ATTACHMENT 4

MHI Document L5-04GA564
Tube Wear of Unit-3 RSG
Technical Evaluation Report

[Proprietary Information Redacted]

Non-proprietary Version

[ ] (P.1)

San Onofre Nuclear Generating Station, Units 2 & 3
REPLACEMENT STEAM GENERATORS

Tube wear of Unit-3 RSG – Technical Evaluation Report

Supplier Status Stamp

VPL No: SO23-617-1-M1538	Rev No: 0	QC: N/A

☐ DESIGN DOCUMENT ORDER NO. 800873488
☒ REFERENCE DOCUMENT–INFORMATION ONLY ☐ VIRP IOM MANUAL

MFG MAY PROCEED: ☐ YES ☐ NO ☒ N/A

STATUS - A status is required for design documents and is optional for reference documents. Drawings are reviewed and approved for arrangements and conformance to specification only. Approval does not relieve the submitter from the responsibility of adequacy and suitability of design, materials, and/or equipment represented.

☐ 1. **APPROVED**
☐ 2. **APPROVED EXCEPT AS NOTED** - Make changes and resubmit.
☐ 3. **NOT APPROVED** - Correct and resubmit for review. NOT for field use.

APPROVAL: (PRINT / SIGN / DATE)
RE: D. Calhoun/David Calhoun 10/1/12
FLS:
Other:

SCE DE(123) 5 REV. 3 07/11 REFERENCE: SO123-XXIV-37.8.26

Purchase Order No.	4500024051
Specification No.	SO23-617-01R3

CONTENT		REMARKS	PURCHASER	ORDER No.	DATE
DESCRIPTION	PAGE			ITEM No.	REFERENCE
FIGURE	SHEET		Edison (MNES)	2591012	
TOTAL	474 PAGE			1003	

Nuclear Plant Component Designing Department
Steam Generator Designing Section

APPROVED BY	
CHECKED BY	
DESIGNED BY	
DRAWN BY	—
—	—
ISSUE DATE	

Distribution		PM(S)	COPY
Edison	1	1	1

DWG. No. L5-04GA564

Rev.No. 9

MITSUBISHI HEAVY INDUSTRIES, LTD.

Revision History

No.	Revision	Date	Approved	Checked	Prepared
0	Initial issue	See cover sheet			
1	Revised in accordance with RSG-SCE/MHI-12-5698 (Since this report has been wholly revised, the revision bar is omitted)				
2	-Revised in accordance with RSG-SCE/MHI-12-5714 -Revised Appendix-10 by using the latest ATHOS outputs -Added Appendix-16				
3	-Revised in accordance with RSG-SCE/MHI-12-5728 -Revised Appendix-8 and 9 in accordance with Expert Panel's comments				
4	-Revised the main report wholly				
5	-Revised Executive Summary and Section 5.2.2				
6	-Revised in accordance with RSG-SCE/MHI-12-5745				
7	- Revised in accordance with RSG-SCE/MHI-12-5757 and RSG-SCE/MHI-12-5762				
8	- Revised in accordance with RSG-SCE/MHI-12-5775 - Revised Appendix-9 to be consistent with the current full bundle model analysis cases				

No.	Revision	Date	Approved	Checked	Prepared
9	- Revised in accordance with RSG-SCE/MHI-12-5786 - Revised Section 4.1.2 and 4.1.3 - Added Fault Tree Evaluation in Section 6 - Undeleted Appendix-16				

Table of Contents

Appendices

Acronyms and Definitions

2A, 2B, 3A, 3B:	Unit 2 SGs A (E089) & B (E088) and Unit 3 SGs A (E089) & B (E088)
3D:	Three-dimensional
Active support:	Tube support at AVB or TSP, which prevents tube motion in the in-plane and out-of-plane directions
ATHOS:	An EPRI sponsored thermal hydraulic computer program for steam generator flow analysis
AVB:	Anti-Vibration Bar
B01-B12 / AVB01-AVB12:	AVB designations with B01 the first above TSP #7 on the hot leg side
B05 and B06:	Cross-section through the U-bend parallel to AVB B05 and B06
Col:	Tube column number
CDS:	Certified Design Specification of SONGS Unit 2&3 RSGs (SO23-617-01, Revision 3)
ECT:	Eddy Current Testing
FEI:	Fluid Elastic Instability
FIV:	Flow Induced Vibration
Free-span:	Tube section between supports
G-value:	Tube diameter in the U-bend region aligned with tube-to-AVB intersections

Thermal-hydraulic conditions:	The term "thermal-hydraulic conditions" refers to flow velocity, void fraction (steam quality) and hydro-dynamic pressure
Inactive support:	Tube support at AVB or TSP, which does not prevent tube motion in both in-plane and out-of-plane directions
ISI:	In-service Inspection
IVHET:	MHI tube wear analysis program
MHI:	Mitsubishi Heavy Industries
N:	Newton, force (1N equals 0.225lbf)
P/D ratio:	Tube pitch-to-diameter ratio
PSI:	Pre-service Inspection
RB	Retainer Bar
R100C88:	Tube address (Row 100, Column 88)
RSG:	Replacement Steam Generator
SCE:	Southern California Edison
SONGS:	San Onofre Nuclear Generating Station
TSP:	Tube Support Plate
TTW:	Tube-to-Tube Wear
T/H	Thermal and Hydraulic
TSP #1-TSP #7:	Tube support plate numbers from the lower most to the upper most

Executive Summary

On January 31, 2012, during the first cycle after steam generator replacement, San Onofre Nuclear Generating Station (SONGS) Unit 3 was shut down due to indications of a steam generator tube leak. Steam generator tube inspections confirmed one small leak on one tube in one of the two steam generators. Further inspections of 100% of the steam generator tubes in both Unit-3 steam generators discovered unexpected wear, including tube-to-tube as well as tube-to-tube-support structural wear.

Tube wear was found in the tube free span sections, at anti-vibration bars (AVBs), at Tube Support Plates (TSPs) and at retainer bars, and was labeled as follows:

(i) Type 1 (Tube-to-Tube Wear)
(ii) Type 2 (AVB wear)
(iii) Type 3 (TSP wear)
(iv) Type 4 (Retainer bar wear)

The cause of the first 3 types of tube wear is tube vibration. The causes of tube vibration are the thermal-hydraulic conditions in the SG secondary side and the condition of the tube bundle supports. Type 4 tube wear is due to vibration of the selected retainer bars, rather than the tubes.

Structures in a two-phase flow field have lower resistance to vibration when the fluid void fraction (and hence steam quality) is high. High void fraction (high steam quality) results in the two-phase flow mixture having low density, which in turn results in a high velocity of the two-phase flow and in a low damping factor. Consequently, the dynamic pressure, which is a function of the flow velocity squared, increases. As the dynamic pressure is a major factor causing the structures in the flow field to vibrate, it is more likely for the structures to vibrate when the void fraction (steam quality) is high (as it affects both the flow velocity and the damping factors).

Based on the investigation of the correlation between the void fraction (steam quality) and the number of tubes with wear in a given void fraction region, a strong correlation between the void fraction (steam quality) and the percentage of tubes with wear was identified. Consequently, it is concluded that the thermal-hydraulic conditions in the SG secondary side, namely high void fraction (steam quality) and high flow velocity, along with lack of sufficient in-plane tube support, discussed next, are the main causes of the excessive tube vibration and unexpected wear in the SONGS Unit 2 and Unit 3 SGs. The higher than typical void fraction is a result of a very large and tightly packed tube bundle, particularly in the U-bend, 9 9

with high heat flux in the hot leg side.
Contemporary experience shows that out-of-plane vibration of the SG U-tube is more likely to occur than in-plane vibration, because tube U-bend natural frequency in the out-of-plane direction is lower than natural frequency in the in-plane direction. In the design stage, MHI assumed that the tube support in the out-of-plane direction with "zero" tube-to-AVB gap in hot condition was sufficient to prevent tube from becoming fluid-elastic unstable during operation. But, the recent SONGS experience shows that the flat bar AVBs does not provide friction forces required to prevent tubes from vibrating in the in-plane direction and eventually becoming fluid-elastic unstable under high local secondary thermal-hydraulic conditions such as in the SONGS RSGs. In addition, MHI concludes that in the Unit-3 RSGs low tube and AVB fabrication dimensional dispersion causes that the tube-to-AVB contact forces are not sufficient to prevent the in-plane motion of tubes.

In order to ensure the structural integrity of the tubes after restarting the plant, all tubes which have a potential for losing their integrity during the next operating period should be plugged and thermal power output of the plant should be decreased. Plugging for the Type 1 wear should include not only the tubes with the Type 1 wear but also tubes which are susceptible to the Type 1 wear, for preventative reasons. Plugging for the Type 2 and 3 wear should include the tubes with wear equal to, or greater than, 35% in accordance with Technical Specifications. Plugging for the Type 4 wear should include 94 tubes which are adjacent to the retainer bars. Decreasing the thermal power output will improve thermal-hydraulic conditions (will lower flow velocities and void fractions in the critical tube bundle U-bend region) and thus will reduce the possibility of the occurrence of tube fluid-elastic instability (FEI) leading to unacceptable tube wear.

1. Introduction

After approximately 11 months of power operation following the steam generator replacement, SONGS Unit-3 underwent an unplanned shut down on Jan. 31, 2012 as a result of leakage of primary coolant to the secondary side from a tube in the 3B (3E-088) steam generator (SG). The maximum leakage rate was at approximately 82 gallon/day (~13 liters/hour). Subsequent investigation revealed that the direct cause of the leakage was tube-to-tube wear.

At the time of the Unit-3 leak, SONGS Unit-2 had already completed one cycle of power operation (~22 months) after the steam generator was replaced in the refueling outage since Jan. 9, 2012. Eddy-Current Testing (ECT) inspections were performed on all tubes in both Unit-3 SGs and wear indications on many of the tubes were found. This report presents the evaluation of the mechanistic cause of tube wear and the countermeasures required for Unit-3 return to service.

2. Summary of RSG Design for SONGS

2.1 Overall RSG Design

The SONGS RSGs were specified, designed and fabricated as replacements on a like-for-like basis for the original steam generators in terms of fit, form and function with limited exceptions, and were replaced under the 10CFR50.59 rule. The CDS for the design and fabrication of the RSGs (SO23-617-01, Revision 3) specified the limiting design parameters and materials. Thus, replacement steam generator design with 3/4" tube diameter arranged in 1" triangular pitch, which was the same as in the original steam generators, and the larger heat transfer area than in the original steam generators, was optimal. The other parameters/materials not specified by CDS were established/ selected in the design process. The SONGS RSGs were designed and fabricated to achieve an "effective zero gap" as required by CDS Rev. 3 in order to minimize its potential for tube wear. The CDS also states that the tube support/tube bundle assembly shall be fabricated such as to ensure no damage to the tubes and subsequent operation of the RSG with minimal vibration.

2.2 Tube Bundle Design

The major concern with the large U-tube SGs is their propensity for tube wear in the tube bundle U-bend region. Consequently, minimizing tube wear was given the first priority in the SONGS RSG specification, design and fabrication, and the tube support design and fabrication was discussed by MHI and SCE in numerous design review meetings. As a result, the tube bundle U-bend support design and fabrication was as follows:

1) Six (6) V-shaped AVBs (three sets of two) were provided between each tube column.
2) The AVB thickness was set such as to provide an effective "zero" tube-to-AVB gap under operating (hot) conditions.
3) The AVB end-caps were welded to the retaining bars with the U-bend in the gravity neutral position to achieve uniformity of the gap size and AVB parallelism, using spacers between the AVBs sized based on a mockup test.

The tube bundle and AVB structure configuration and components (AVBs, retaining bars, bridges and retainer bars) are shown in Fig.2-1. MHI investigated field experience with U-bend tube degradation using INPO, NRC and NPE data bases, and concluded that tube wear in the operating U-tube SGs was mostly being caused by out-of-plane tube motion. Consistent with this and Reference 7, only out-of-plane vibration of the SG U-tubes was evaluated because tube U-bend natural frequency in the out-of-plane direction is lower than natural frequency in the in-plane direction and out-of-plane vibration is more likely to occur than in-plane vibration. No SG problems stemming from in-plane tube motion were identified by MHI and thus MHI concluded that the design and fabrication processes described above were sufficient for minimizing tube wear in the SONGS RSGs.

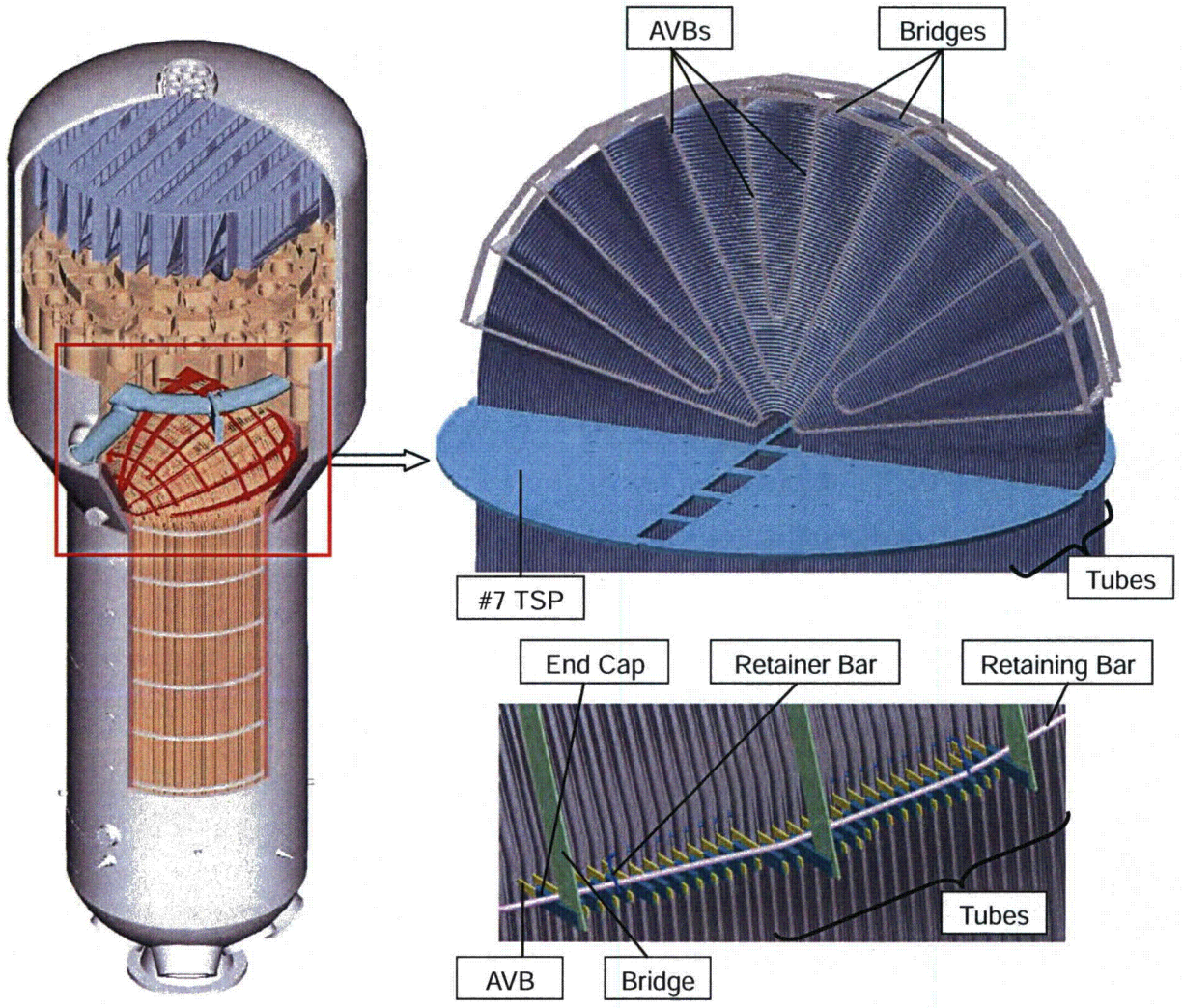

Fig.2-1 Tube Bundle and AVB Structure Configuration

3. Description of Events

3.1 Unit-2

3.1.1. Abstract

During the first refueling outage following steam generator replacement, ECT inspection of the unit 2 steam generator tubes identified a total of 10 tubes with wear depths of 28 to 90% of the tube wall thickness. Six of the affected tubes were located adjacent to the retainer bars. The retainer bars are part of the floating anti-vibration bar (AVB) structure that supports the U-bend region of the tubes. The remaining tubes had detectable wear associated with AVB support points elsewhere in the AVB structure.

3.1.2. Sequence of Events

Fall of 2009

The original Combustion Engineering (CE) SGs were replaced with MHI SGs during the Cycle 16 Refueling Outage. 9

May, 2010

Unit 2 completed the Cycle 16 Refueling and Steam Generator Replacement outage and returned to service at nominal 100% reactor power.

January 9, 2012

Unit 2 started the Cycle 17 Refueling Outage.

February 5, 2012

Routine ECT inspections of the SGs identified wear indications greater than 35% at two tube locations adjacent to the retainer bars.

3.2 Unit-3

3.2.1. Abstract

During the first cycle after steam generator replacement, on Jan.31, 2012, Unit 3 was shut down due to indication of a steam generator tube leak. Steam generator tube inspections confirmed one small leak on one tube in one of the two steam generators. Continuing inspections of 100% of the steam generator tubes in both Unit-3 steam generators discovered unexpected wear, including tube-to-tube as well as tube-to-tube-support wear.

3.2.2. Sequence of Events

Fall, 2010

The original CE SGs were replaced with MHI SGs during the Cycle 16 Refueling Outage.

February, 2011

Unit 3 completed the Cycle 16 Refueling and Steam Generator Replacement Outage and returned to service at nominal 100% reactor power.

January 31, 2012

During 100% power operation, a high radiation alarm from the condenser air ejector line revealed a primary-to-secondary leak in a SG. SONGS operators responded by rapidly reducing power and then shutting down the plant.

4. Investigation of Wear Condition

4.1 ECT Inspection Results

The basis of ECT data evaluations in this report (except Table 4.1.2-1 and Table 4.1.3-1) is described in Appendix-3 of Reference 8.

Table 4.1.2-1 and Table 4.1.3-1 are based on the information provided by SCE (Reference 9 and 11). 9

Wear indications obtained from ECT inspection are shown in Fig.4.1-1 and 4.1-2.

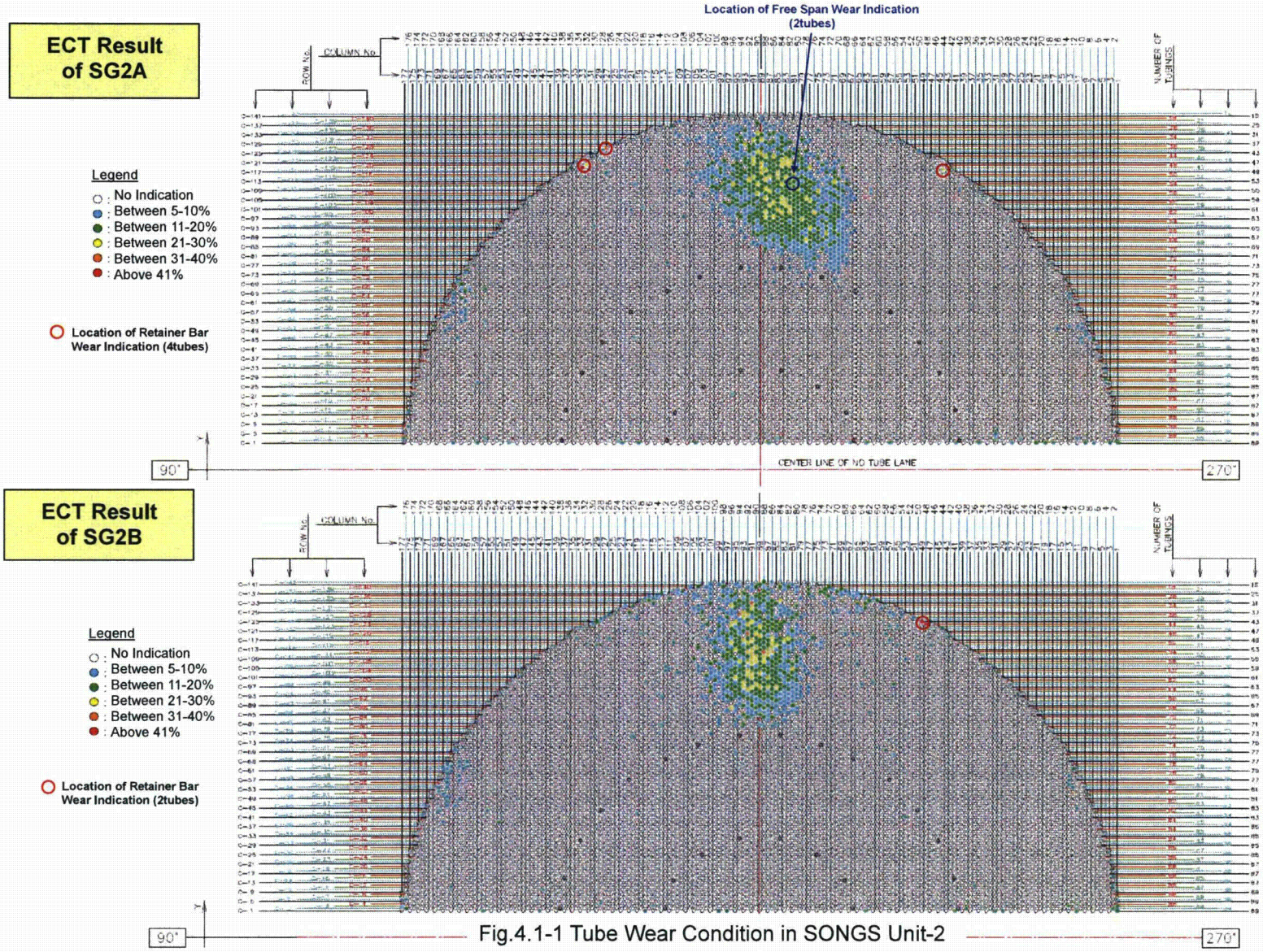

Fig.4.1-1 Tube Wear Condition in SONGS Unit-2

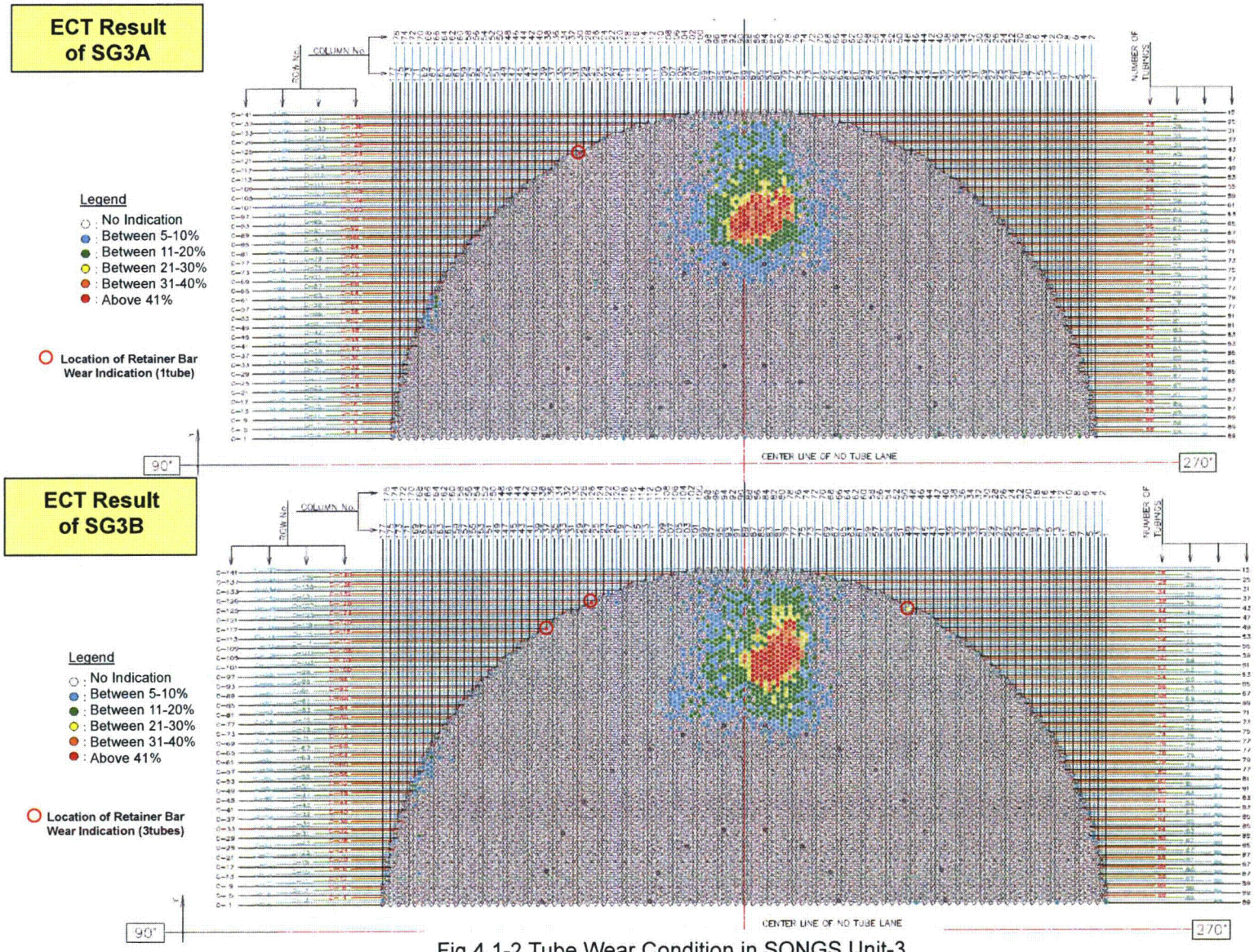

Fig.4.1-2 Tube Wear Condition in SONGS Unit-3

4.1.1. Types of Tube Wear

Tube wear indications were found in the tube free span sections, AVB region and TSP region and were grouped into 4 types as follows:

(i) Type 1 (TTW)

Wear in the tube free-span sections between the AVBs located in the U-bend region. Most of the tubes with this type of wear have also wear indications at AVBs and TSPs. In this case, it is considered that the entire tube, including the straight leg, was vibrating excessively. These tubes are shown in Fig.4.1.1-1.

(ii) Type 2 (AVB wear)

Wear at the tube-to-AVB intersections only with no wear indications in the tube free-span sections. Some of these tubes have wear indications at the TSPs as well. In this case, it is considered that mainly the U-bend section of the tube was vibrating. These tubes are shown in Fig.4.1.1-2.

(iii) Type 3 (TSP wear)

Wear at the tube-to-TSP intersections only in the straight section of the tubes. In this case, it is considered that only the straight section of the tube was vibrating. The tubes with wear at TSPs without wear in the U-bend section are shown in Fig. 4.1.1-3; the tubes with wear at TSPs and with wear in the U-bend section are shown in Fig. 4.1.1-4).

(iv) Type 4 (RB wear)

Wear at the AVB structure retainer bars in the tube U-bend section. These tubes have no wear indications in the free span, at AVBs or at TSPs. In this case, it is considered that the retainer bar itself was vibrating and the tube was not vibrating. These tubes are shown in Fig.4.1.1-2 and in Appendix-1.

Table.4.1.1-1 Wear Type Locations

Wear Pattern	Wear Location			
	Free Span	AVB	TSP	Retainer Bar
Type 1 (TTW)	Yes	Yes	(Yes)	No
Type 2 (AVB wear)	No	Yes	(Yes)	No
Type 3 (TSP wear)	No	No	Yes	No
Type 4 (RB wear)	No	No	No	Yes

Yes : Wear indication was found

(Yes) : Wear indication may be present since some tubes with AVB wear indications have no indications at TSP locations

No : No wear indication

Tube wear indications at each AVB and TSP elevation for all wear categories are shown in

Fig.4.1.1-5, 4.1.1-6, 4.1.1-7 and 4.1.1-8.

3A-SG

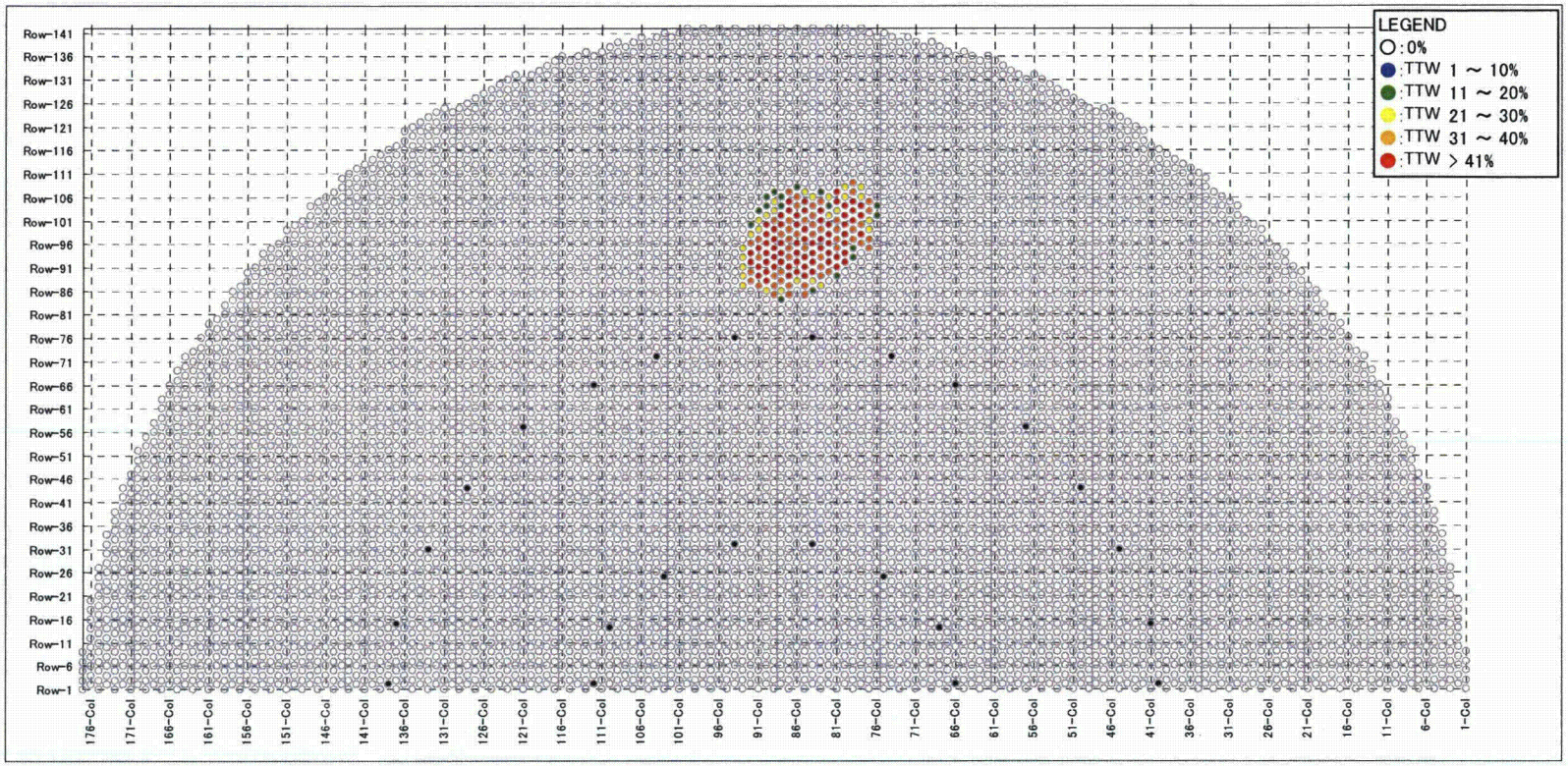

Fig 4.1.1-1(1/2) Tubes with TTW indications in U-bend region

3B-SG

Fig 4.1.1-1(2/2) Tubes with TTW indications in U-bend region

3A-SG

Fig 4.1.1-2(1/2) Tubes with wear indications at AVBs and at retainer bars

3B-SG

Fig 4.1.1-2(2/2) Tubes with wear indications at AVBs and at retainer bars

3A-SG

Fig 4.1.1-3(1/2) Tubes with wear indications at TSPs only

3B-SG

Fig 4.1.1-3(2/2) Tubes with wear indications at TSPs only

3A-SG

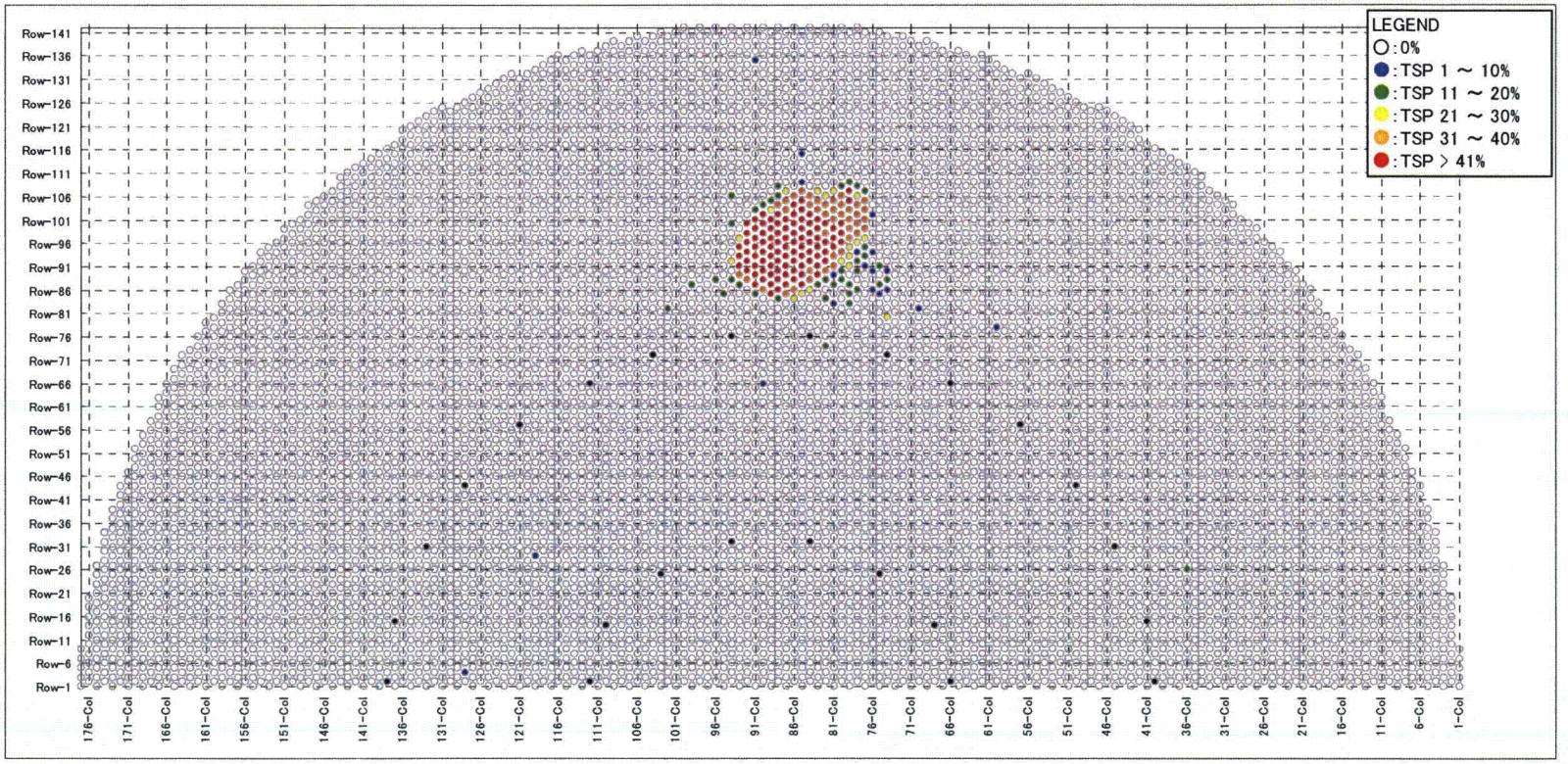

Fig 4.1.1-4(1/2) Tubes with wear indications at TSPs and TTW indications

3B-SG

Fig 4.1.1-4(2/2) Tubes with wear indications at TSPs and TTW indications

3A-SG AVB01

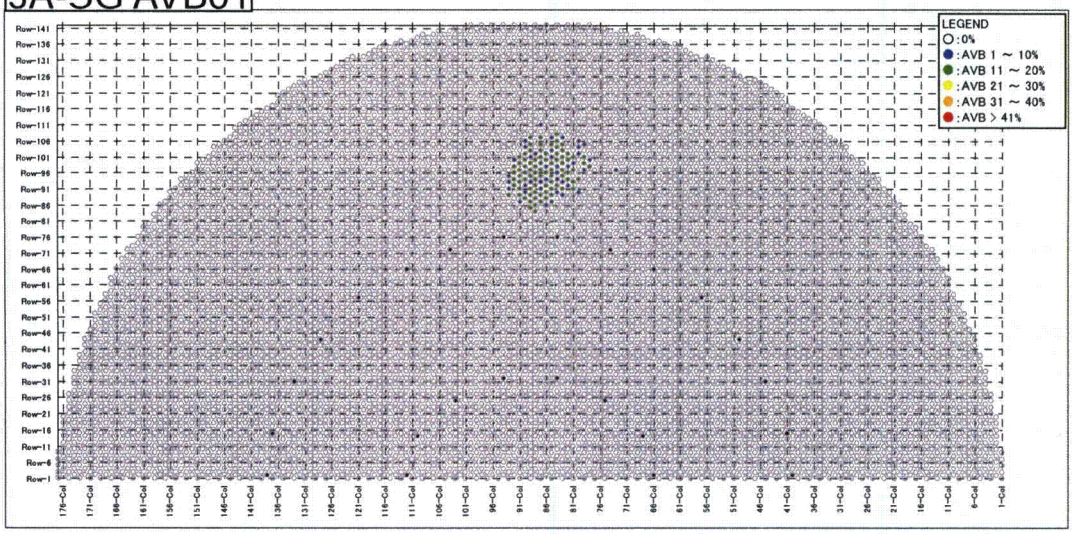

3A-SG AVB02

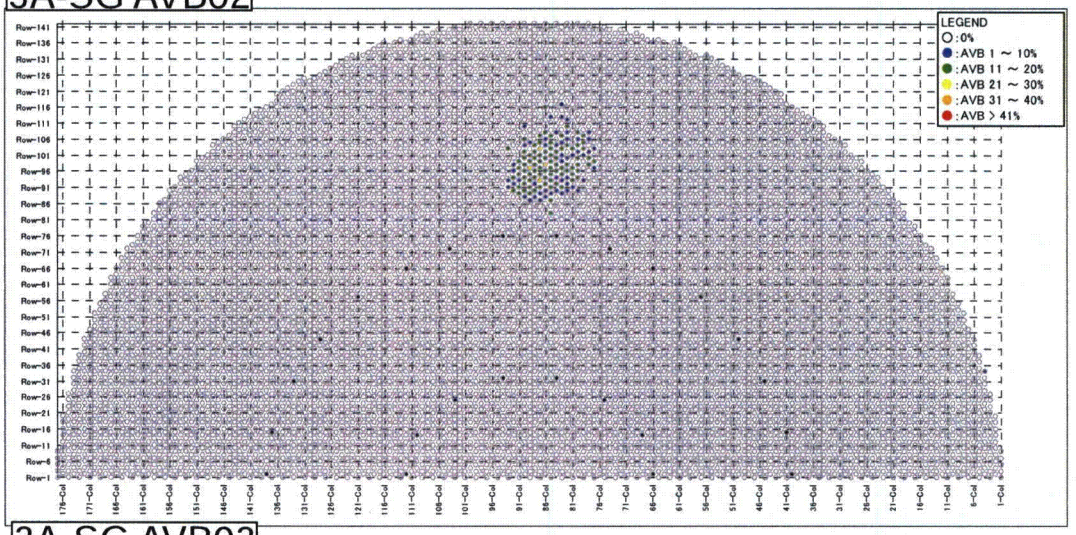

3A-SG AVB03

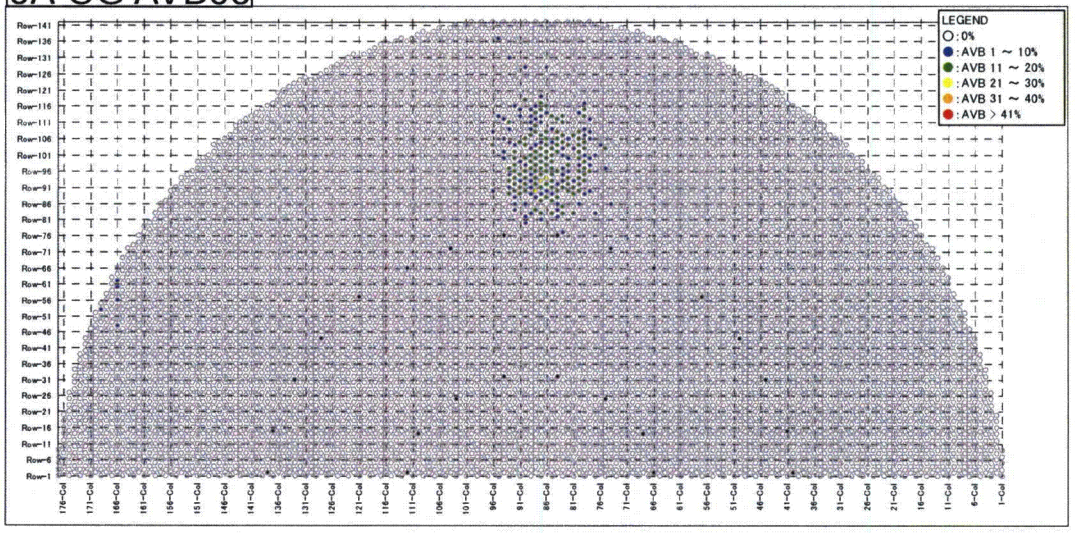

Fig 4.1.1-5 (1/4) Tubes with wear indication (at AVBs)

3A-SG AVB04

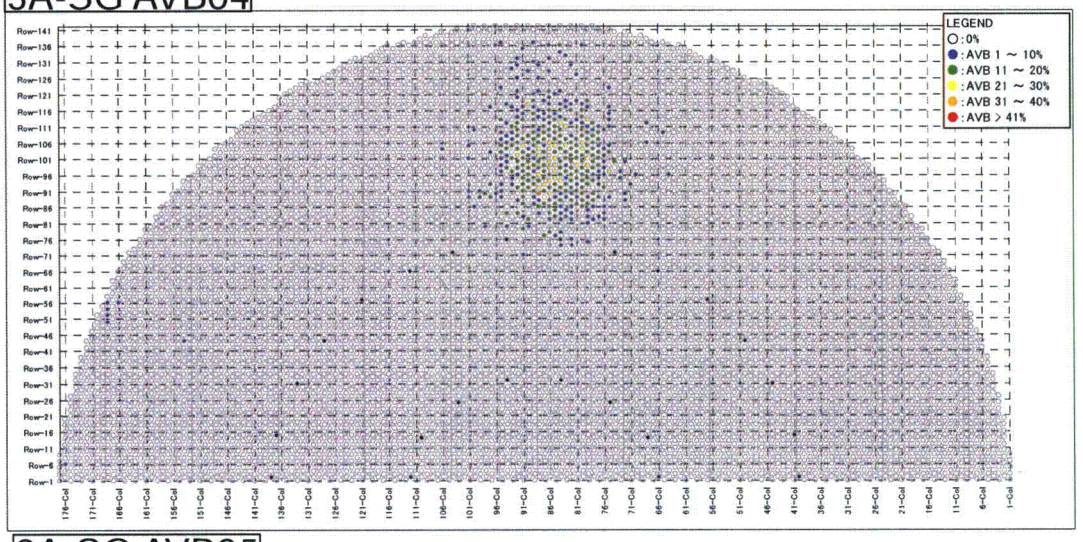

3A-SG AVB05

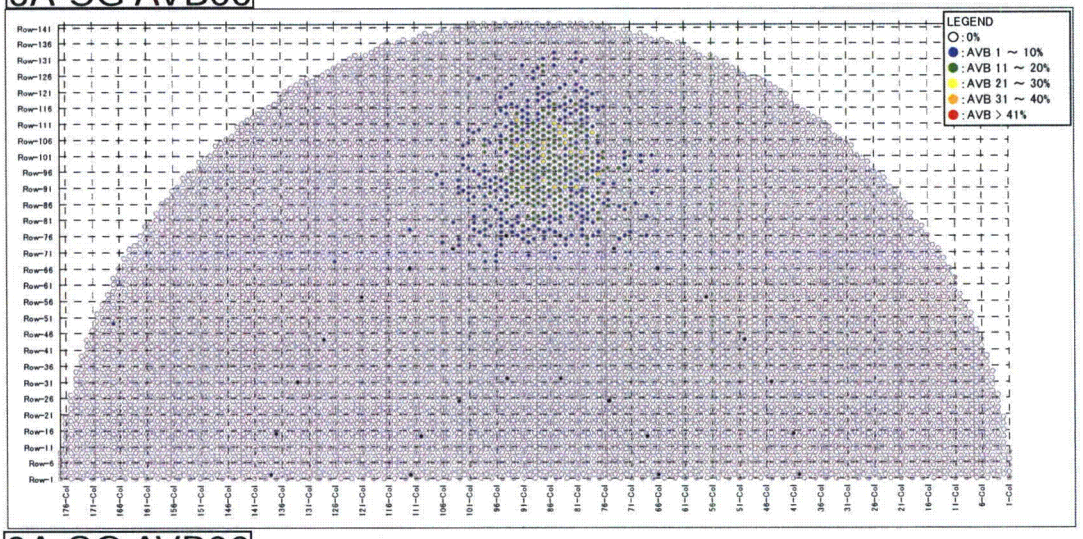

3A-SG AVB06

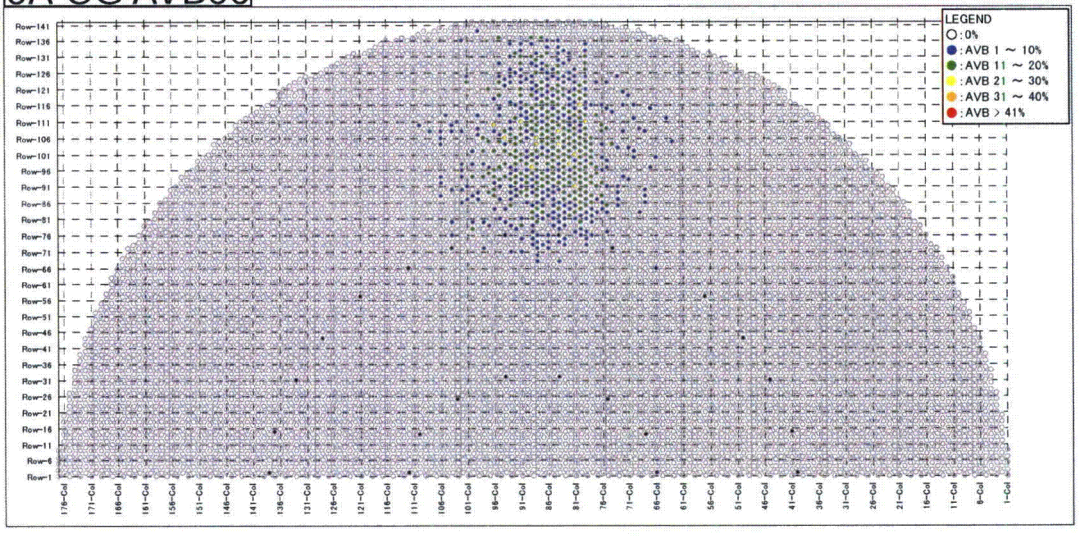

Fig 4.1.1-5 (2/4) Tubes with wear indication (at AVBs)

3A-SG AVB07

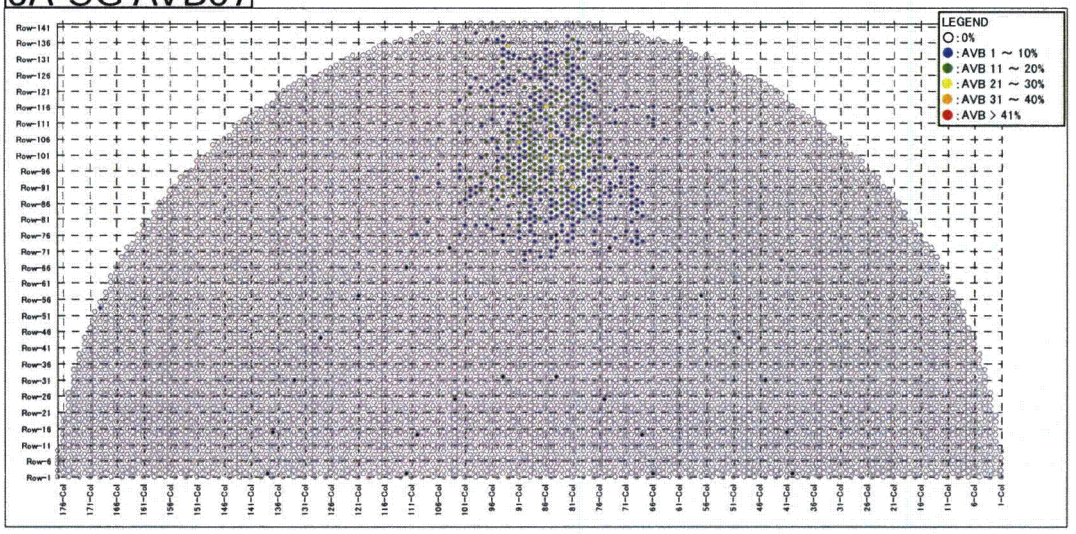

3A-SG AVB08

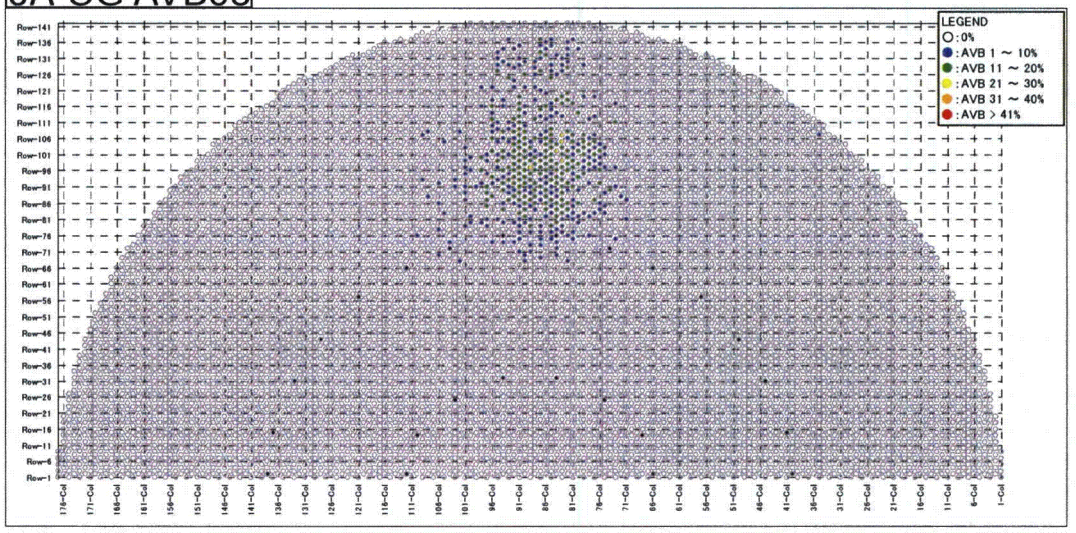

3A-SG AVB09

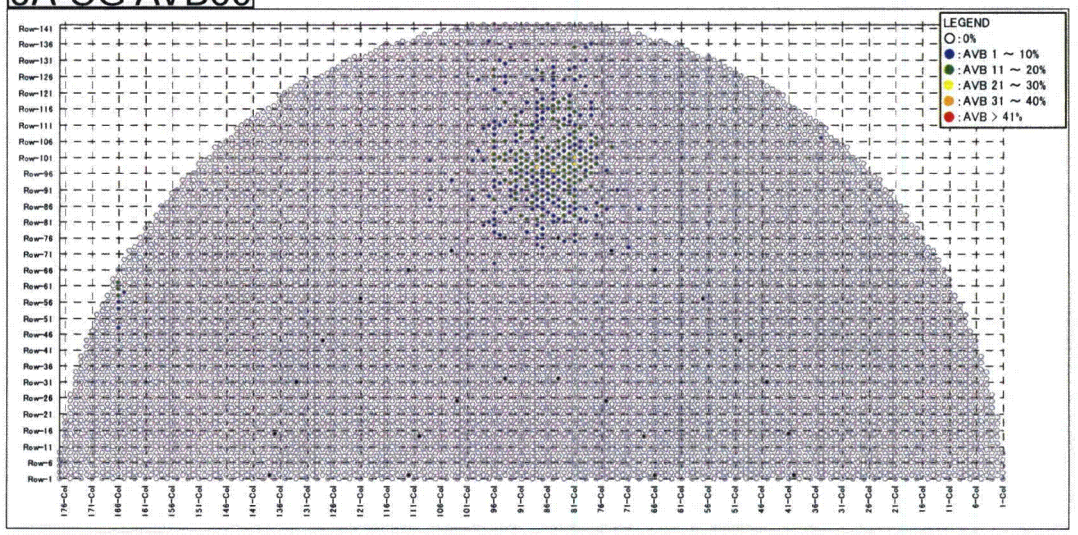

Fig 4.1.1-5 (3/4) Tubes with wear indication (at AVBs)

3A-SG AVB10

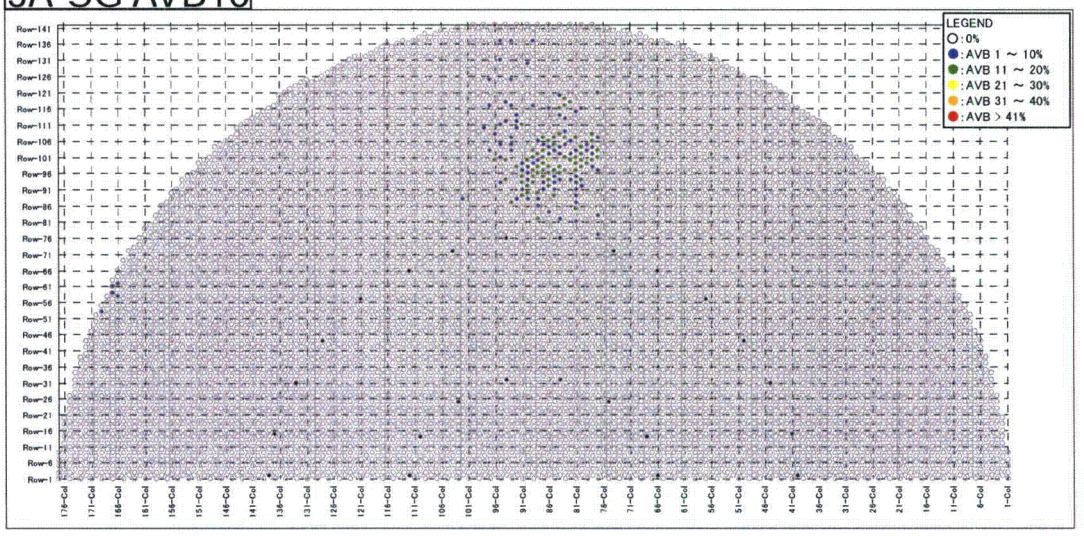

3A-SG AVB11

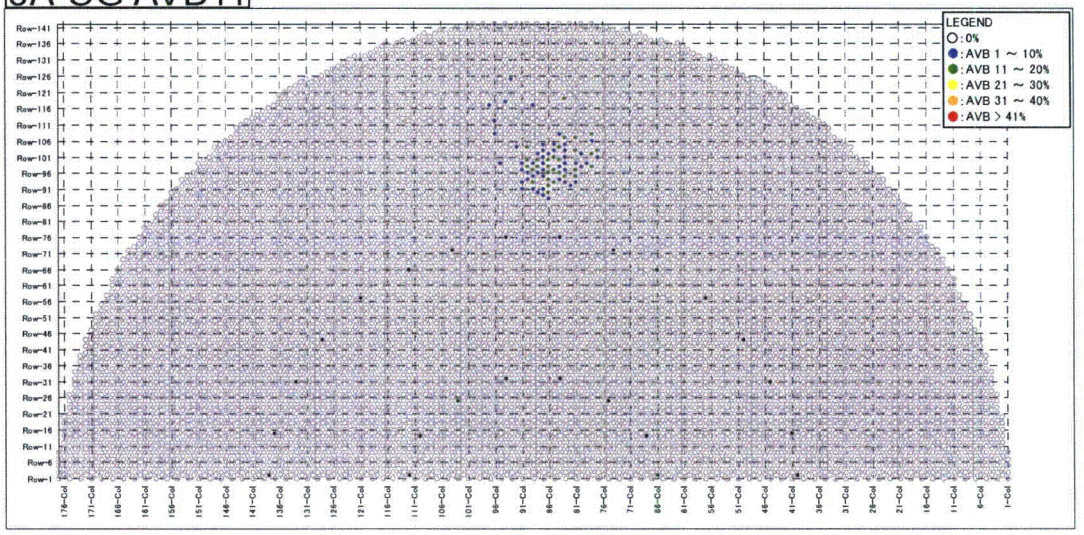

3A-SG AVB12

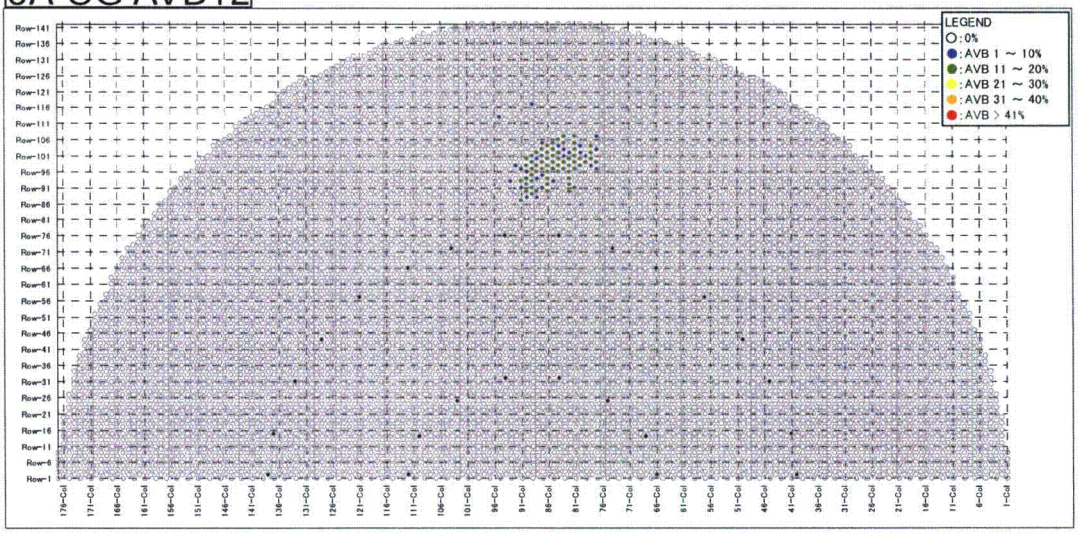

Fig 4.1.1-5 (4/4) Tubes with wear indication (at AVBs)

3A-SG #1TSP

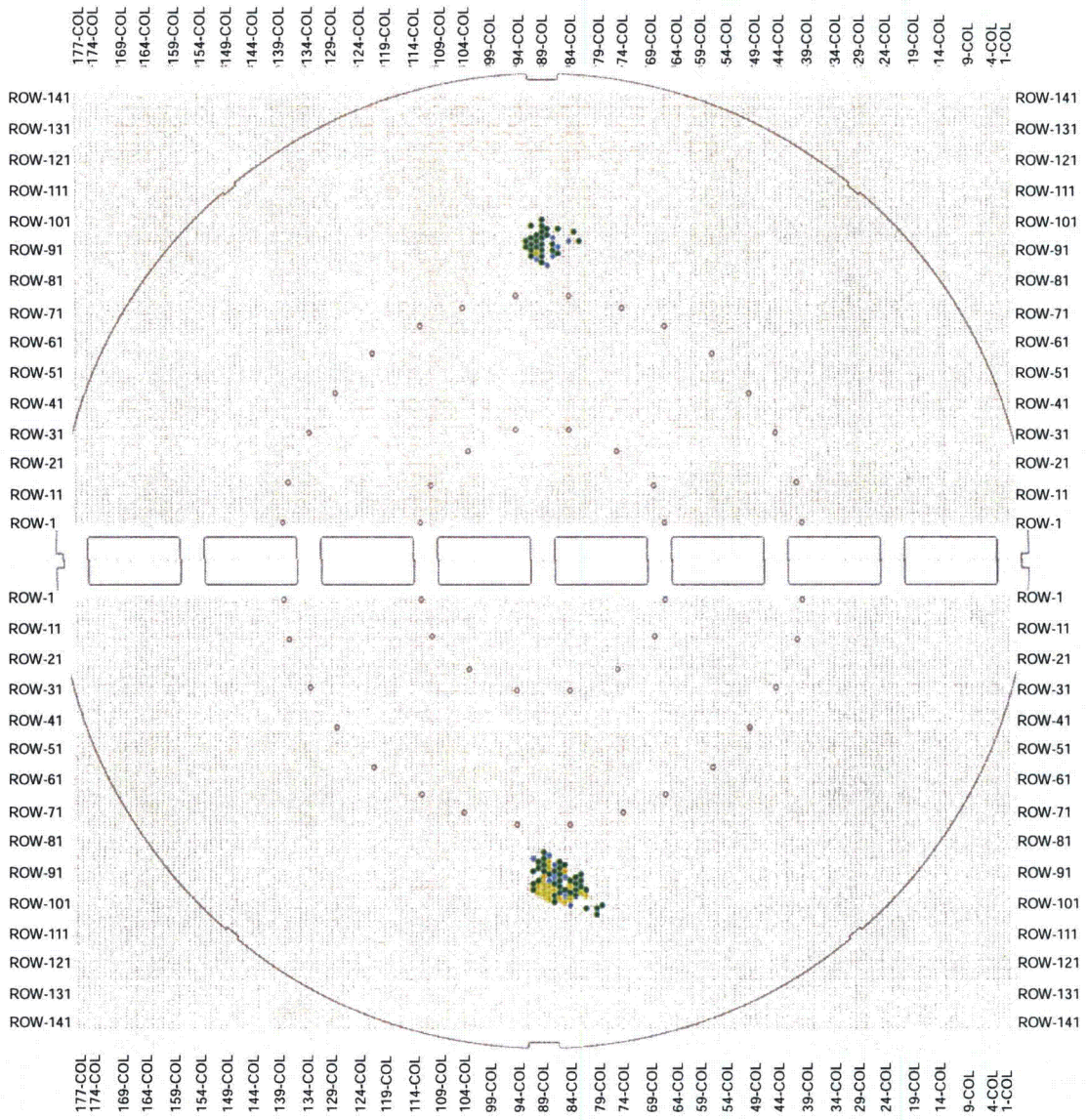

Fig 4.1.1-6 (1/7) Tubes with wear indications at TSPs

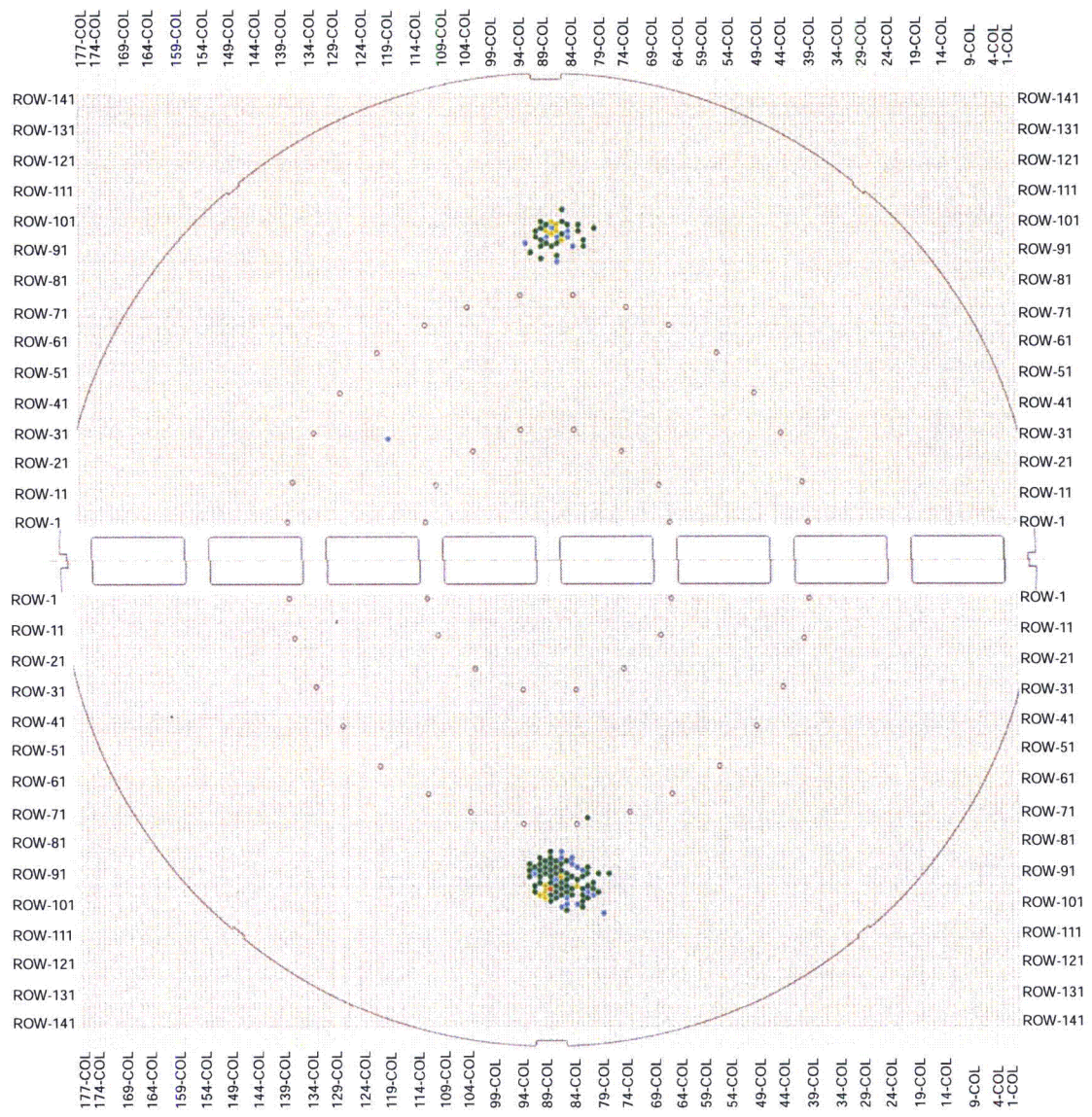

Fig 4.1.1-6 (2/7) Tubes with wear indications at TSPs

3A-SG #3TSP

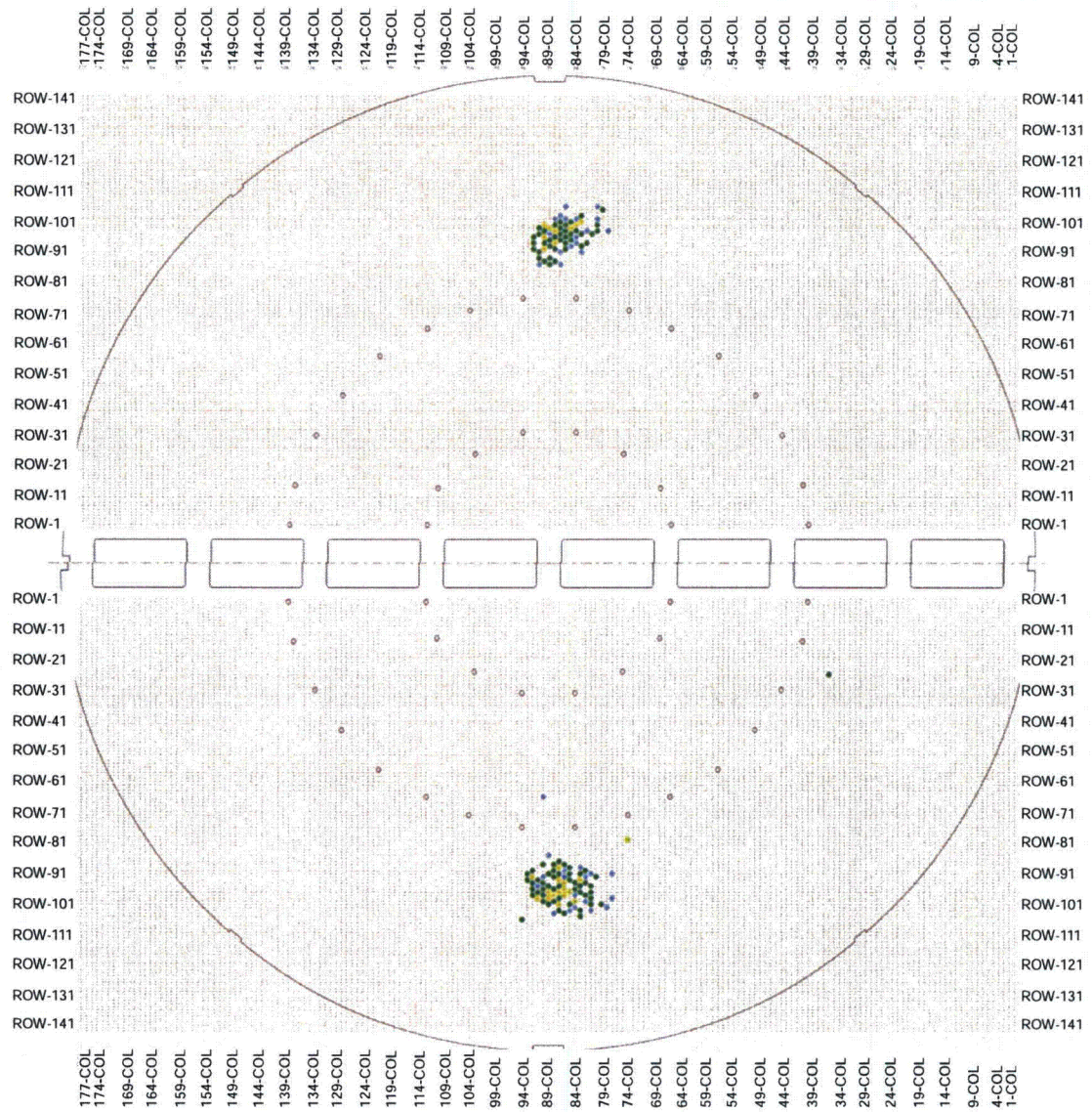

Fig 4.1.1-6 (3/7) Tubes with wear indications at TSPs

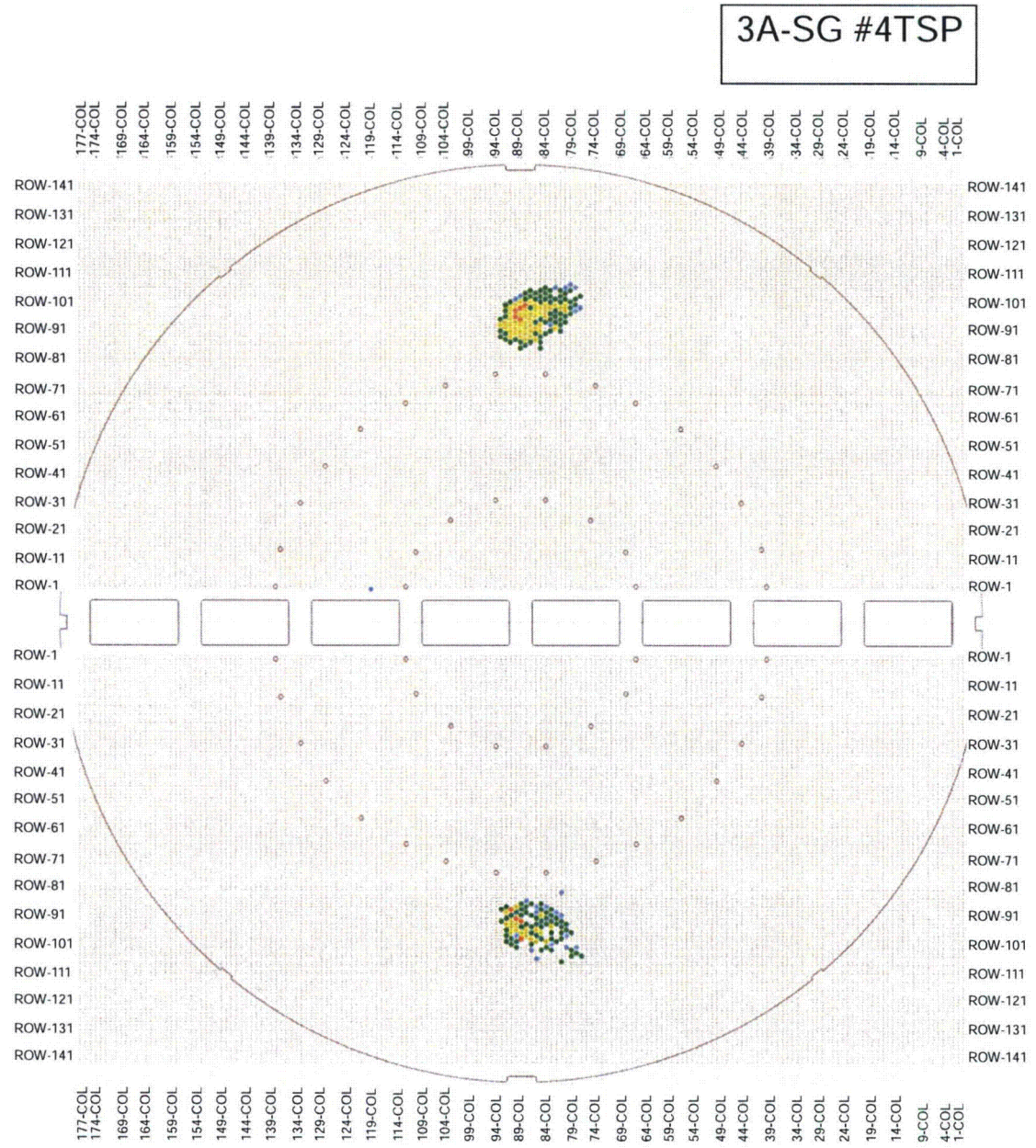

Fig 4.1.1-6 (4/7) Tubes with wear indications at TSPs

3A-SG #5TSP

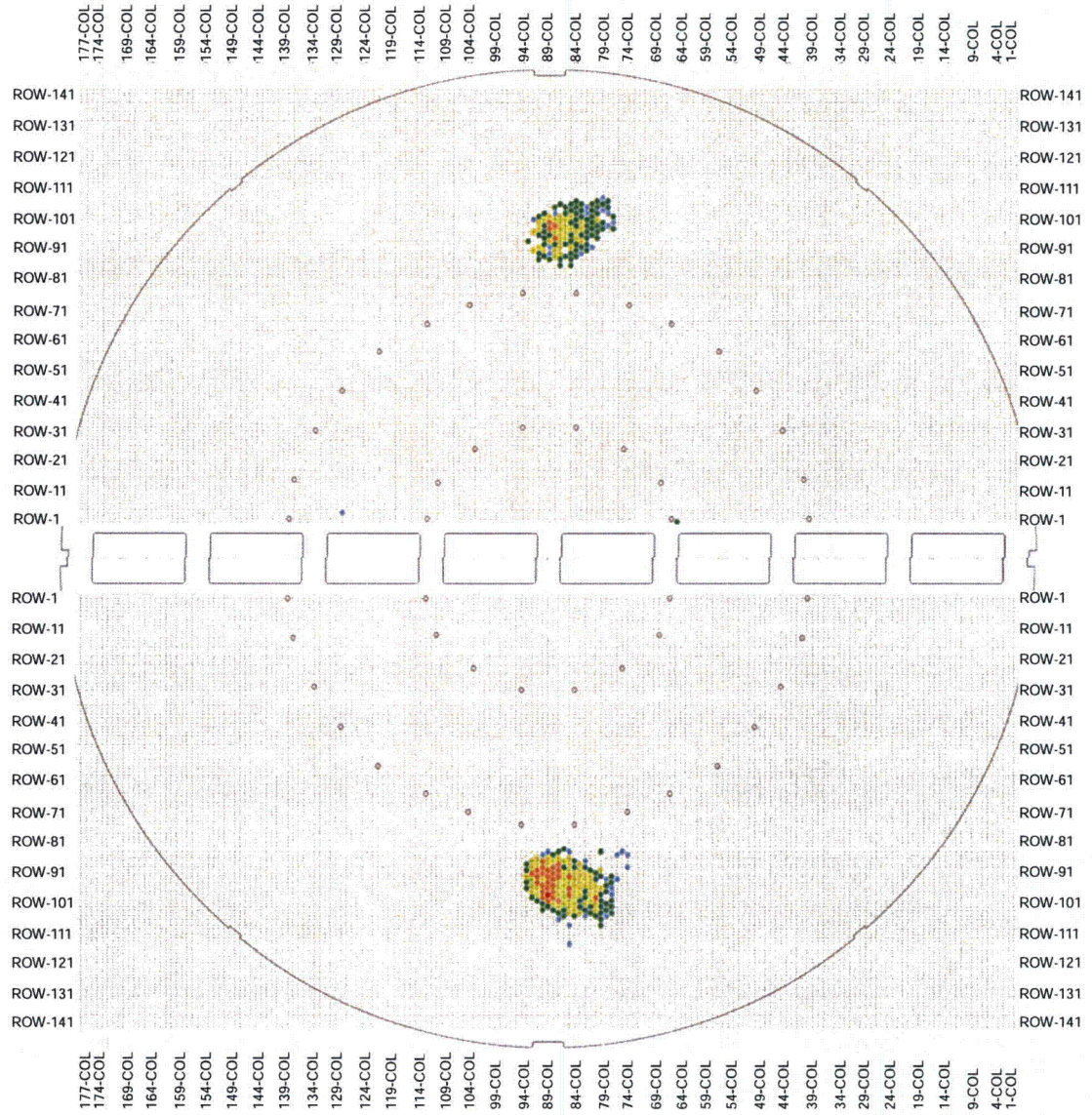

Fig 4.1.1-6 (5/7) Tubes with wear indications at TSPs

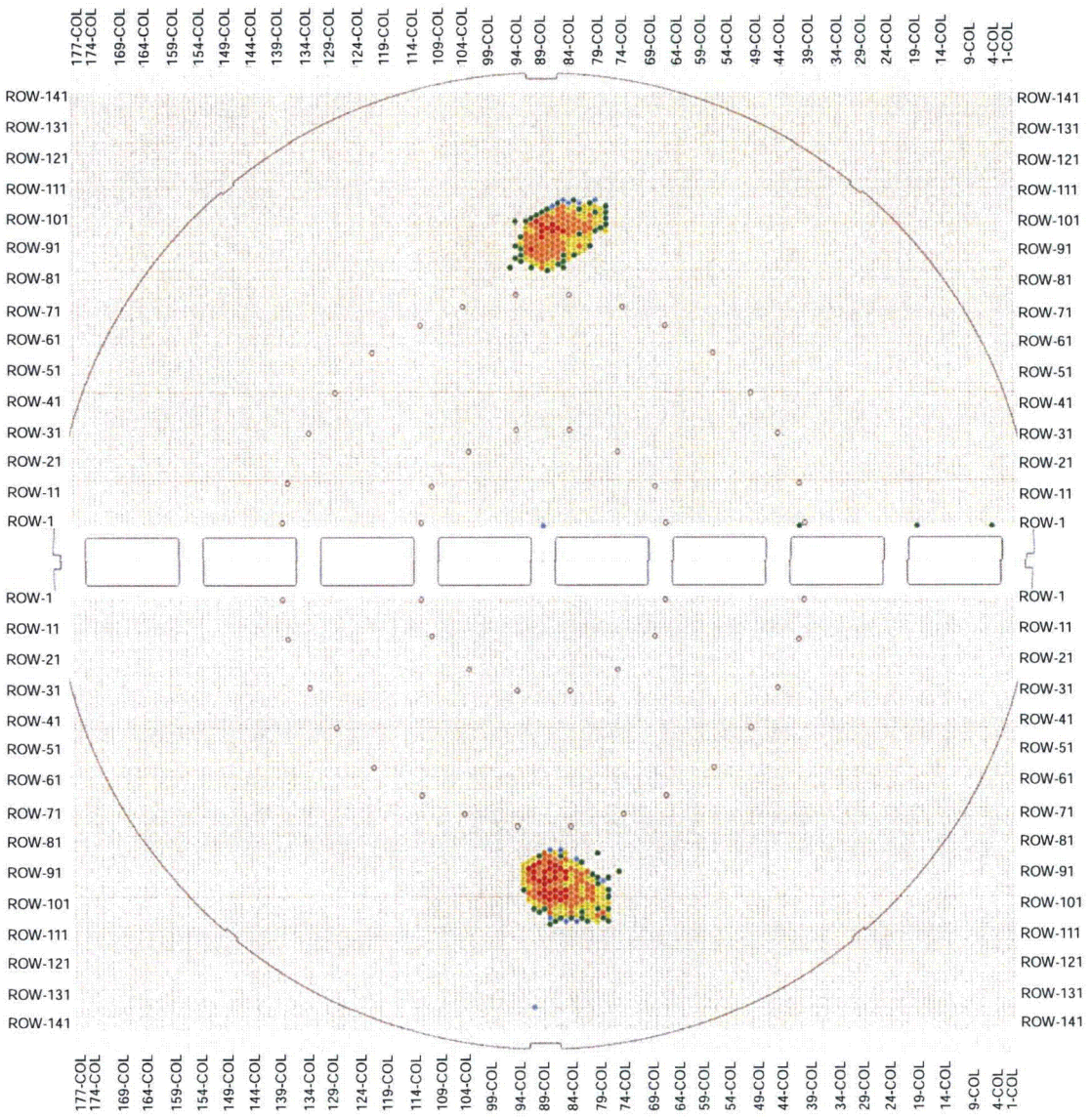

Fig 4.1.1-6 (6/7) Tubes with wear indications at TSPs

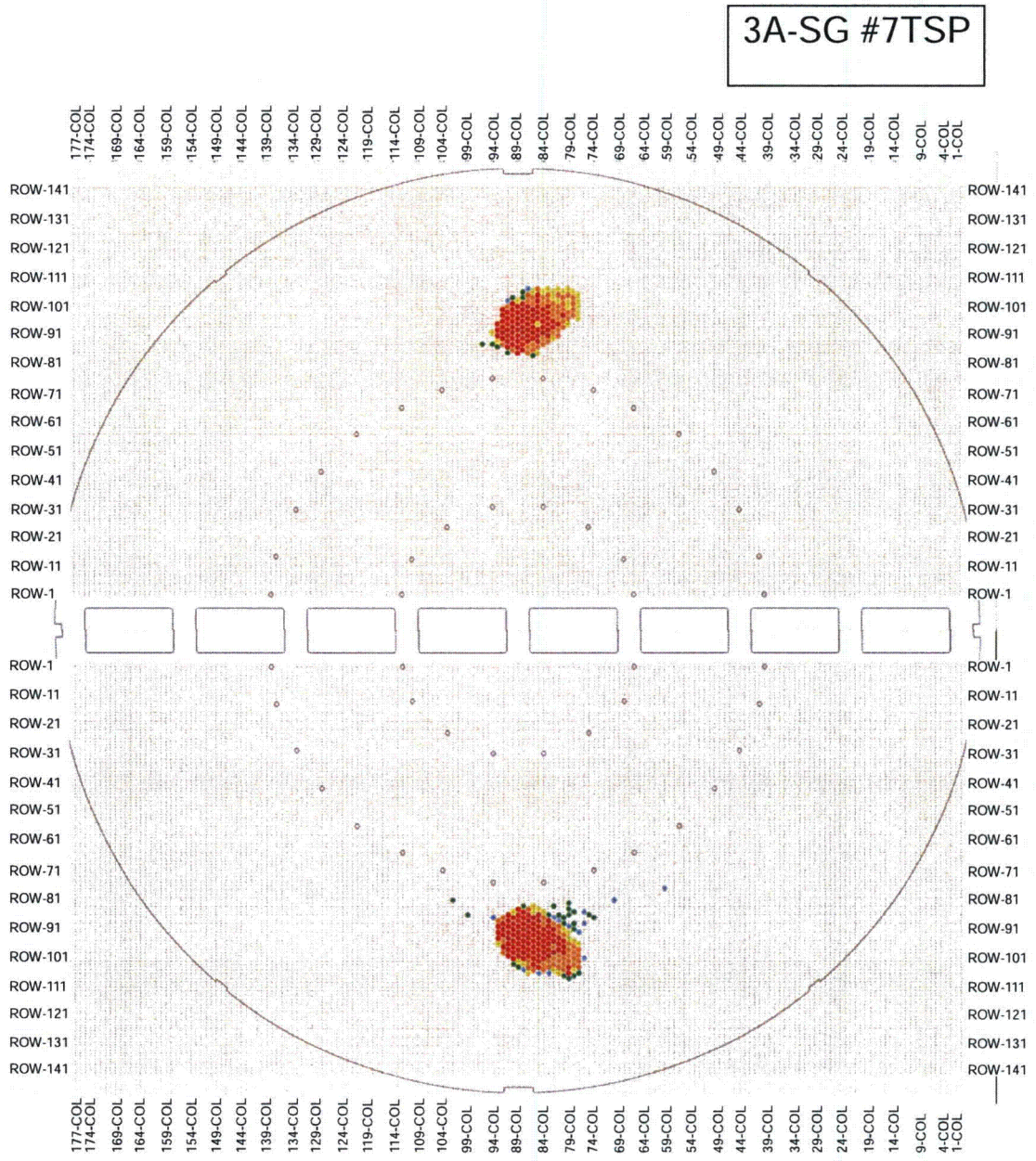

Fig 4.1.1-6 (7/7) Tubes with wear indications at TSPs

3B-SG AVB1

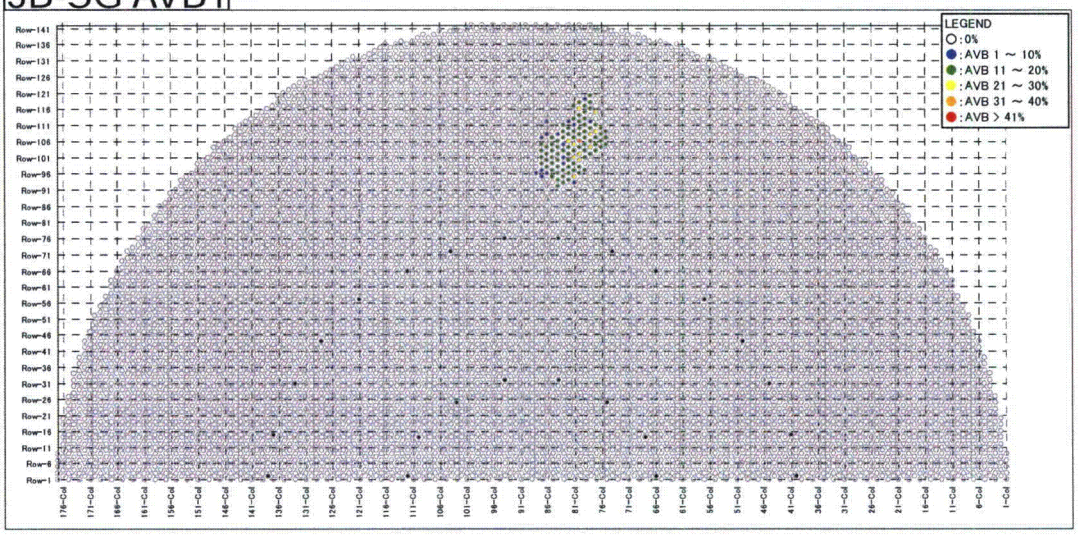

3B-SG AVB2

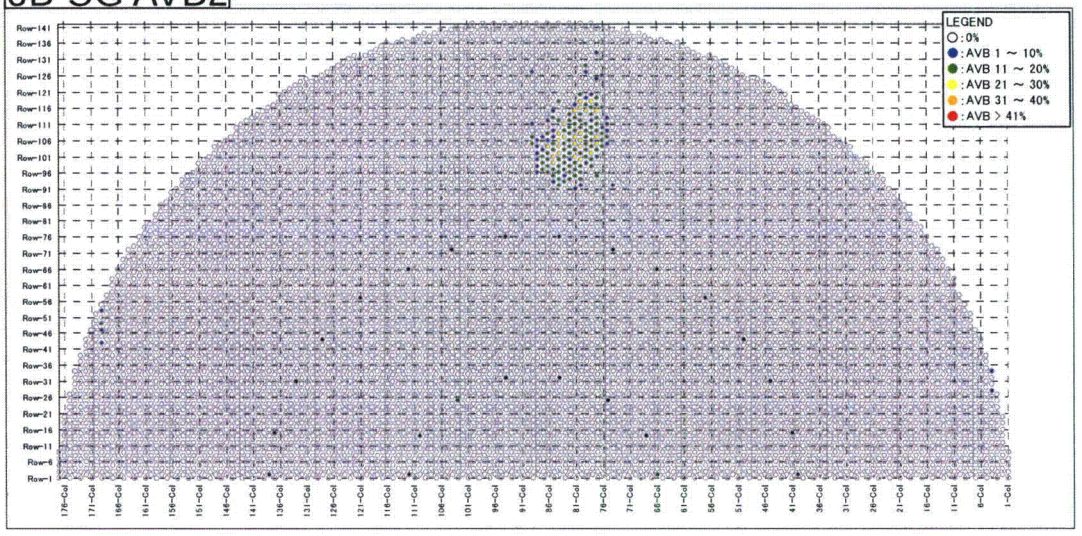

3B-SG AVB3

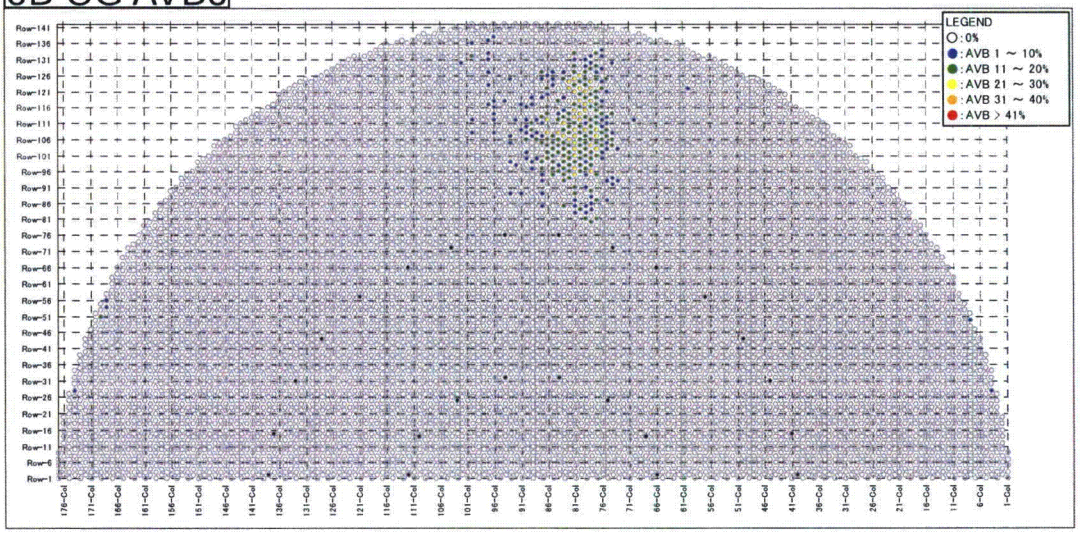

Fig 4.1.1-7 (1/4) Tubes with wear indication (at AVBs)

3B-SG AVB4

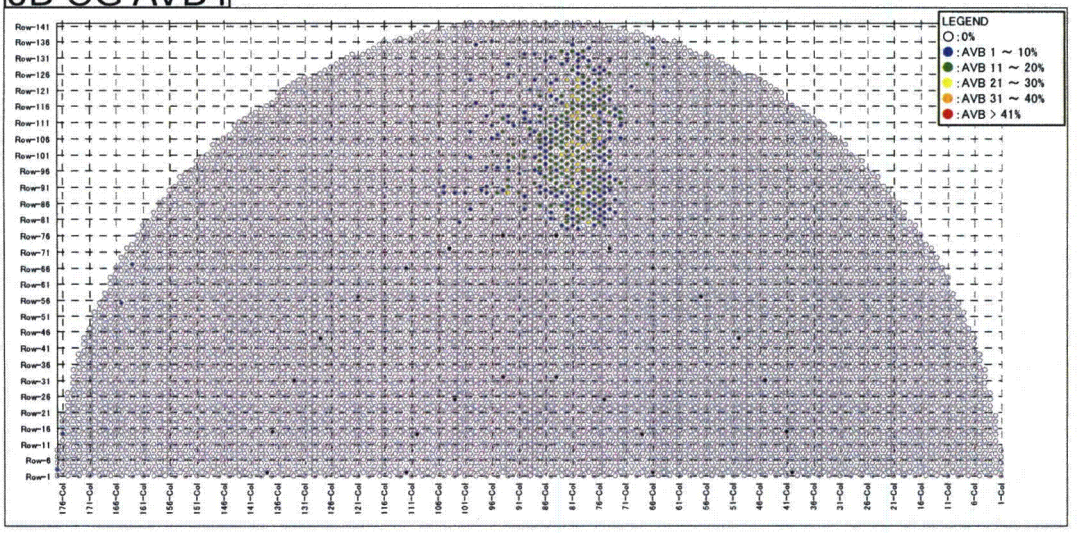

3B-SG AVB5

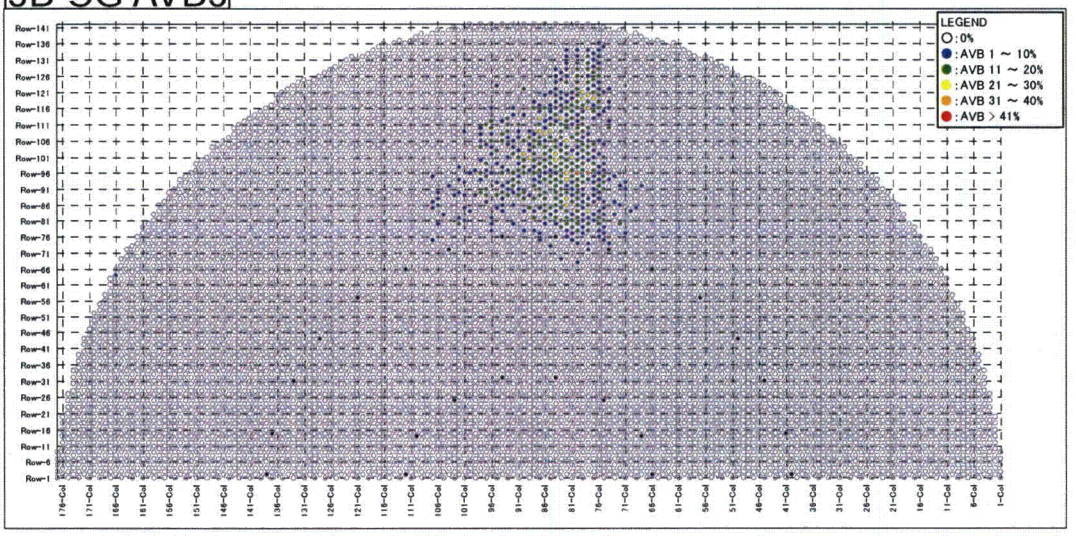

3B-SG AVB6

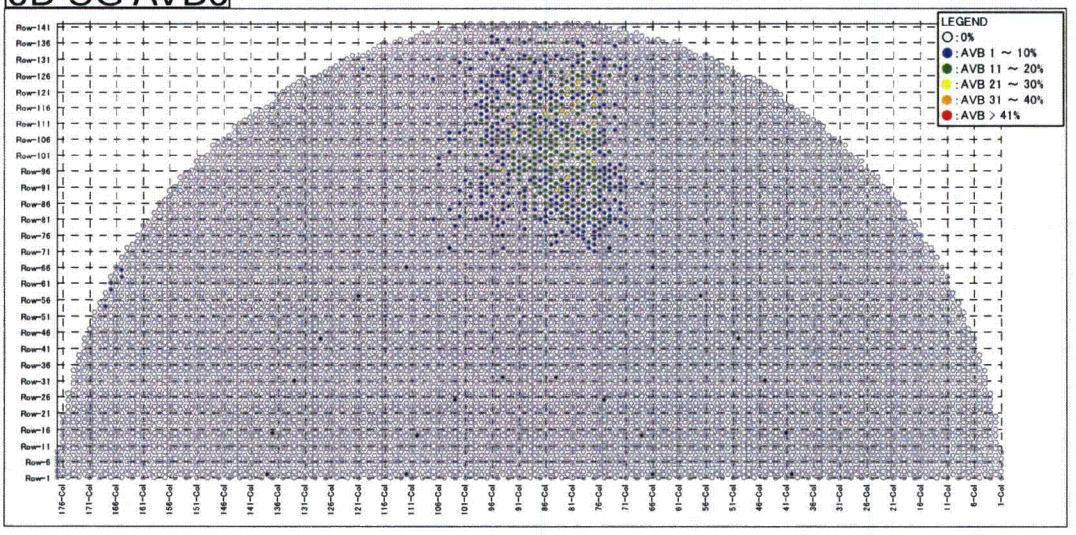

Fig 4.1.1-7 (2/4) Tubes with wear indication (at AVBs)

3B-SG AVB7

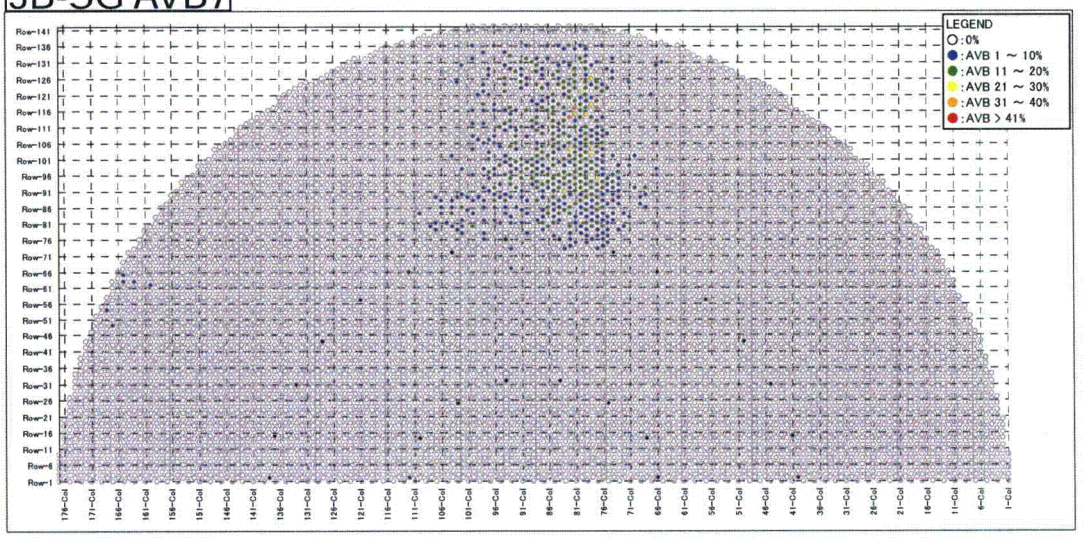

3B-SG AVB8

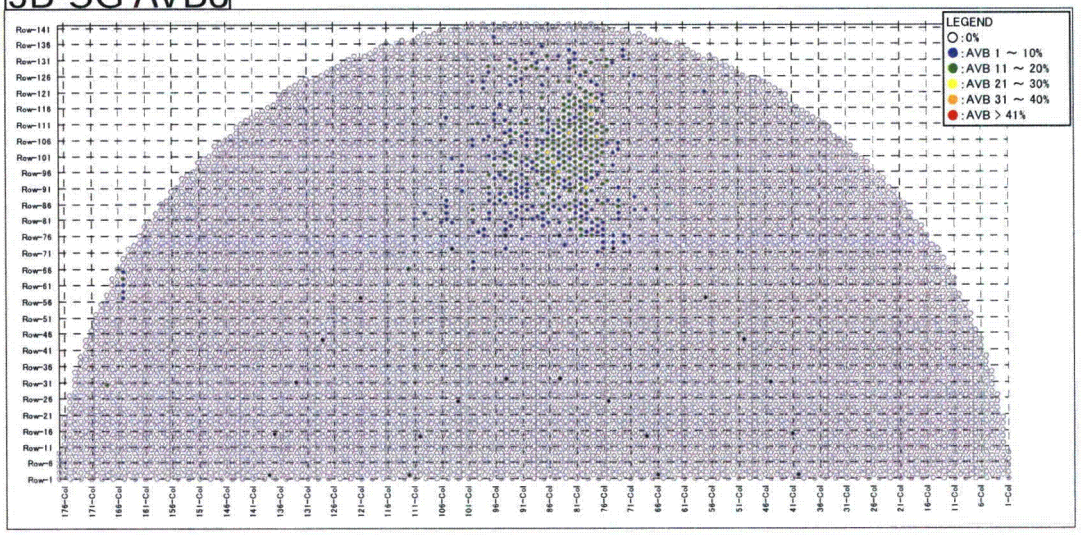

3B-SG AVB9

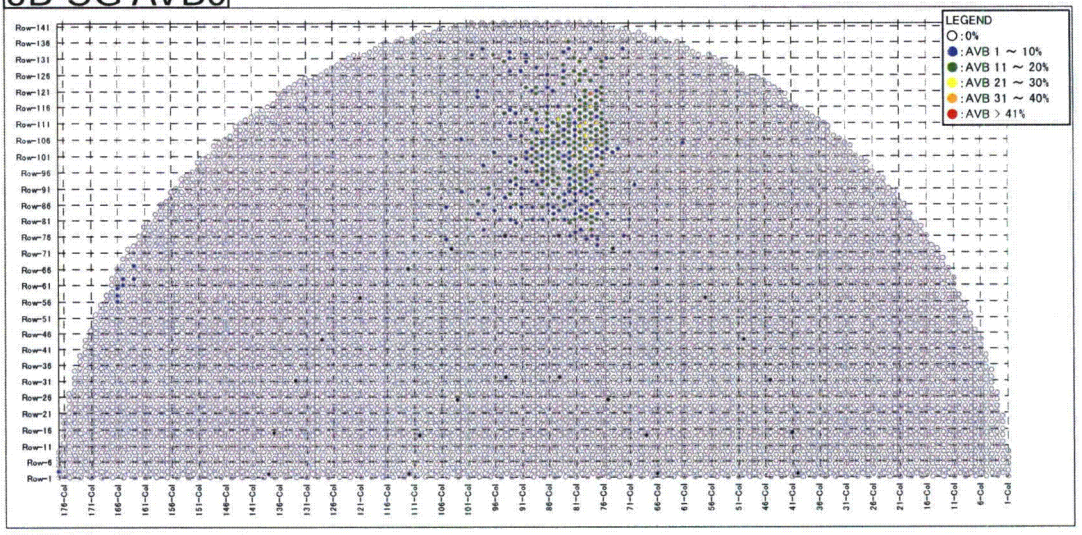

Fig 4.1.1-7 (3/4) Tubes with wear indication (at AVBs)

3B-SG AVB10

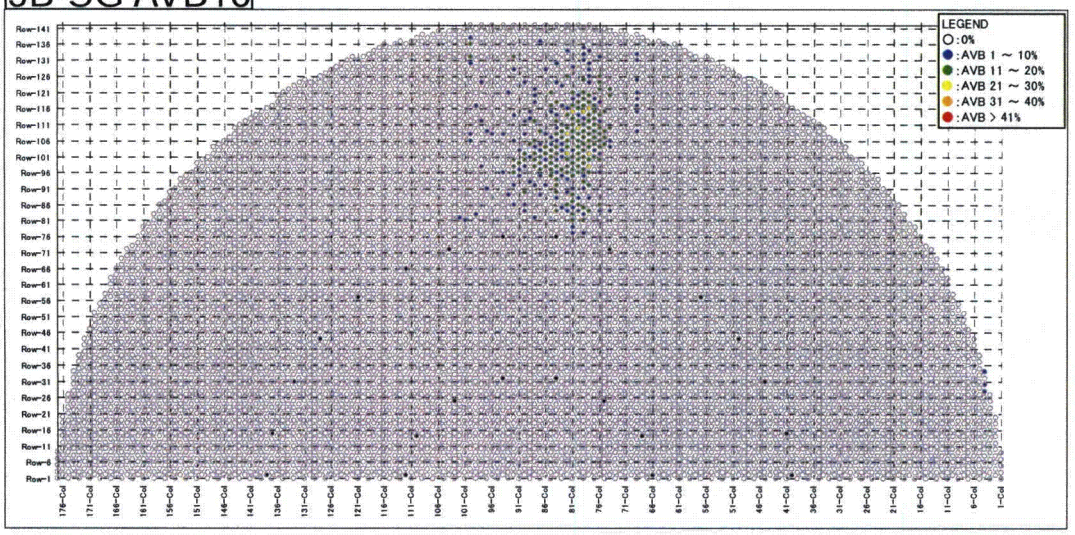

3B-SG AVB11

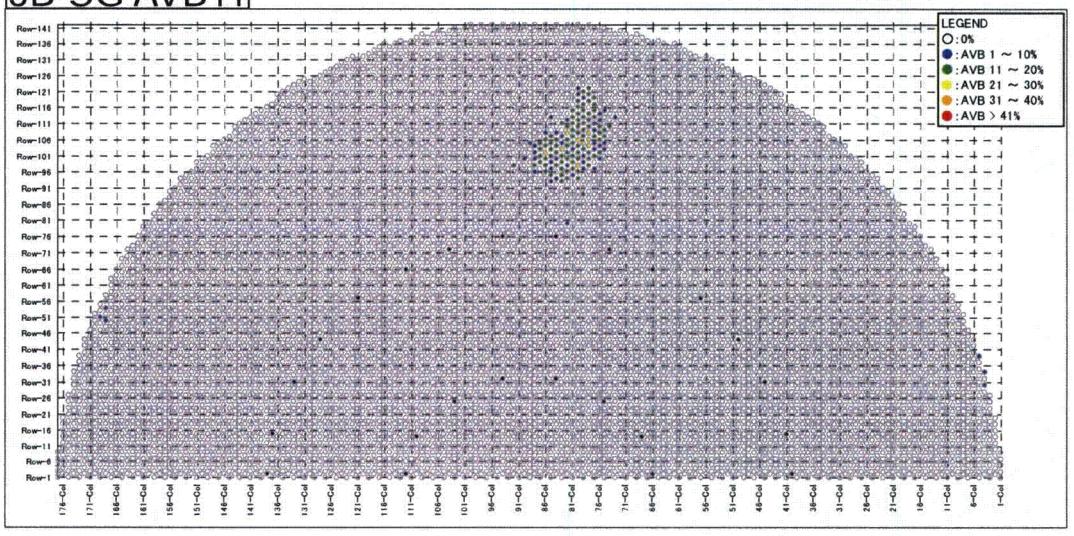

3B-SG AVB12

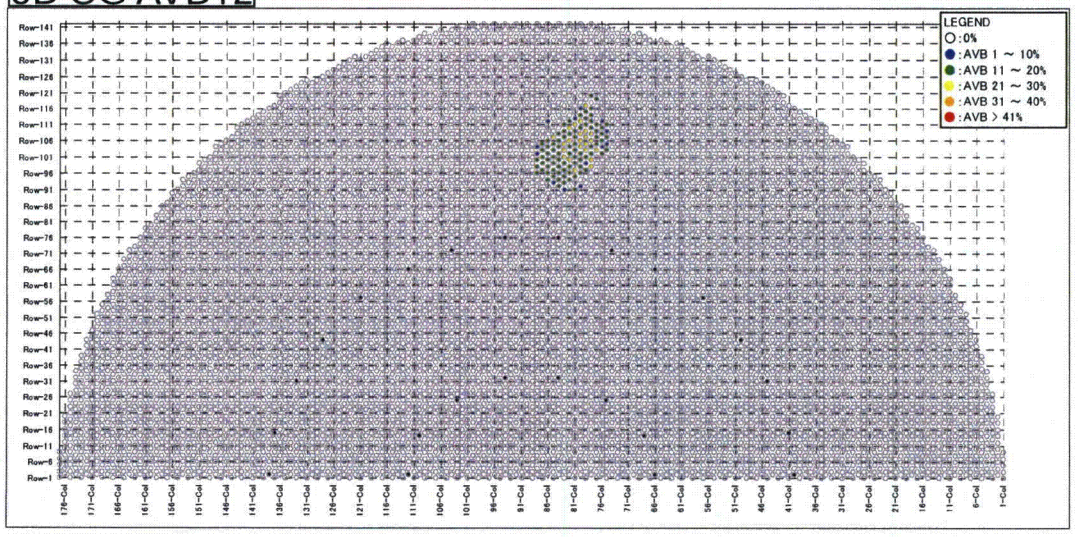

Fig 4.1.1-7 (4/4) Tubes with wear indication (at AVBs)

3B-SG #1TSP

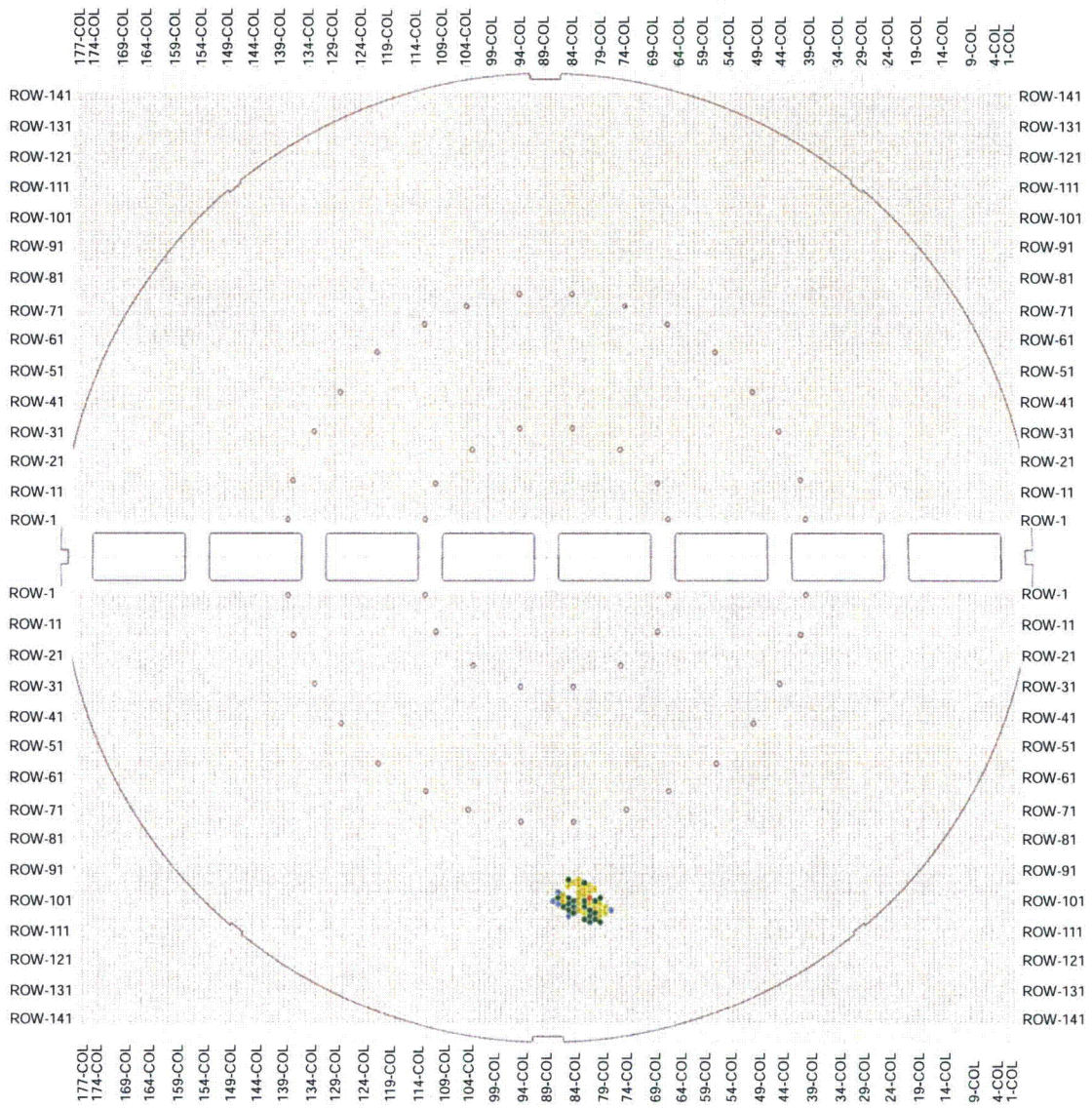

Fig 4.1.1-8 (1/7) Tubes with wear indications at TSPs

3B-SG #2TSP

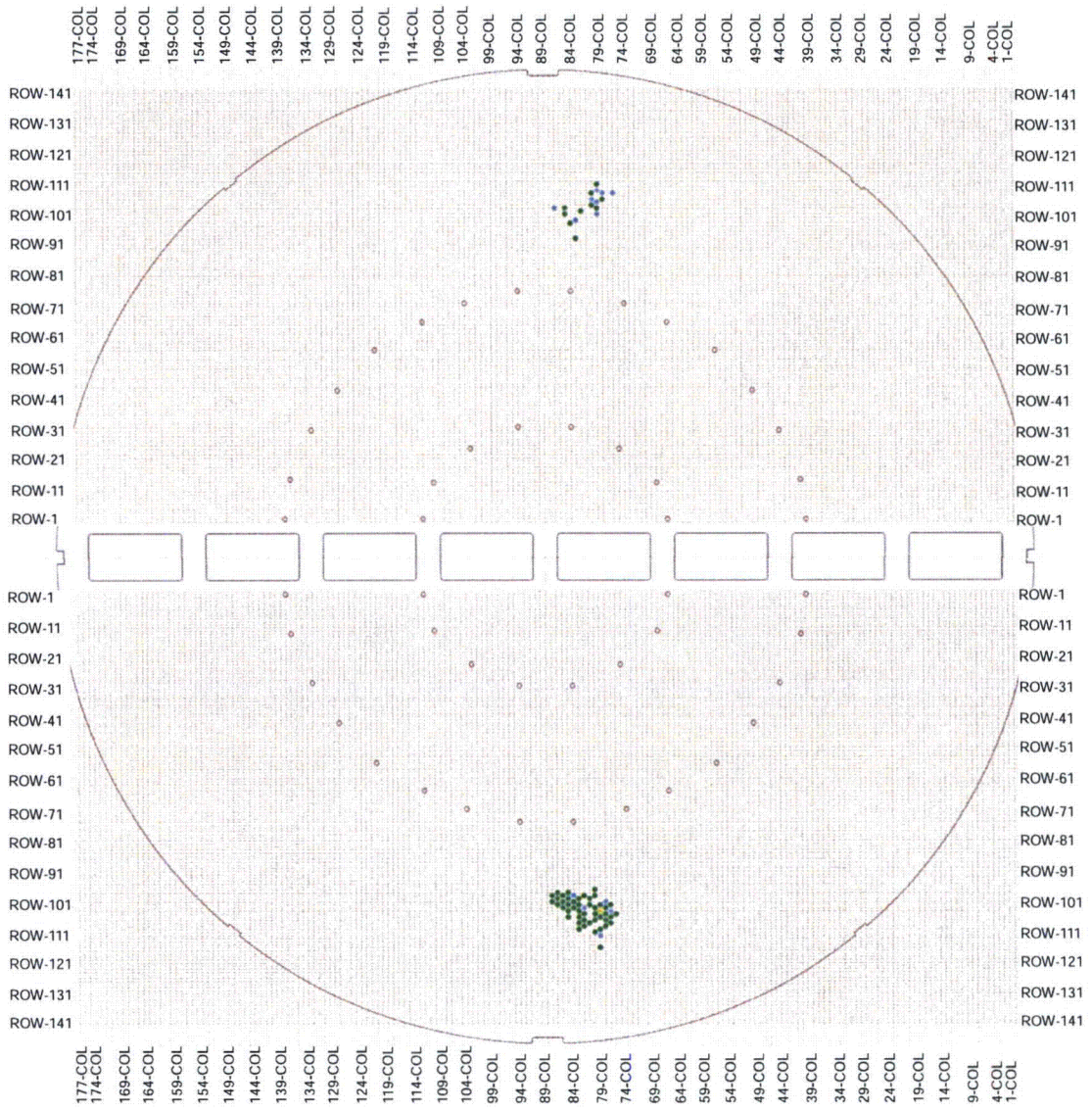

Fig 4.1.1-8 (2/7) Tubes with wear indications at TSPs

3B-SG #3TSP

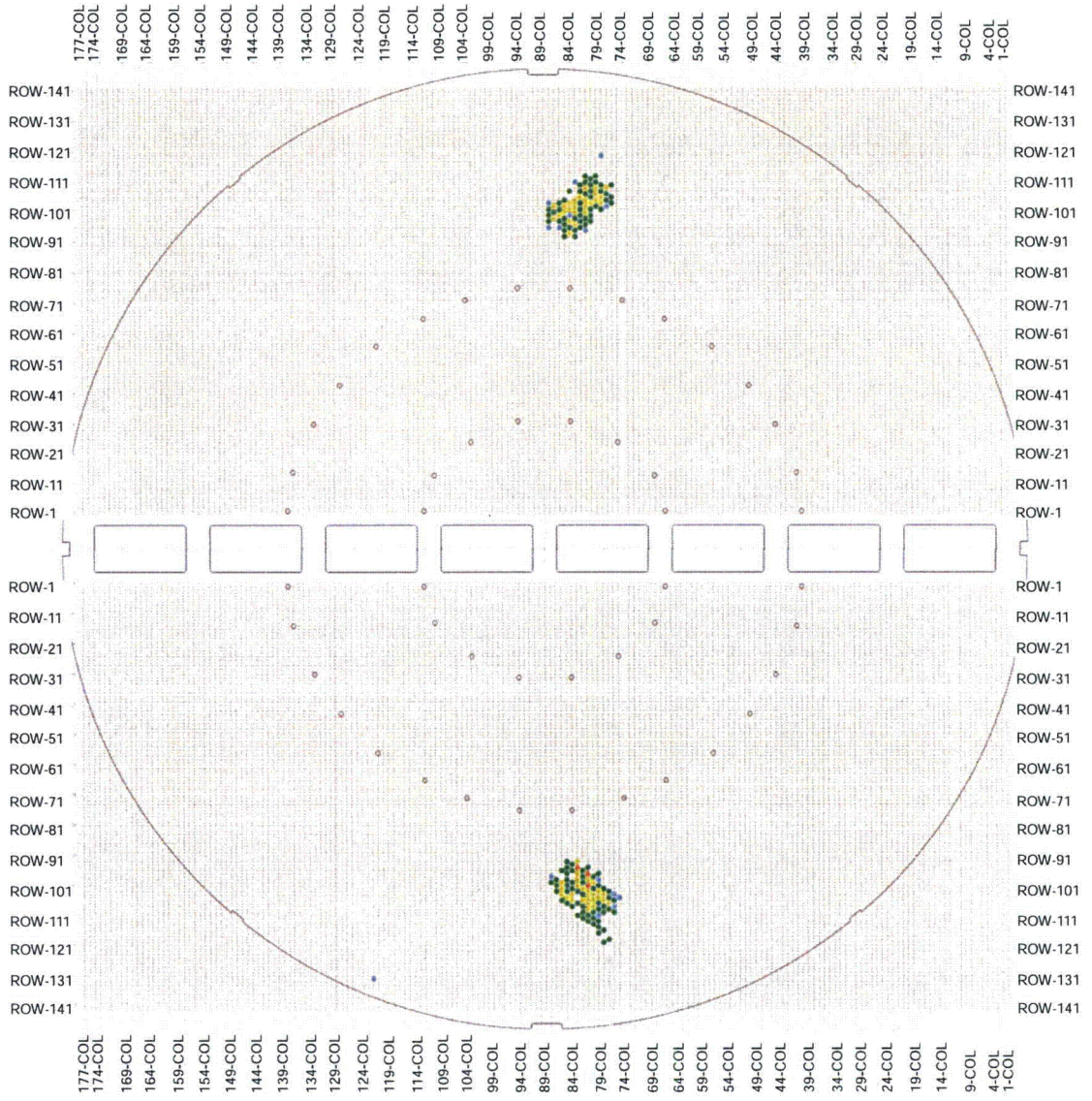

Fig 4.1.1-8 (3/7) Tubes with wear indications at TSPs

3B-SG #4TSP

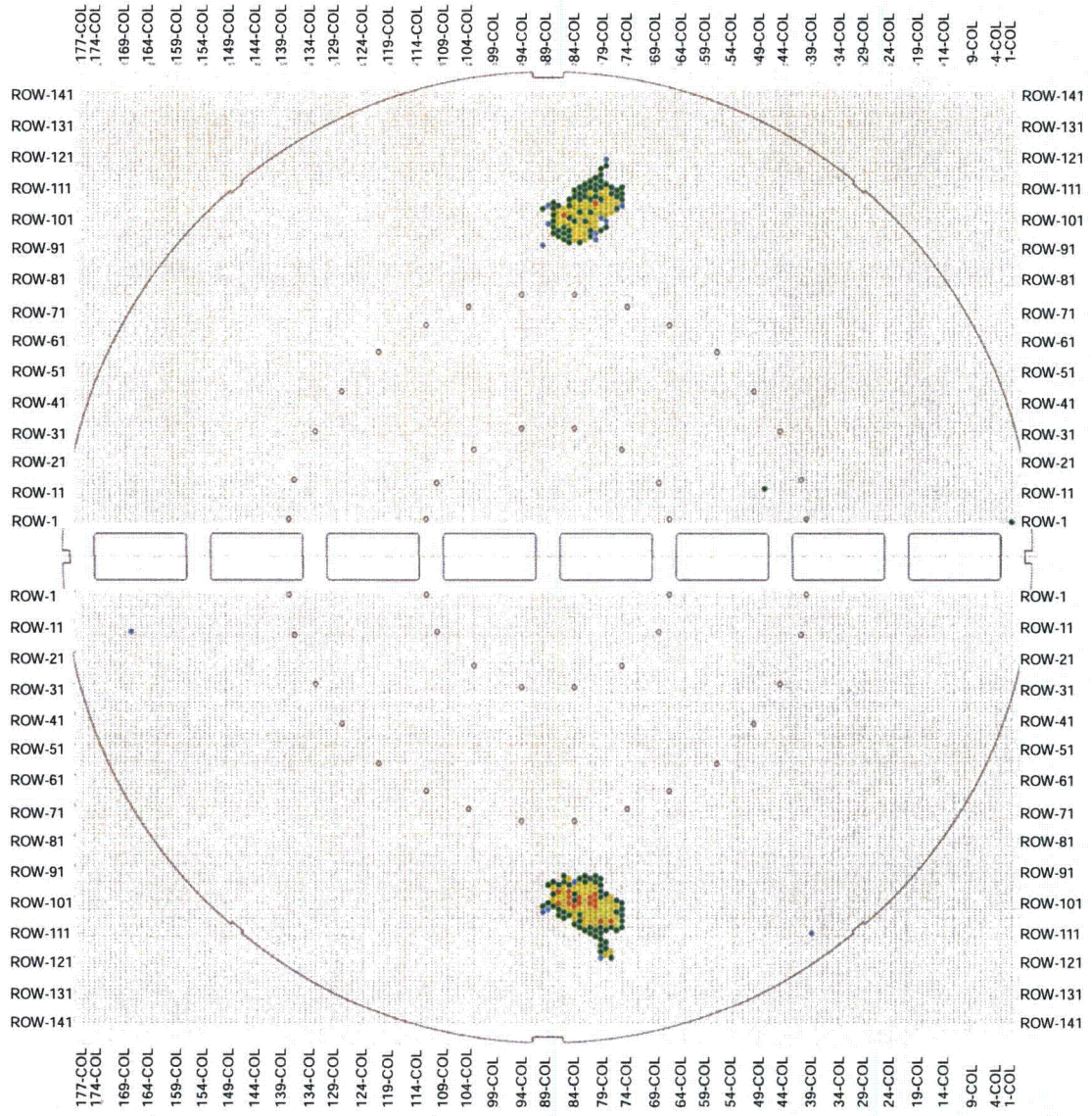

Fig 4.1.1-8 (4/7) Tubes with wear indications at TSPs

3B-SG #5TSP

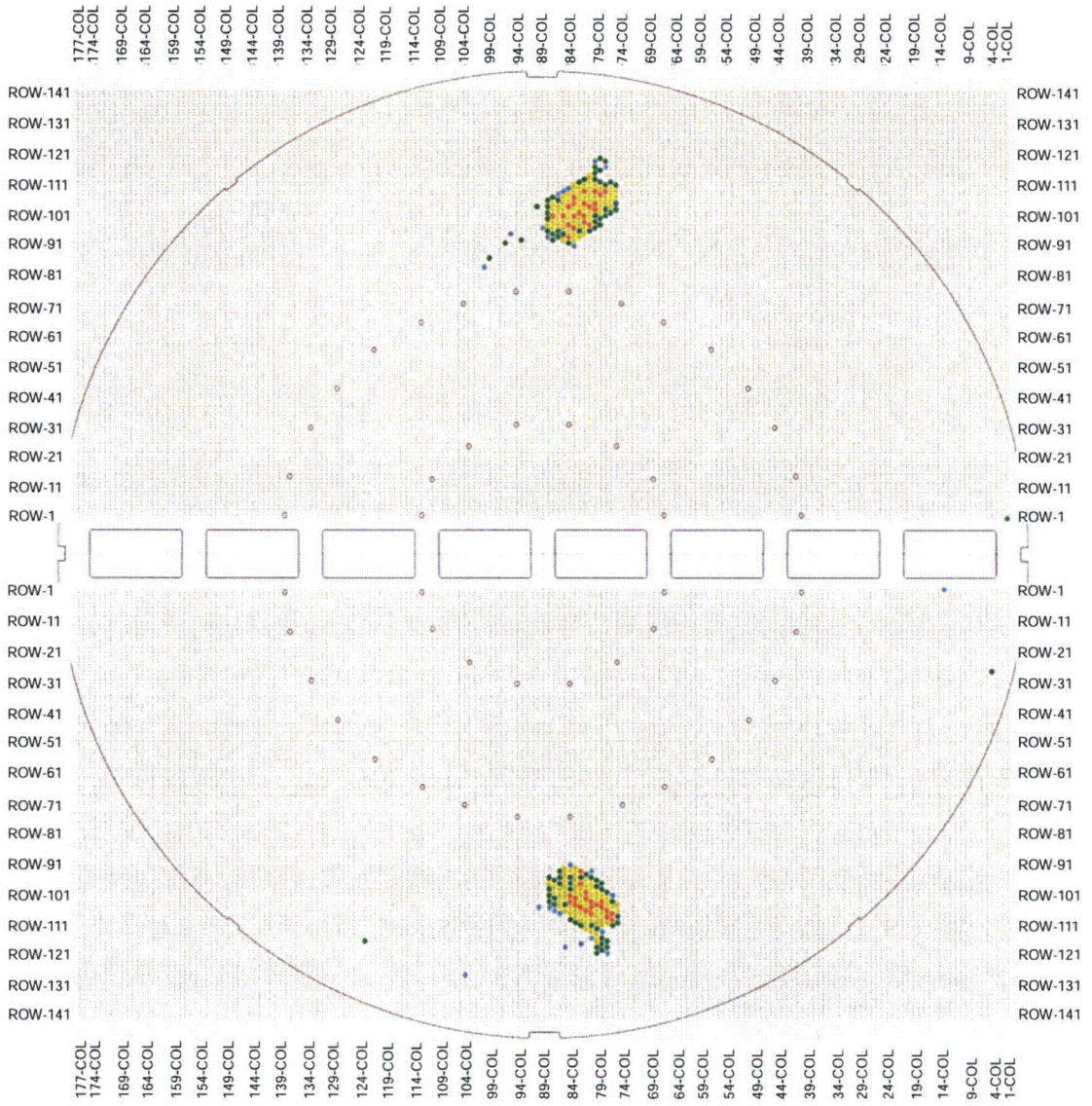

Fig 4.1.1-8 (5/7) Tubes with wear indications at TSPs

3B-SG #6TSP

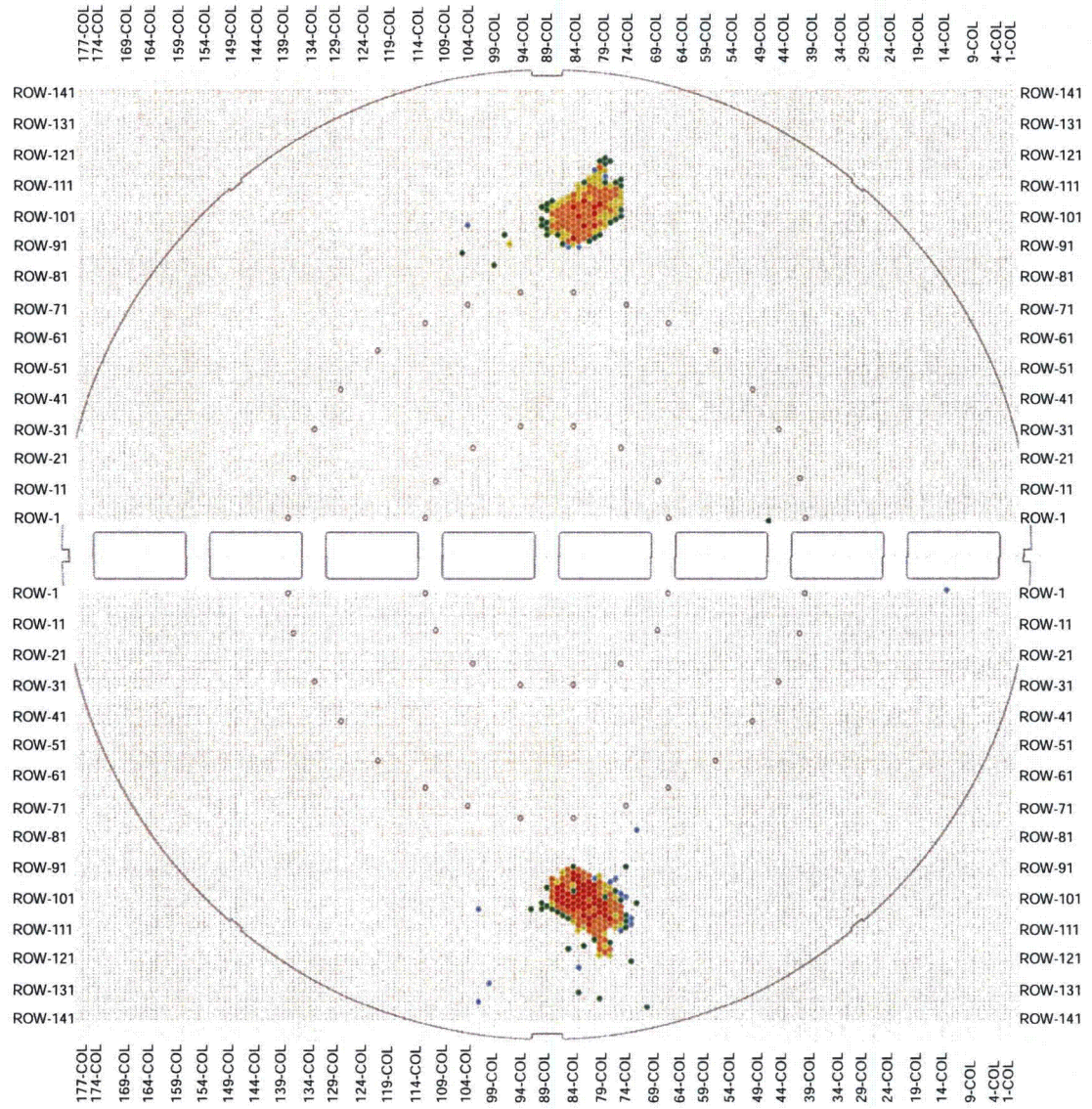

Fig 4.1.1-8 (6/7) Tubes with wear indications at TSPs

3B-SG #7TSP

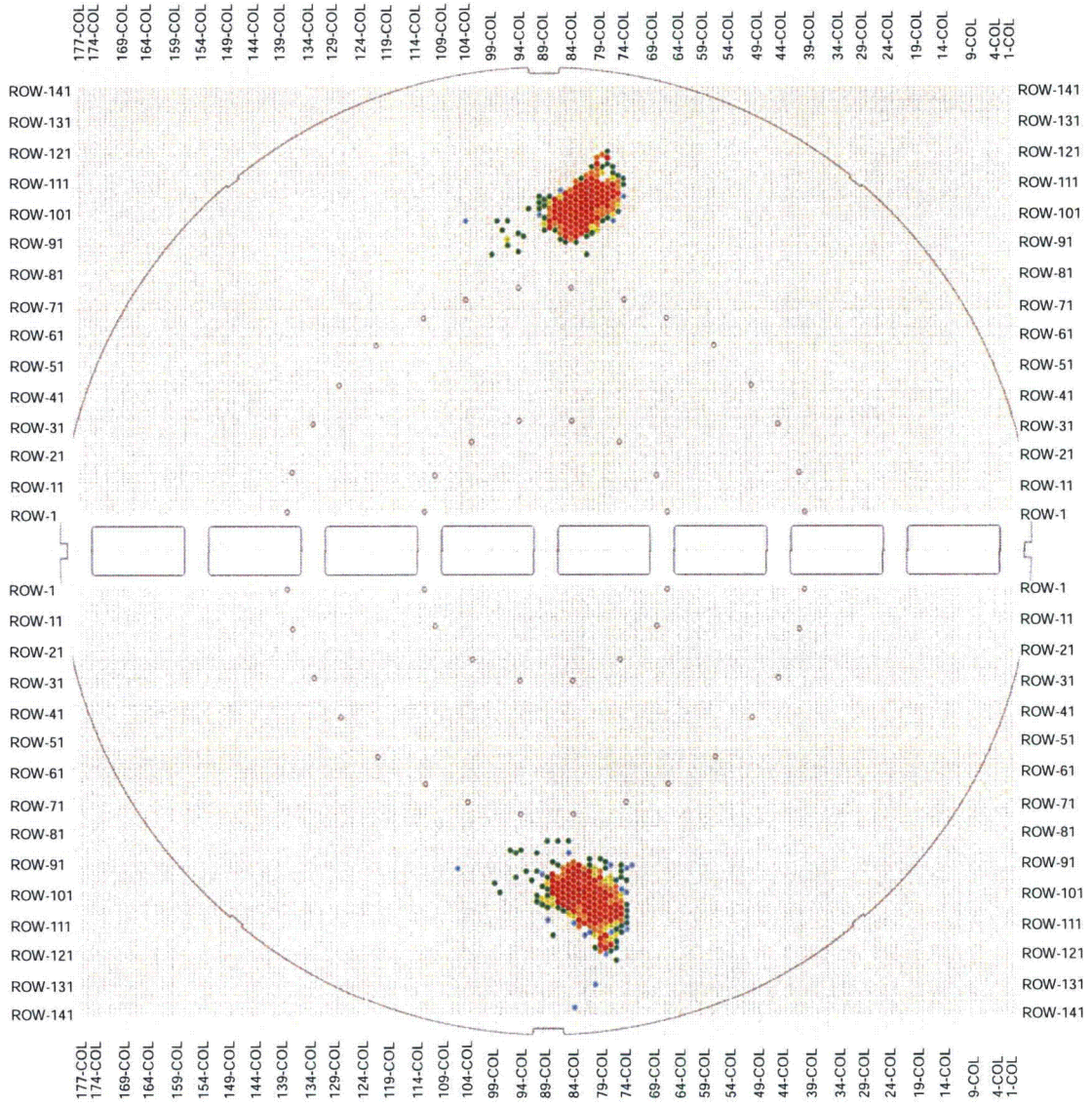

Fig 4.1.1-8 (7/7) Tubes with wear indications at TSPs

4.1.2. Tube Wear in Unit-2 (for reference only)

The tubes in Unit 2 have experienced wear at 4 locations, i.e. wear in the free span area, wear at the AVB bars, wear at the TSPs and wear at retainer bars, as well as wear due to a foreign object. Table 4.1.2-1 shows the number of tubes that have shown wear at these four different locations as well as foreign object wear and is provided by SCE (Reference 9 and 11).

Table 4.1.2-1 Number of Tubes with Wear in SONGS Unit-2

Wear Type	SG 2A (2E-089)	SG 2B (2E-088)	Total
Tube-to-Tube Wear	2	0	2*
AVB Wear	804	595	1399*
TSP Wear	119	180	299*
Retainer Bar Wear	4	2	6*
Foreign Object	0	2	2*
Total	861**	734**	1595**

Notes:

*) The total number of tubes with wear at a given location

**) The total number of tubes with wear at any location

9

For purposes of analysis in this report, MHI has categorized the tube wear into the four types of wear as defined in Section 4.1.1 (Types of Tube Wear). Table 4.1.2-2 shows the number of tubes in the Unit 2 RSGs that fall into each of these types of wear.

Table 4.1.2-2 Number of Tubes with Type of Wear in SONGS Unit-2

Wear Type	SG 2A (2E-089)	SG 2B (2E-088)	Total
Type 1 (TTW)	2	0	2
Type 2 (AVB wear)	802	595	1397
Type 3 (TSP wear)	53	137	190
Type 4 (RB wear)	4	2	6
Foreign Object	0	2	2
Total	861	736	1597

In this table each of the tubes is only counted once with priority given to Type 1 followed by Type 2, Type-3, Type 4 and Foreign Object. The data in this table is based on the ECT data evaluations described in Appendix-3 of Reference 8 which includes both bobbin ECT and rotated ECT data. The total number of tubes differs from that in table 4.1.2-1 because, as explained in Appendix 3, Reference 8, the data in Table 4.1.2-1 for wear at AVBs and TSPs is based solely on bobbin ECT data. △9

4.1.3. Tube Wear in Unit-3

The number of tubes for each type of tube wear in Unit-3 is listed in Table.4.1.3-1.

The tubes in Unit 3 have experienced wear at 4 locations, i.e. wear in the free span area, wear at the AVB bars, wear at the TSPs and wear at retainer bars. Table 4.1.3-1 shows the number of tubes that have shown wear at these four different locations and is provided by SCE (Reference 9 and 11).

Table.4.1.3-1 Numbers of Tubes with Wear in SONGS Unit-3

Wear Type	SG 3A (3E-089)	SG 3B (3E-088)	Total
Tube-to-Tube Wear	165	161	326*
AVB Wear	871	896	1767*
TSP Wear	214	250	464*
Retainer Bar Wear	1	3	4*
Total	887**	919**	1806**

Notes:

*) The total number of tubes with wear at a given location

**) The total number of tubes with wear at any location

For purposes of analysis in this report, MHI has categorized the tube wear into the four types of wear as defined in Section 4.1.1 (Types of Tube Wear). Table 4.1.3-2 shows the number of tubes in the Unit 3 RSGs that fall into each of these types of wear. 9

Table 4.1.3-2 Number of Tubes with Type of Wear in SONGS Unit-3

Wear Type	SG 3A (3E-089)	SG3B (3E-088)	Total
Type 1 (TTW)	165	161	326
Type 2 (AVB wear)	714	737	1451
Type 3 (TSP wear)	15	20	35
Type 4 (RB wear)	1	3	4
Total	895	921	1816

In this table each of the tubes is only counted once with priority given to Type 1 followed by Type 2, Type-3, and Type 4. This data in this table is based on the ECT data evaluations

described in Appendix-3 of Reference 8 which includes both bobbin ECT and rotated ECT data. The total number of tubes differs from that in Table 4.1.3-1 because as explained in Appendix 3, Reference 8 the data in Table 4.1.3-1 for wear at AVBs and TSPs is based solely on bobbin ECT data. △9

4.2 Visual Inspection Results of the Tube Bundle

Based on the visual inspection performed along AVBs No.B04 and B09, the following observations were made (see to Appendix-7 for details).

4.2.1. Observations Common to Unit-2 and Unit-3

The AVBs, end caps, and retainer bars were manufactured according to the design. It was confirmed that there were no significant gaps between the AVBs and tubes which might have contributed to excessive tube vibration because the AVBs appear to be virtually in contact with tubes as shown in Fig.4.2-1, Fg.4.2-2 and Fig.4.2-3. ECT wear indications are identified as the Type 1 and Type 2 wear. △9

4.2.2. Observations in Unit-3

Pattern 1 wear indicating high amplitude in-plane motion of the tube, as shown in Fig 4.2-2, was seen on the tubes with Type 1 wear. Pattern 2 wear, as shown in Fig 4.2-3, was seen on the tubes with the Type 2 wear.

4.2.3. Observations in Unit-2

Pattern 2 wear seen in Unit-3 was also seen on the tubes with the Type 2 wear tubes.

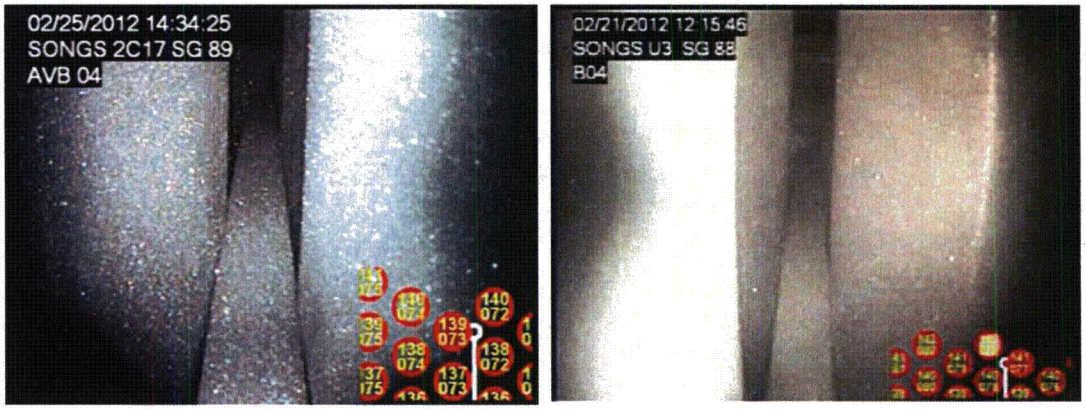

Sample from SG-2A **Sample from SG-3B**

Fig.4.2-1 Condition of Tube Wear in SONGS Unit-2 and Unit-3

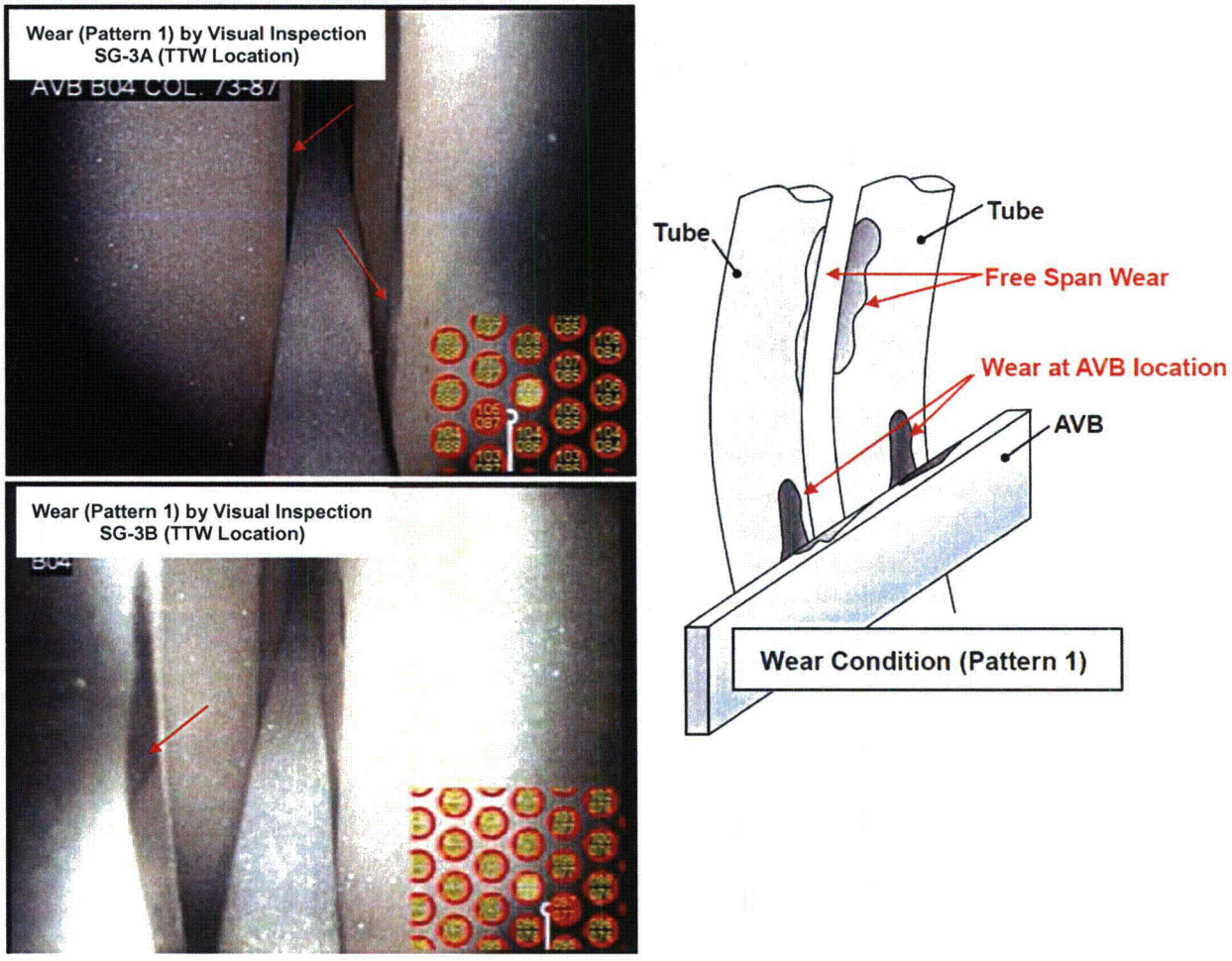

Fig.4.2-2 Illustration of Tube Wear Pattern 1

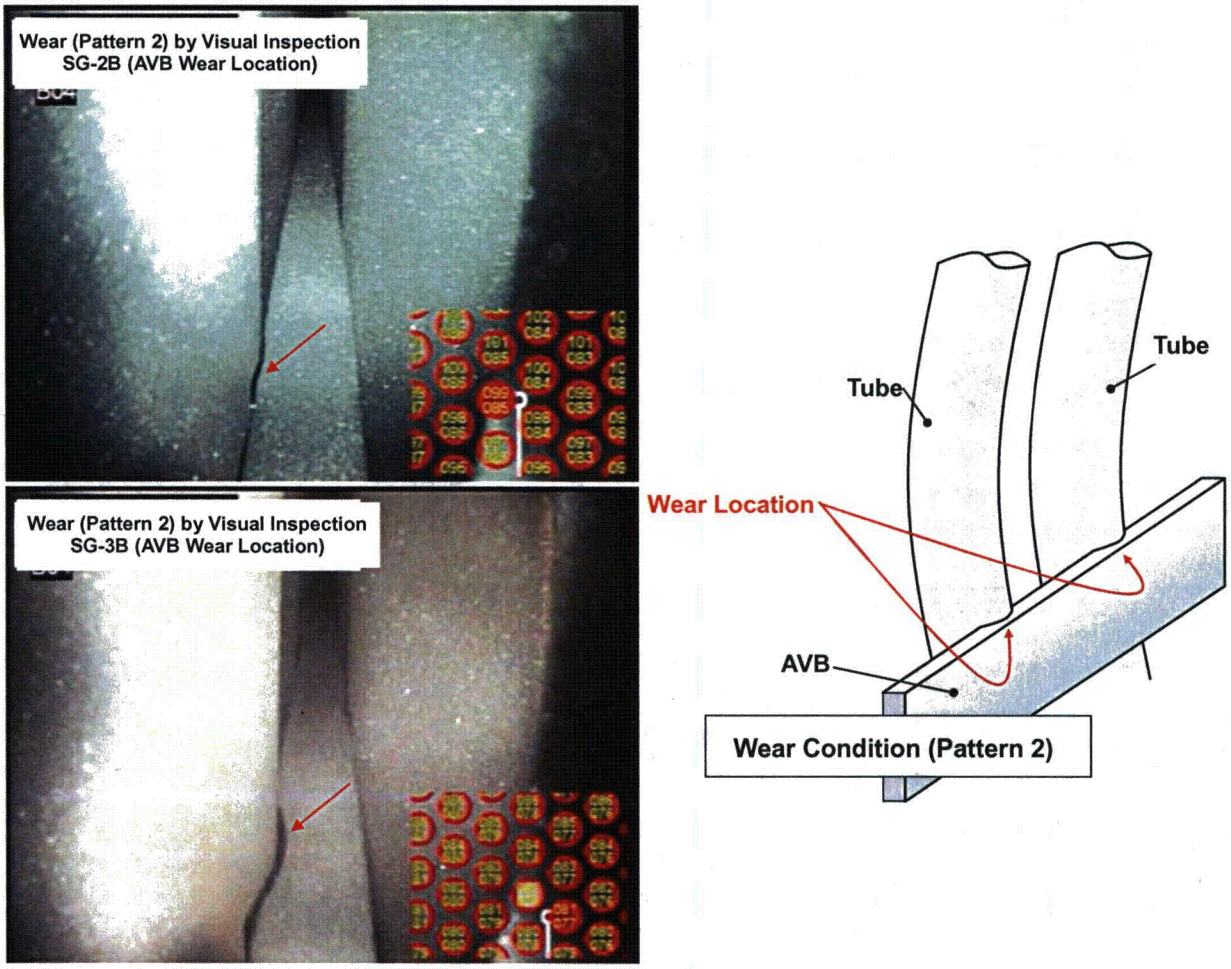

Fig.4.2-3 Illustration of Tube Wear Pattern 2

5. Mechanistic Cause Analysis

The cause of the first 3 types of tube wear (i.e. TTW, AVB wear, TSP wear) is excessive tube vibration. Generally, the causes of tube excessive vibration are the thermal-hydraulic operating conditions of the SG secondary side and lack of sufficient in-plane tube support for the tubes (condition of the tube supports in terms of their effectiveness; active versus inactive tube supports).The cause of the Type 4 tube wear (RB wear) is vibration of the retainer bar itself which is described in Section 6.

5.1 Thermal Hydraulic Condition in the Secondary Side

In general, structures in a two-phase flow field have lower resistance to vibration when a void fraction (percentage of vapor volume in a saturated mixture) or steam quality (percentage of vapor mass in a saturated mixture) is high. The high void fraction (steam quality) results in the two-phase fluid having a low density, which in turn results in an increase of the flow velocity of the two-phase fluid, and in a low damping factor. The increase of the flow velocity (v) causes the increase of the hydrodynamic pressure (ρv^2) which causes structures to vibrate in the flow field. The hydrodynamic pressure is a measure of energy imparted on the structure by the flow field, and damping is a measure of how easily the structure can dissipate this energy. If the amount of energy imparted on the structure is higher than the amount of energy dissipated, the structure (in this case the tubes) will vibrate with progressively increasing amplitudes, which eventually may lead to the tubes becoming fluid-elastic unstable. Also, the unstable tubes will excite the surrounding tubes via two-way coupling with the fluid. Therefore, it is more likely for the tubes to vibrate when the void fraction (steam quality) is high.

Fig.5.1-1 shows the results of the three-dimensional thermal hydraulic analysis of SONGS Unit-2 and 3 SGs (see Reference 5 for detail). This analysis was performed recently using the ATHOS computer code developed by EPRI. As can be seen from the void fraction profile, the highest void fraction is estimated to be [ ](and the steam quality is[ ]), which is high compared to the [ ]void fraction (when steam quality is less than[ ]) for the other SGs designed by MHI based on ATHOS computer code. The higher than typical void fraction is a result of a very large and tightly packed tube bundle, particularly in the U-bend, with high heat flux in the hot leg side. Because this high void fraction is a potentially major cause of the tube FEI, and consequently unexpected tube wear (as it affects both the flow velocity and the damping factors), the correlation between the void fraction (steam quality) and the number of tubes with wear in a given void fraction region was investigated. From this investigation, a strong correlation between the void fraction (steam quality) and the percentage of tubes with the Type 1 and Type 2 wear was identified (see Fig.5.1-2 and Fig.5.1-4). The correlation

△9

△9

between flow velocity and the number of tubes with wear was also investigated. The results show that when the flow velocity is high, the percentage of tubes with wear increases, even though this correlation is not as strong as that between the void fraction (steam quality) and the percentage of tubes with wear (see Fig.5.1-3 and Fig.5.1-5).

Consequently, it is concluded that the thermal-hydraulic conditions in the SG secondary side, namely high void fraction (steam quality) and high flow velocity along with lack of sufficient in-plane tube support, are the main causes of the excessive tube vibration and unexpected wear in the SONGS Unit 2 and Unit 3 RSGs.

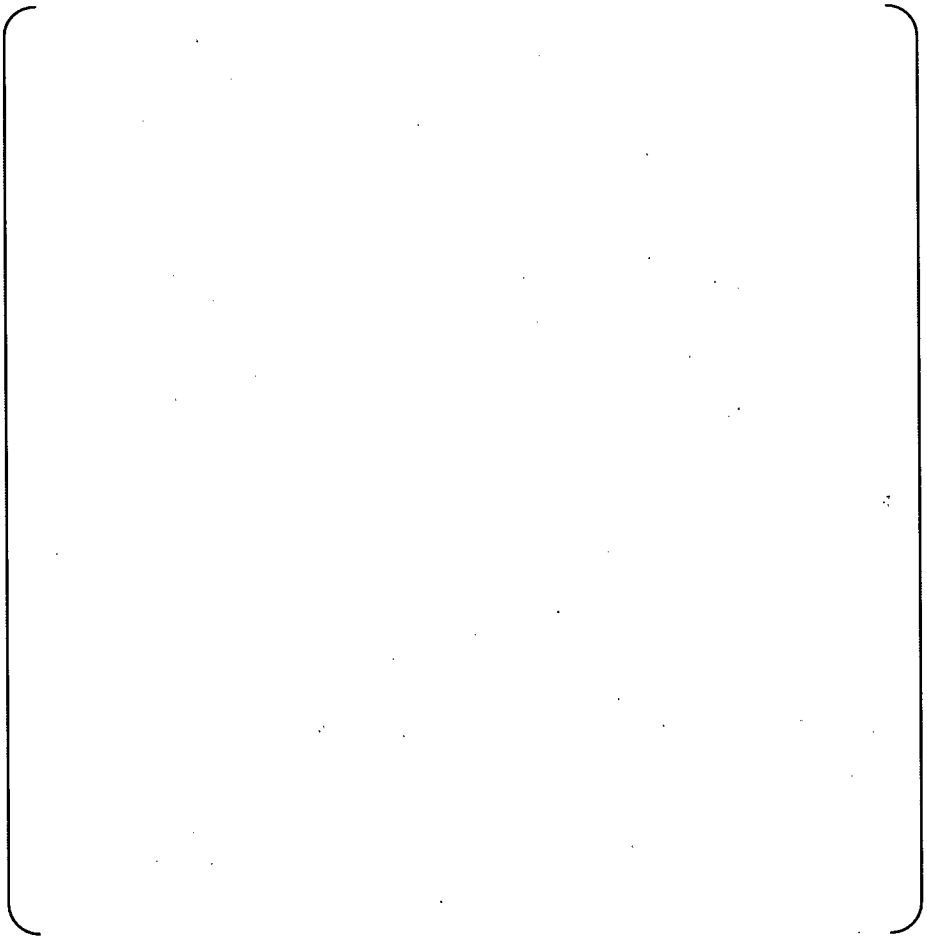

Fig.5.1-1 Thermal Hydraulic Analysis for the Unit-2 and Unit-3 SGs

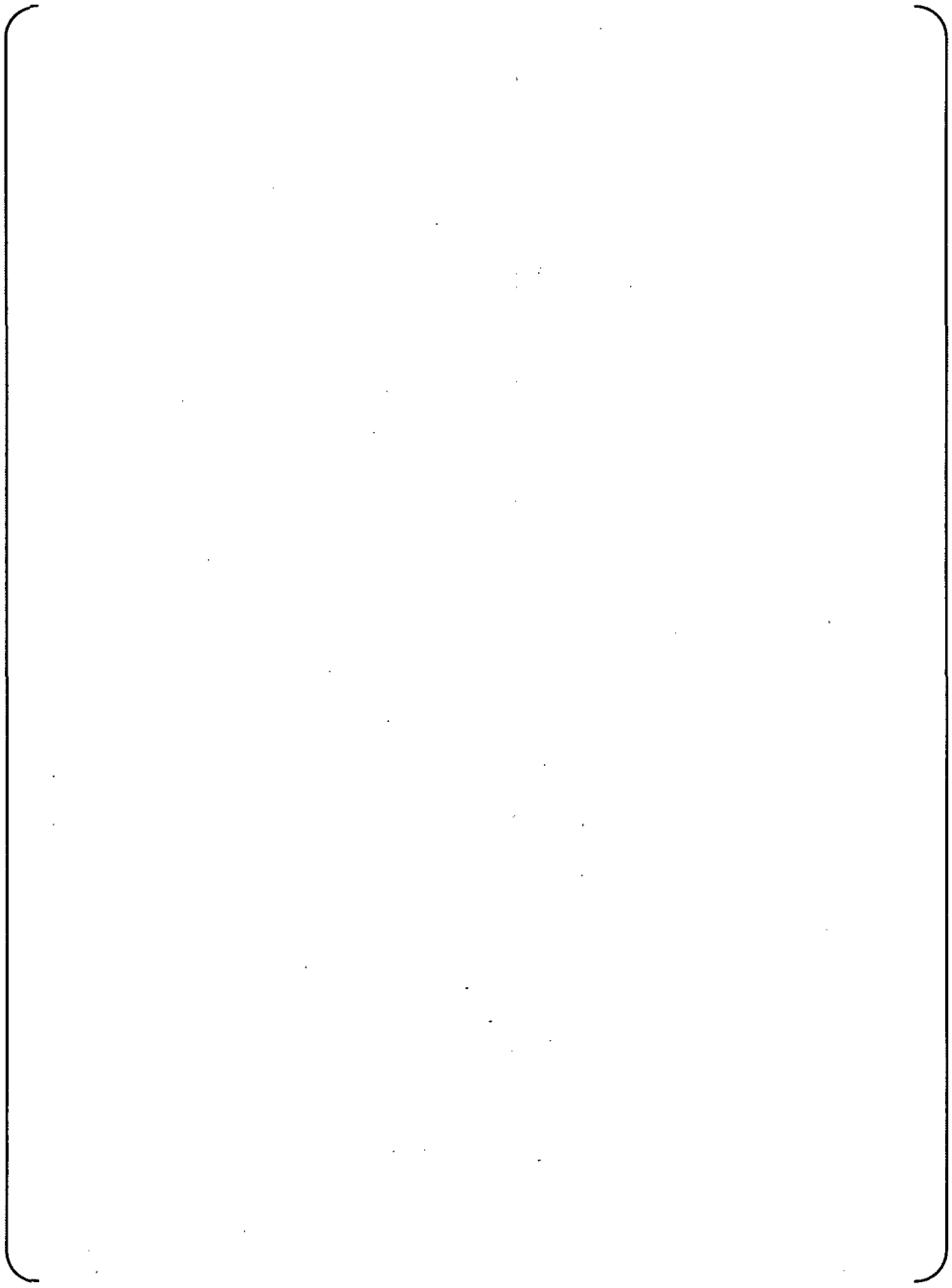

Fig.5.1-2 Correlation between Type 1 Wear (TTW) and Void Fraction (Steam Quality)

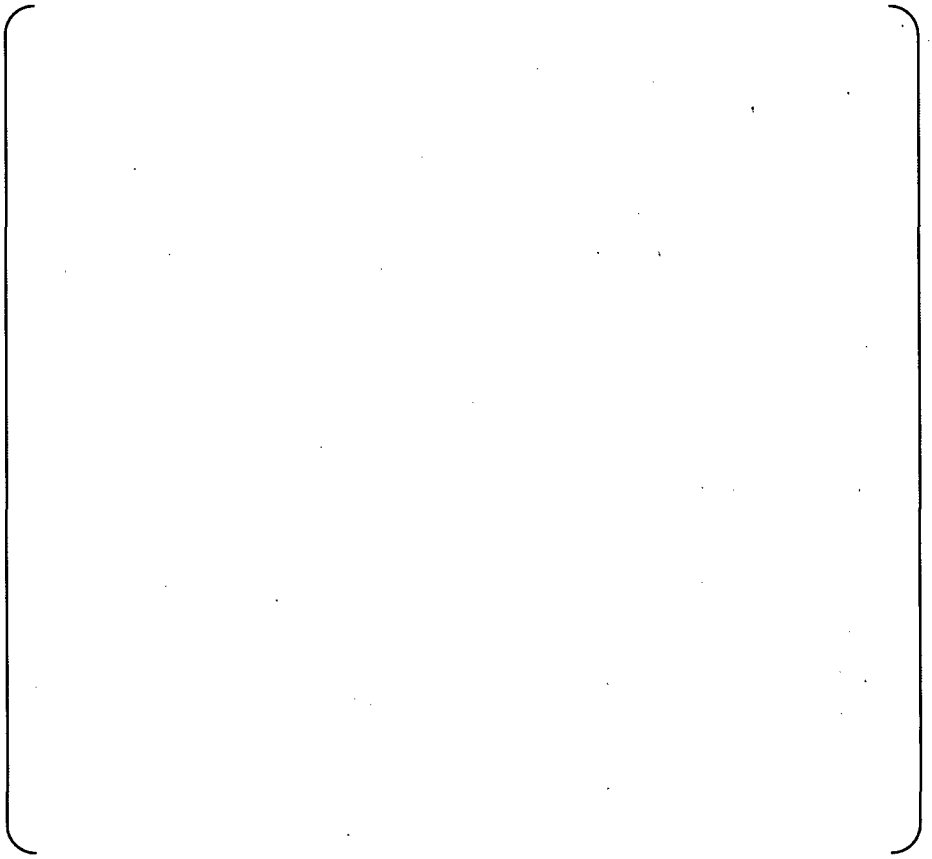

Fig.5.1-3 Correlation between Type 1 Wear (TTW) and Flow Velocity

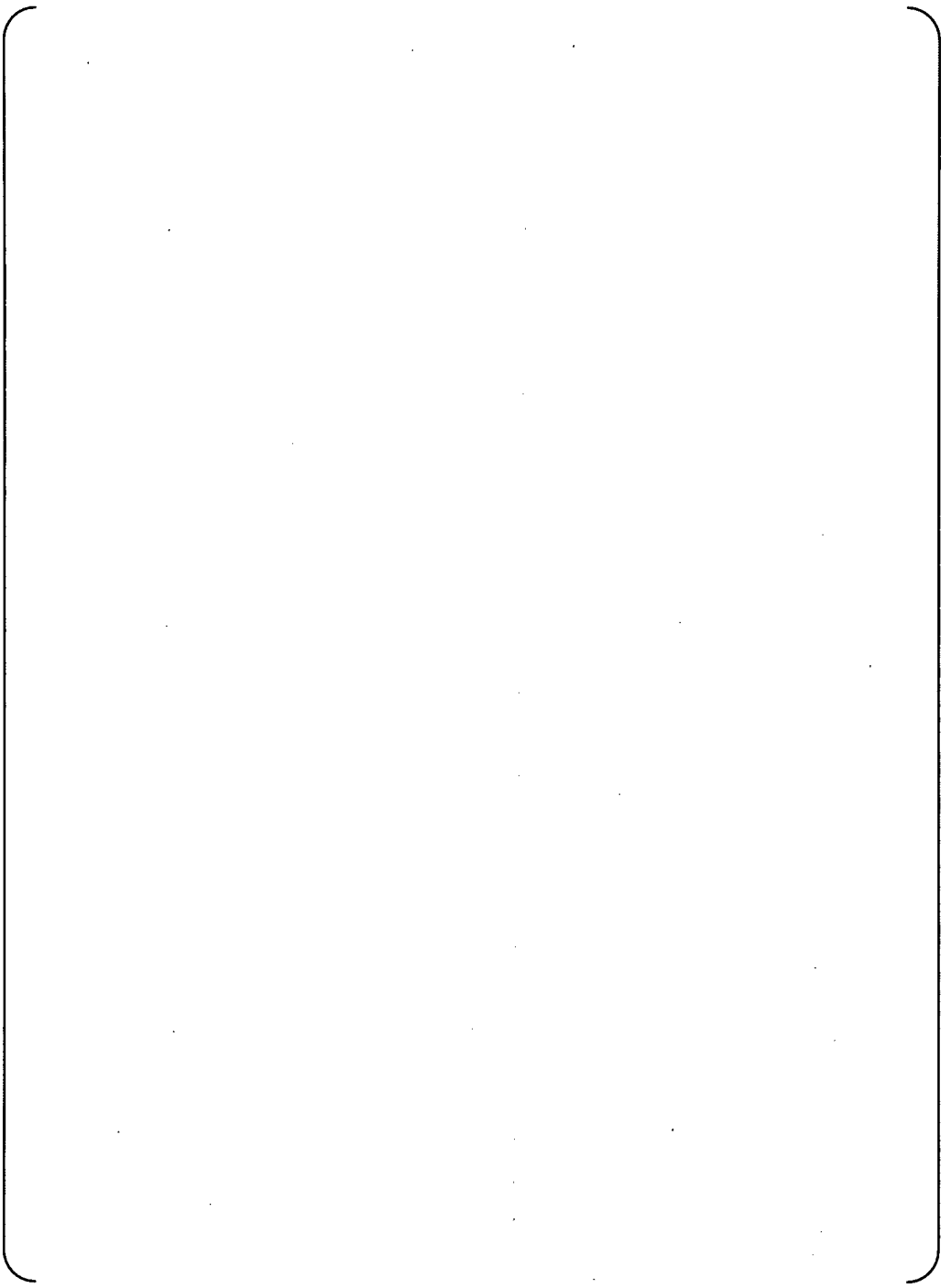

Fig.5.1-4 Correlation between Type 2 Wear (AVB wear) and Void Fraction (Steam Quality)

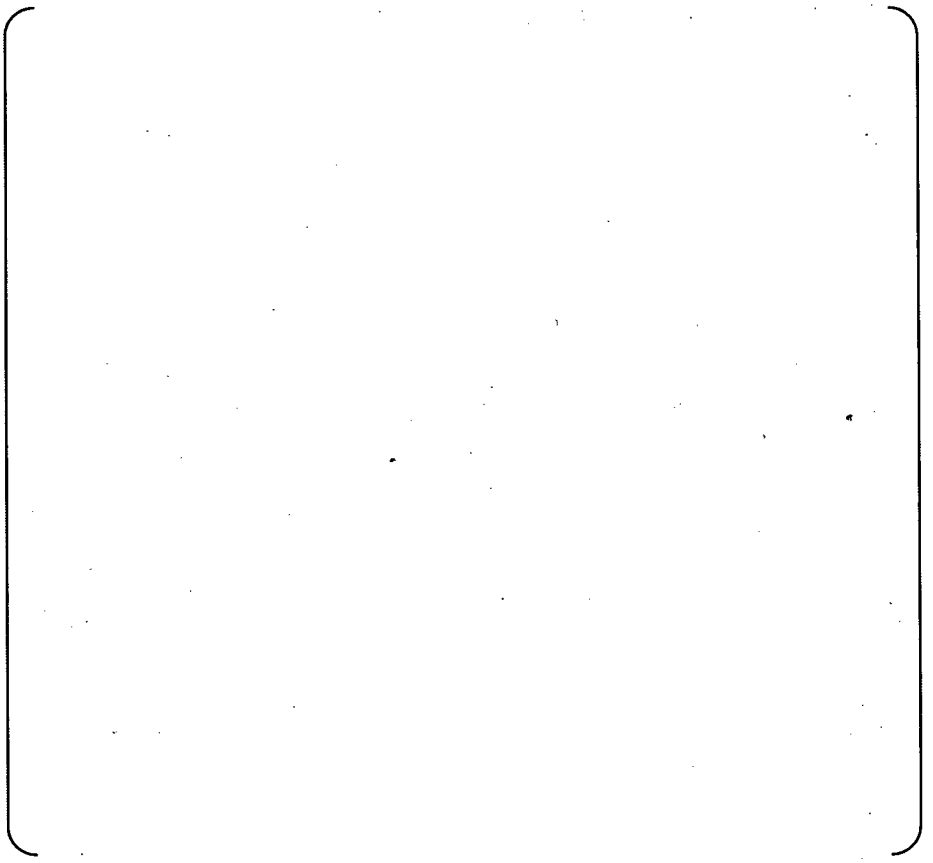

Fig.5.1-5 Correlation between Type 2 Wear (AVB Wear) and Flow Velocity

5.2 Evaluation of U-bend Supports Condition

5.2.1. Out-of-Plane Direction Support

The SONGS SG tube bundles were designed for out-of-plane U-bend support only with "zero" gaps in the hot condition. Based on visual inspections, the tube-to-AVB gaps in cold condition were as could be expected, i.e., most likely meeting the design premise of "zero gap" in the hot condition.

The recent tube bundle deformation analysis (refer to Appenidx-8), which takes into account the tube and AVB dimensional fabrication tolerance dispersion, indicates that the contact forces between the tubes and AVBs produce the friction forces which prevent the distortion of the AVB structure assembly and the dynamic pressure during operation does not increase the tube-to-AVB gaps (see Fig.5.7-3 and Fig.5.7-4 of Appendix-8 for details).

Therefore, MHI has concluded that U-bend support in the out-of-plane direction is adequate.

5.2.2. In-Plane Direction Support

By design, U-bend support in the in-plane direction was not provided for the SONGS SGs. In the design stage, MHI considered that the tube U-bend support in the out-of-plane direction designed for "zero" tube-to-AVB gap in hot condition was sufficient to prevent the tube from becoming fluid-elastic unstable during operation based on the MHI experiences and contemporary practice as described in Section 2.2.

Secondary side thermal-hydraulic conditions in the SONGS SGs during operation appear to be such that the effective fluid flow velocities are higher than the critical velocities in the U-bend in-plane direction for several tubes in a particular region of the tube bundle where the void fraction is very high as described in Section 5.1.

MHI concludes that under the secondary thermal-hydraulic conditions such as in the SONGS SGs, certain tube-to-AVB minimum contact force is required to prevent tubes from vibrating in the in-plane direction and eventually becoming fluid-elastic unstable. Furthermore, MHI concludes that the tube and AVB fabrication dimensional tolerance dispersion results in contact forces between the tubes and AVBs, however, these forces are not sufficient to provide friction forces ample to prevent in-plane motion of the tubes (See reference 10 for details).

5.2.3. Differences between Unit-2 and Unit-3

According to the manufacturing dimensional tolerance analysis (refer to Appendix-4 and Appendix-9 for details), the average contact force in the Unit-3 SGs was found to be smaller than the average contact force in the Unit-2 SGs. Consequently, the contact forces caused by the manufacturing dimensional variations in the Unit-2 SGs are more than two times larger than in the Unit-3 SGs, which is consistent with the tolerance analysis results shown in Fig. 5.2.1.Therefore, it is concluded that the contact forces of Unit-3 were more likely to be insufficient to prevent the in-plane motion of tubes and the Unit-3 SGs were more susceptible to in-plane tube vibration. 9 9

The difference in the contact forces between the Unit-2 and Unit-3 SGs was caused by the manufacturing dimensional tolerance variations, mainly due to improvement of AVB dimensional control. For the Unit-3 AVBs, a[ ]pressing force was used for the AVB nose portion after bending in order to control the twist and flatness of the AVB more precisely, while [ ] pressing force was used for the Unit-2 AVBs. Because the manufacturing dimensional variations of the Unit-2 SGs are larger than those of the Unit-3 SGs (AVB twist at AVB nose portion of Unit-2 is larger than that of Unit-3), the tube-to-AVB contact forces of the Unit-2 SGs are greater than those in the Unit-3 SGs, especially at the AVB nose locations, which is evidenced by more ding signals in the Unit-2 SGs than in the Unit-3 SGs. 9 9

A comparison of the Unit-2 and Unit-3 materials, fabrication processes and inspections that might have had an impact on the condition of the U-bend supports is summarized in Table 5.2-1 (refer to Appendix-4 for details) and the evaluations for the factors other than the difference in the AVB pressing forces are summarized below.

(i) Number of Rotations due to Divider Plate Repair

The Unit-3 SGs underwent[ ]more rotations than the Unit-2 SGs due to the divider plate repair. However, the change in the tube support condition between the Unit-3 and Unit-2 SGs due to the difference in number of rotations was found to be negligibly small (refer to Appendix-5 for details).

(ii) Number of Hydrostatic Tests

Primary side hydrostatic tests were performed three times for the 3A SG and two times for the 3B SG, compared to only one time for both 2A and 2B SGs. However, the change in the tube support condition between the Unit-3 and Unit-2 SGs due to the number of hydrostatic tests was found to be negligibly small (refer to Appendix-5 and 14 for details).

(iii) Dimensional Control of Tubes and AVBs

The standard deviation of the AVB thickness, the tube outer diameter (G-value), and the number of adjustments to the tube bending radius was smaller in the Unit-3 SGs than in the Unit-2 SGs. Furthermore, the gaps between the outermost tubes and the AVBs are more uniform in the Unit-3 SGs than in the Unit-2 SGs. These findings indicate that the tube and AVB dimensions of the Unit-3 SGs are more uniform, and hence the reaction forces from tubes and AVBs are smaller than the Unit-2 SGs. Consequently, the contact forces caused by the manufacturing dimensional variations in the Unit-3 SGs are smaller than in the Unit-2 SGs, which is consistent with the tolerance analysis results shown in Fig.5.2-1.

The average of all gaps between the tubes in the outermost rows and AVBs along the retaining bars is smaller in the Unit-3 SGs than in the Unit-2 SGs. However, the gaps between the outer-most tubes and AVBs in the center columns do not have significant effect on the contact forces in the inside of the tube bundle and the main reason for this difference is the fact that the gaps in the outer-most rows of the peripheral columns in the Unit-2 SGs were larger than those in the Unit-3 SGs. The average of the gaps between the outermost tubes and AVBs in the center 60 columns (Column 59 to 119), where the wear indications were found, were essentially the same in the Unit-2 and Unit-3 SGs as shown in Fig.5.2-2. Therefore, the difference of the contact forces between Unit-2 and Unit-3 is caused by the difference of the manufacturing dimensional tolerances other than the outer-most tube-to-AVB gaps.

Manufacturing Tolerances

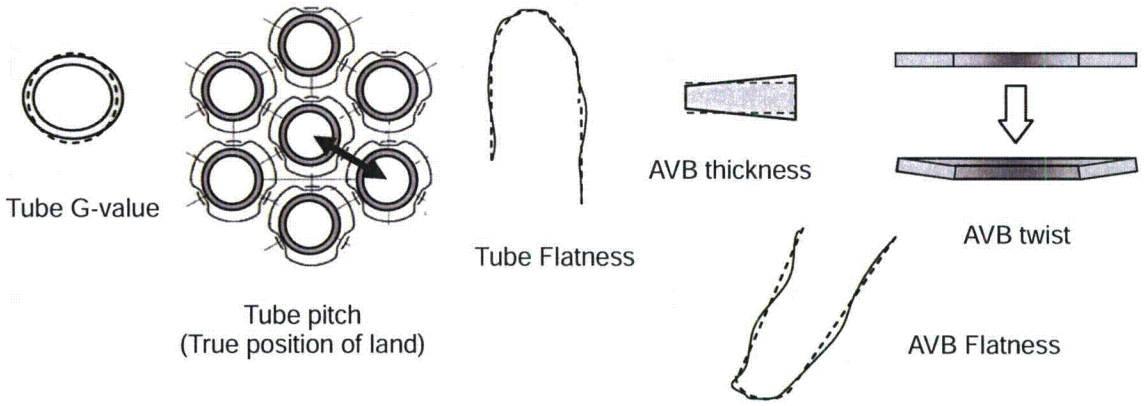

[ ]

Contact forces of Unit-2 are more than
2 times larger than those of Unit-3.

[ ]

Fig.5.2-1 Contact Force Simulation with Manufacturing Tolerances

Table 5.2-1 Manufacturing Differences Between Unit-2 and Unit-3 SGs

Item	Unit-2	Unit-3	Reason / Effect
Rotations	[	]	Due to divider plate repair
Hydrostatic Test			Due to seal-weld leakage and divider plate repair
AVB pressing force			AVB twist and flatness of Unit-3 SGs are controlled more precisely
Standard Deviation of Tube Outer Diameter (G-value*1) mils (mm)			Unit-3 has smaller standard deviation
Adjustment of Tube Bending Radius			Unit-3 had fewer adjustments of tube bending radii
Average Gap between Outermost Tube and AVB*2 mils (mm)			Unit-3 has smaller gaps. Most of the difference is in the peripheral columns not the central columns (where the wear indications are found).

Note)

*1: G-values were measured by micrometer.

*2: Outermost peripheral gaps near the retaining bar-to-AVB welds were measured by feeler gages.

Fig.5.2-2 Comparison of the outer-most tube-to-AVB gaps in the center 60 columns

6. Tube Wear Causes

In general, there are 3 types of tube bundle vibration phenomena occurring in fluid environment (see Fig.6-1):

(1) Vortex Shedding Vibration (vibration due to Karman vortex)

In a single-phase flow when fluid is flowing perpendicularly to a tube, a pair of vortices, known as Karman vortices, will form periodically on the right and left side, and downstream of the tube. When the vortices move away from the tube surface periodically, the reaction forces created by them will cause the tube to vibrate. This phenomenon is called vortex shedding vibration.

The fluid flow across the SG tubes in the region of interest (U-bend region) is a two-phase flow with high void fraction (>[ ]). Therefore, no Karman vortices are expected to form periodically downstream of the tube and no vortex shedding induced tube vibration is expected to occur. Empirical data confirms that vortex shedding vibration typically does not occur in two-phase flow environments where the void fraction is greater than 15% (see Reference 1).

(2) Random Vibration

Random vibration is a phenomenon where the tubes vibrate due to forces created by turbulent flow as a result of fluid velocity and density fluctuations. Vibration amplitudes due to random vibration are generally small (smaller than those due to tube fluid-elastic instability).

(3) Fluid Elastic Instability (FEI)

FEI is a phenomenon where the tubes vibrate with increasingly larger amplitudes due to the fluid effective flow velocity exceeding its specific limit (critical velocity) for a given tube and its supporting conditions and a given thermal hydraulic environment. This occurs when the amount of energy imparted on the tube by the fluid is greater than the amount of energy that the tube can dissipate back to the fluid and to the supports.

In the case when vibration occurs in a two-phase flow such as in the SG tube U-bend region, there is a possibility that it is either due to random vibration or FEI. Based upon the abovementioned study of vibration phenomena, the mechanism of each tube wear type is evaluated next based on the fault tree evaluations shown in Fig.6-2 and Fig.6-3. △9

6.1 Type 1 Wear (TTW)

Based on the results from the rotating pancake coil ECT inspections and visual inspections, MHI concluded that the Type 1 wear (TTW) occurred due to tube in-plane motion (vibration) with a displacement (amplitude) greater than the distance between the tubes in the adjacent rows, resulting in tube-to-tube contact. Tube in-plane motion might have been caused by tube random vibration or FEI. Because the amplitude of random vibration is generally very small, the mechanistic cause of this type of wear is typically tube FEI (refer to Fig.6-1 for the difference between random vibration and FEI).

U-tube out-of-plane direction is more susceptible to flow-induced excitation than the in-plane direction due to lower U-bend natural frequency in the out-of-plane direction. U-tube FEI in the in-plane direction has never been observed in the U-tube SGs before its occurrence in the SONGS SGs. However, recent academic studies (Reference 2 and 3) report that FEI may also occur in the in-plane direction, if tube motion in the in-plane direction is possible (no tube in-plane supports or low tube contact forces with the out-of-plane supports, as concluded by MHI). 9

As described in Section 5.1, the void fraction (steam quality) and the flow velocity are high in the SONGS SGs which means that their tubes are generally more susceptible to vibration. Furthermore, the average tube-to-AVB contact force in the Unit-3 SGs is concluded to be smaller than in the Unit-2 SGs, as described in Section 5.2, which makes the Unit-3 tubes to be even more susceptible to vibration and likely to FEI. Therefore, MHI concludes that in-plane tube motion which caused the Type 1 wear was due to tube FEI. The wear at the AVBs and at TSPs on some of the tubes with the Type 1 wear is an additional effect of these tubes being unstable (refer to Fig.6.1-1). 9

6.2 Type 2 Wear (AVB wear)

Based on the visual inspections, MHI concluded that the Type 2 wear occurred due to tube vibration which caused the tubes to wear against the AVBs at the tube-to-AVB intersections. 9
Tube wear at AVB intersections might have been caused by tube random vibration or FEI. However, because most likely there were no significant gaps between the tubes and AVBs during operation (see Section 5.2.1), the occurrence of tube motion due to FEI is very unlikely 9
(refer to Appendix-3). As described in Section 5.1, the SONGS SG tubes are susceptible to vibration (high void fractions and high flow velocities). Therefore, MHI concludes that the tube

wear at AVB intersections, which caused the Type 2 wear, was due to the random vibration (refer to Fig.6.2-1). 9

The Type 1 and Type 2 wear are simulated in the tube wear analysis as shown in Appendix-10.

6.3 Type 3 Wear (TSP wear)

The tubes with the Type 3 wear are located mostly near the TSP flow slots and at the periphery of the tube bundle where the velocities of cross-flow are high (refer Fig.6.3-1). Tube vibration in cross-flow may be caused by tube random vibration or FEI. However, the size of the gap between the TSP tube hole land surface and the tube is limited (design size is[ ]). Thus, the occurrence of tube FEI is unlikely. Therefore, MHI concludes that the Type 3 wear is caused by cross-flow induced random vibration in the region where secondary fluid cross-flow velocities are high (refer Fig.6.3-2). The results of the FEI and random vibration analysis are shown in Appendix-2.

6.4 Type 4 Wear (RB wear)

The tubes with the Type 4 wear have no indications of TTW or AVB wear, or TSP wear, which suggests that it is caused by only the retainer bars vibrating. SONGS SGs have two types of retainer bars,[ ]mm ([ ]) in diameter and[ ]mm ([ ]) in diameter. Tube wear was found on the tubes adjacent to the retainer bars, but only at the smaller diameter retainer bars. The retainer bars with the smaller diameter have also a relatively long span as compared with the other SGs fabricated by MHI, which means that the natural frequency of these retainer bars is lower and thus they are more likely to vibrate. Therefore, MHI concludes that the Type 4 wear is caused by random vibration of the retainer bars induced by the secondary fluid exiting the tube bundle(see Reference 4 for details).

✓ Vortex Shedding Vibration (Vibration due to Karman vortex)

➢In a single-phase flow when fluid is flowing perpendicularly to a tube, a pair of vortices, known as Karman vortices, will form periodically on the right and left side, and downstream of the tube. When the vortices move away from the tube surface periodically, the reaction forces created by them will cause the tube to vibrate. This phenomenon is called vortex shedding vibration.

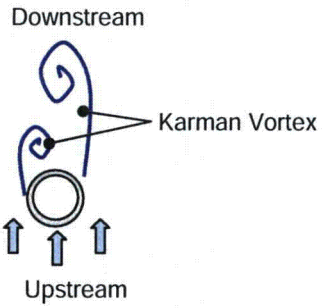

✓Random Vibration

➢Random vibration is a phenomenon where the tubes vibrate due to forces created by turbulent flow as a result of fluid velocity and density fluctuations. Vibration amplitudes due to random vibration are generally small (smaller than those due to tube fluid-elastic instability).

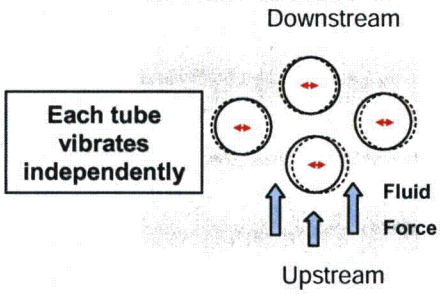

✓Fluid Elastic Instability (FEI)

➢FEI is a phenomenon where the tubes vibrate with increasingly larger amplitudes due to the fluid effective flow velocity exceeding its specific limit

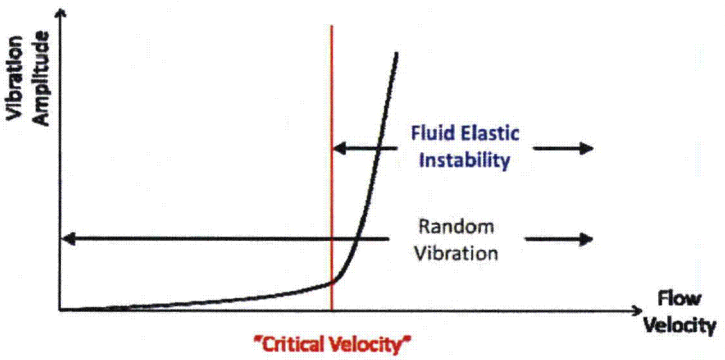

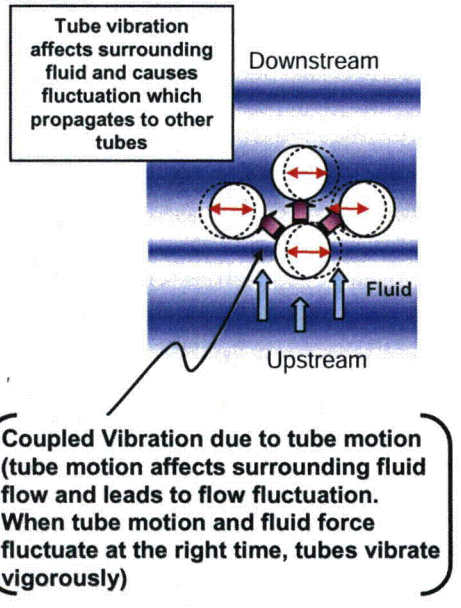

Fig.6-1 Flow Induced Tube Bundle Vibration

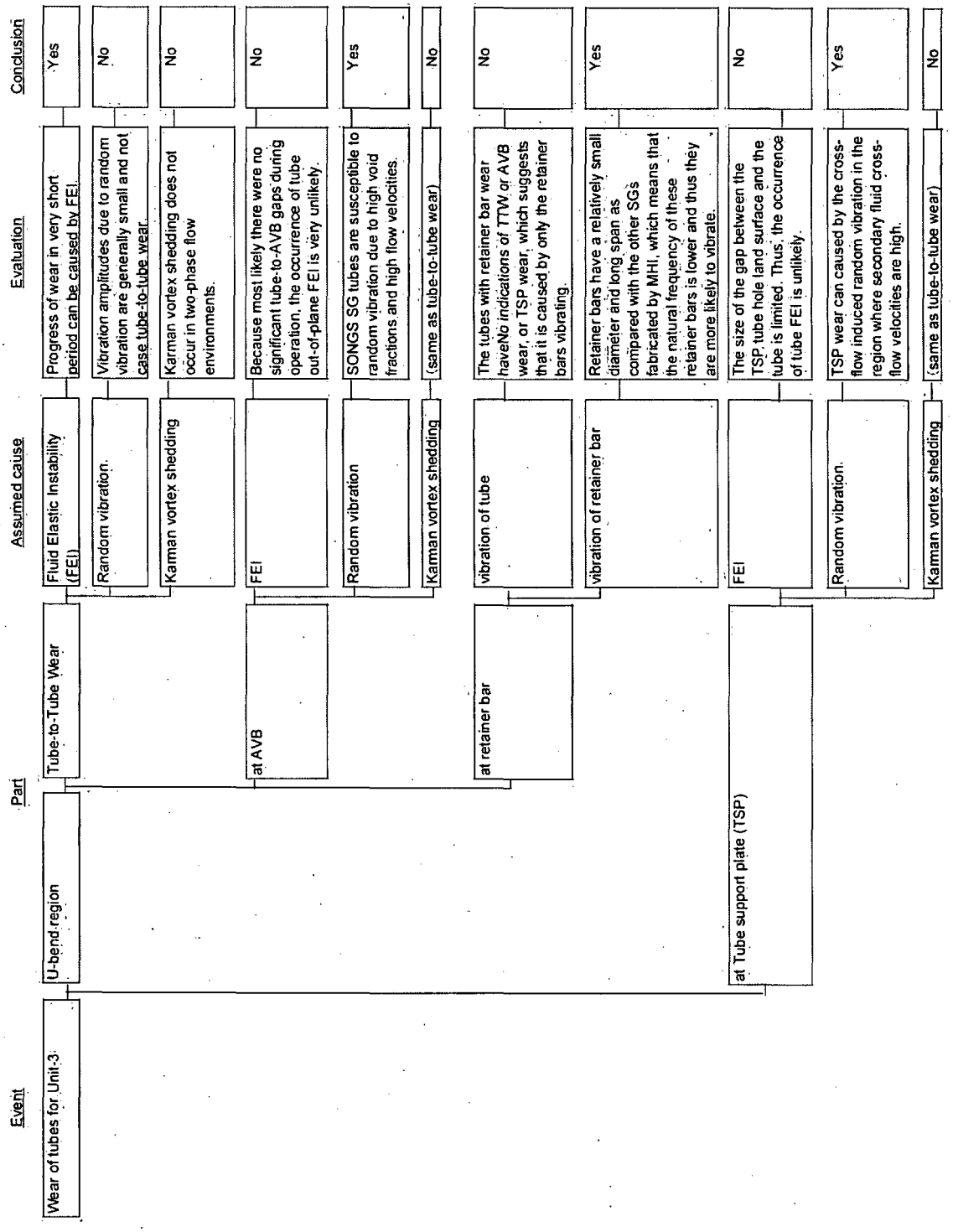

Fig.6-2 Fault Tree Evaluation for the Causes of Wear

9

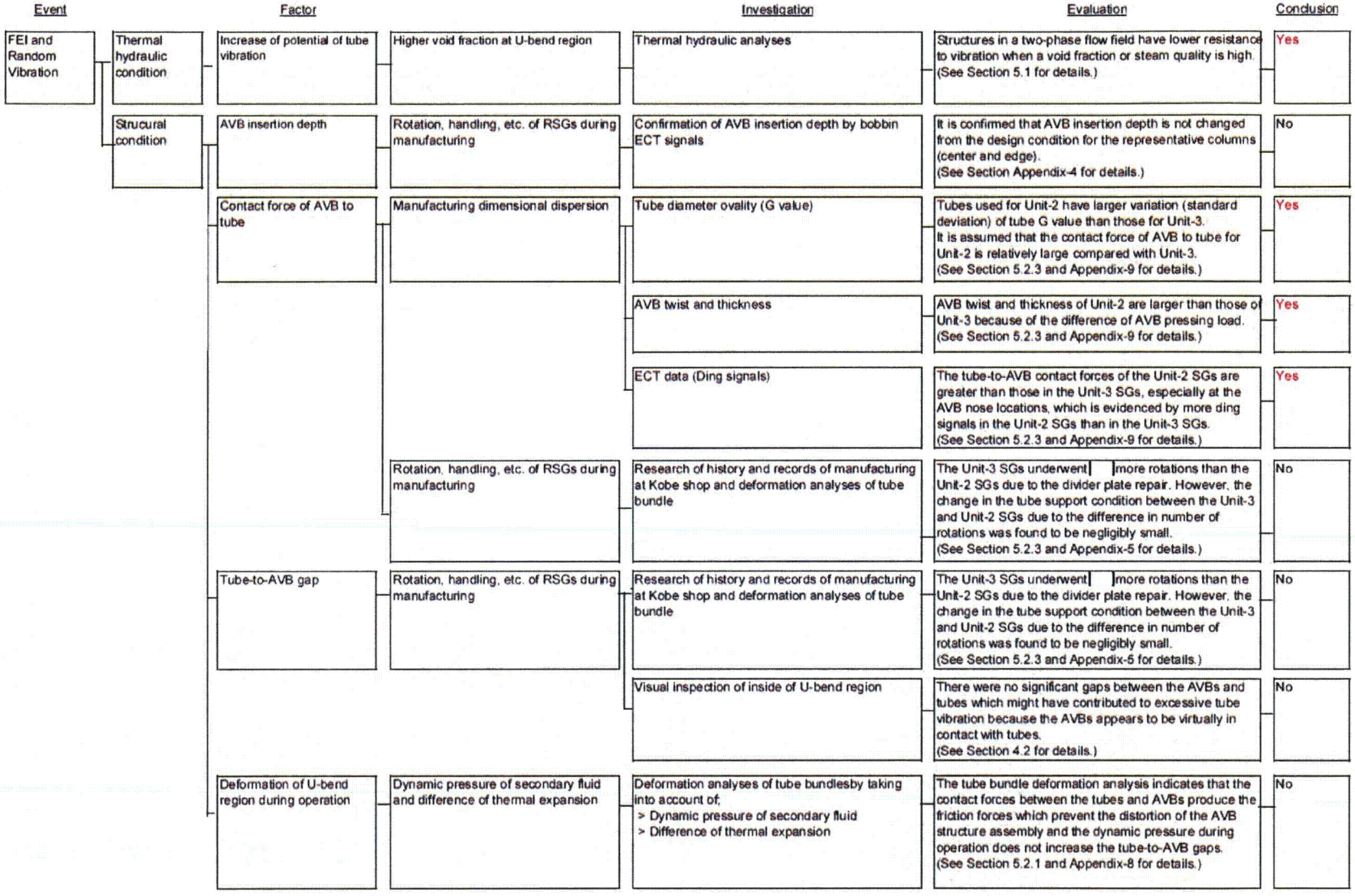

Fig.6-3 Fault Tree Evaluation for the Causes of FEI and Random Vibration

Characteristics of SONGS RSG

【Thermal Hydraulics】

✓ Design with High Steam Quality in U-Bend (max[ ])

【AVB Structure】

✓ Tube between 2 flat AVBs
- AVB Design Assumes Out-of Plane Vibration

Since out-of-plane FEI is more likely to happen compared to in-plane FEI, AVBs are placed at the sides of tube to preven out-of-plane vibration

✓ 6 V-Shaped AVBs (12support points)
- Number of AVB Support Points are designed by FEI Evaluation based on ASME Sec.III

(Out-of-Plane FEI will not occur even if one of supports is inactive as design basis)

✓ Designed and fabricated for "Zero" Gap between Tube and AVB in hot condition

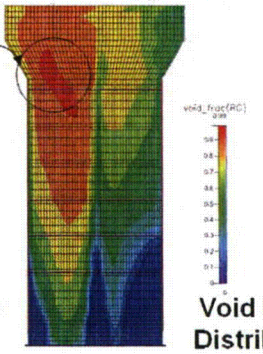

Void Fraction Distribution in 100% Output

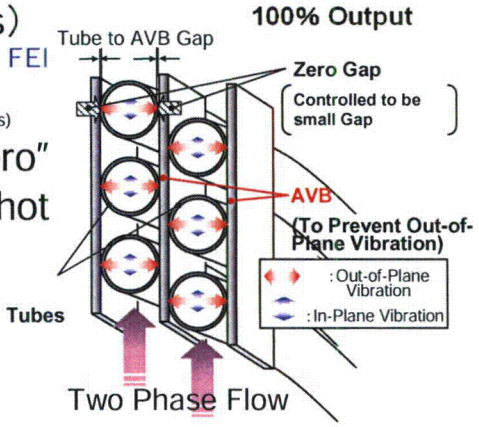

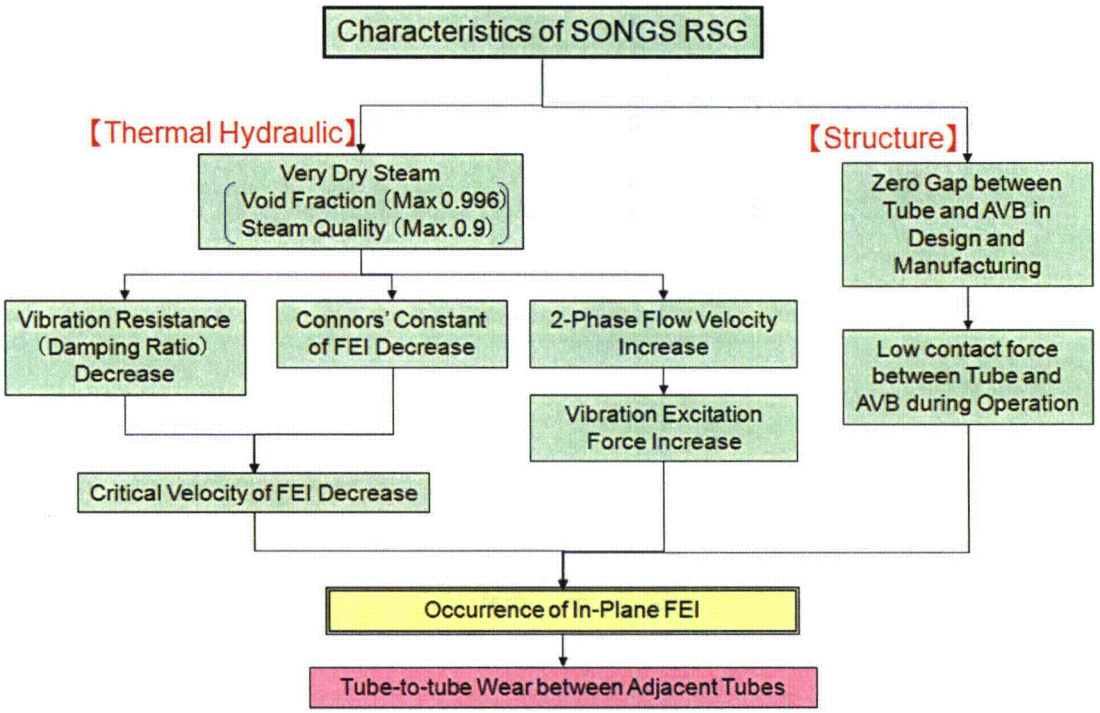

Fig.6.1-1 Type 1 Wear (TTW) Mechanism

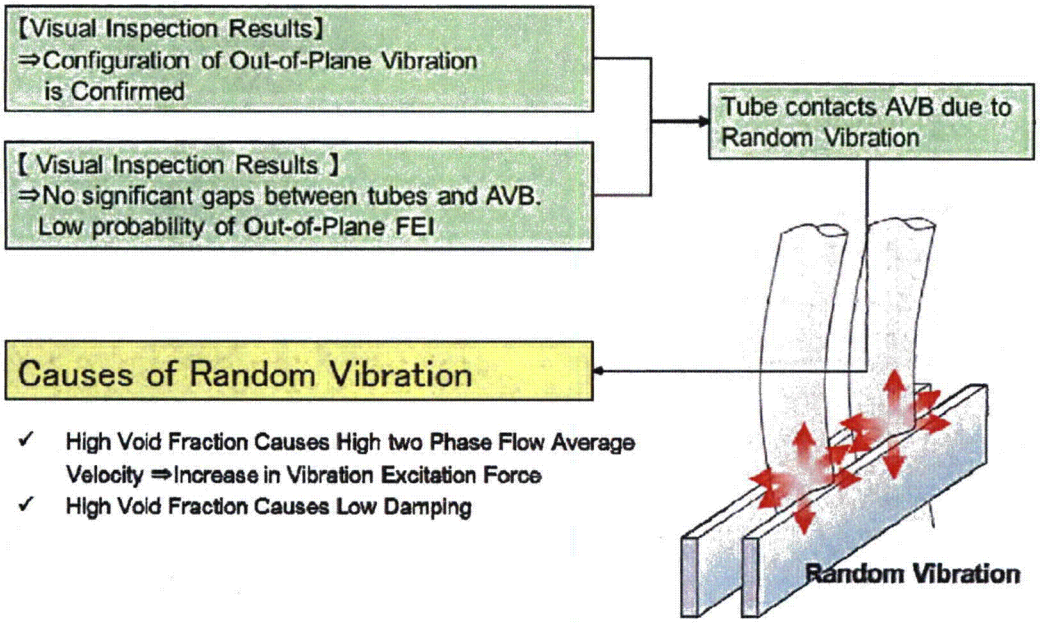

9

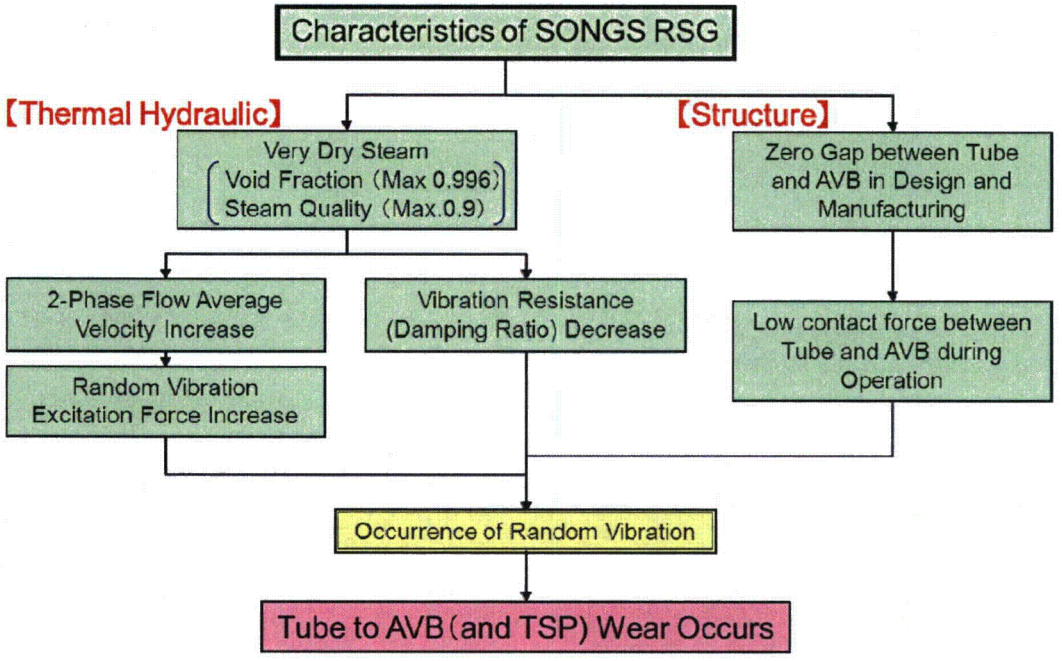

9

Fig.6.2-1 Type 2 Wear (AVB wear) Mechanism

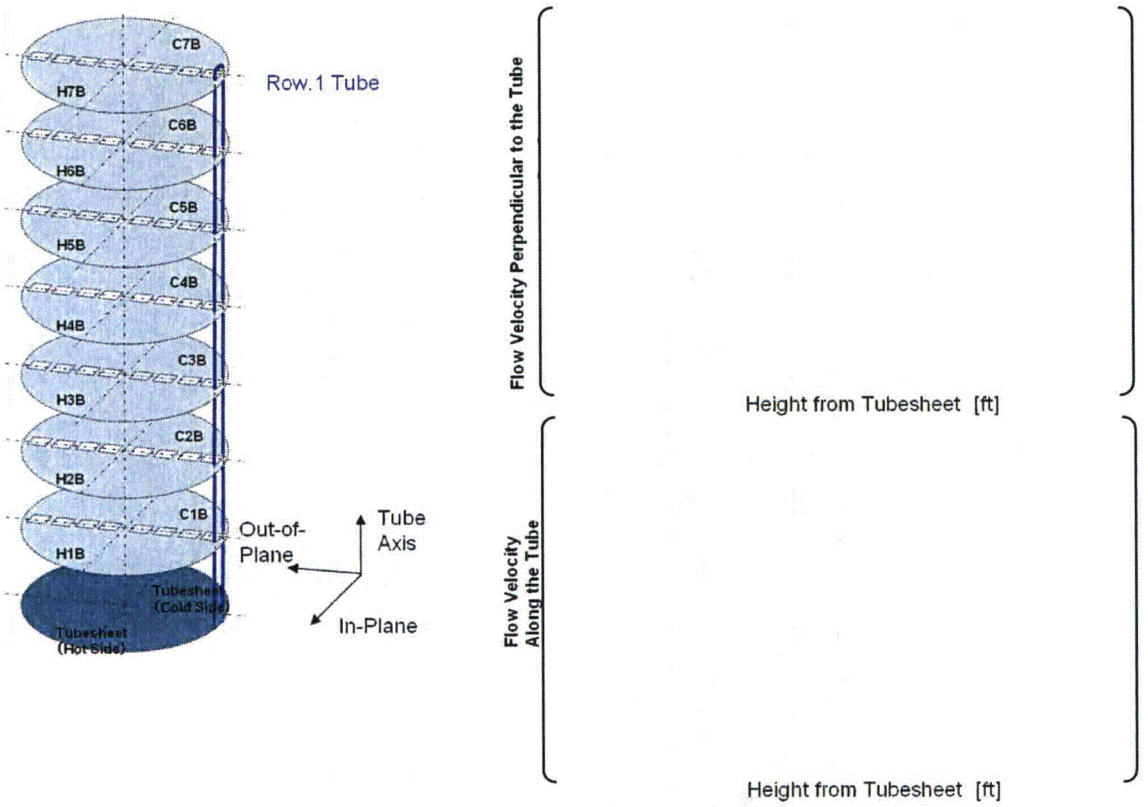

Fig.6.3-1 Flow Velocity Distribution at TSPs

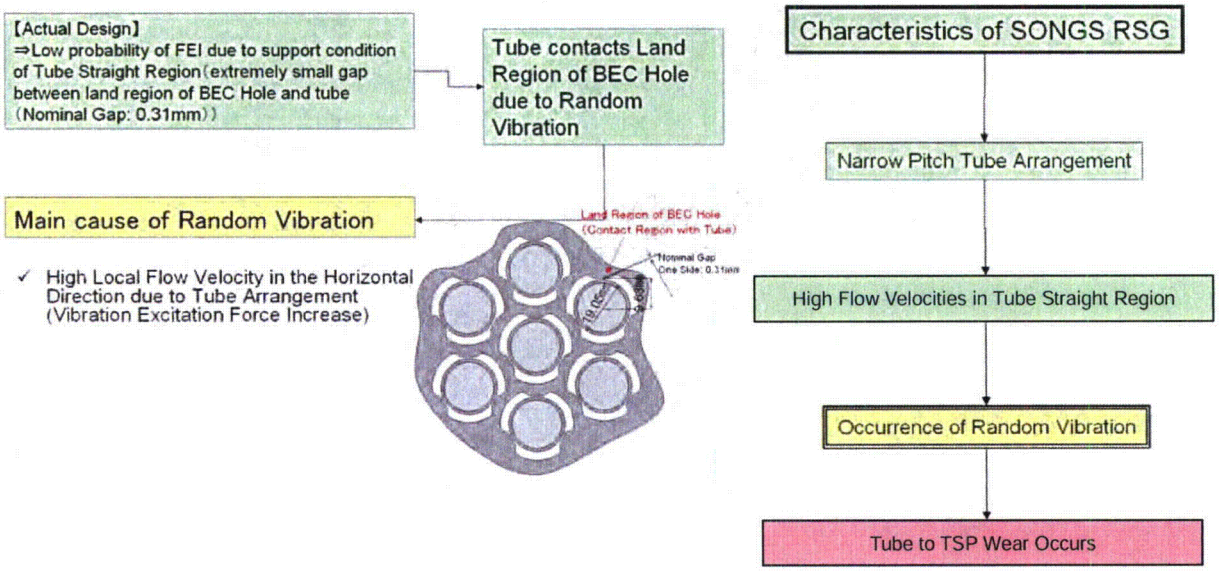

Fig.6.3-2 Type 3 Wear (TSP wear) Mechanism

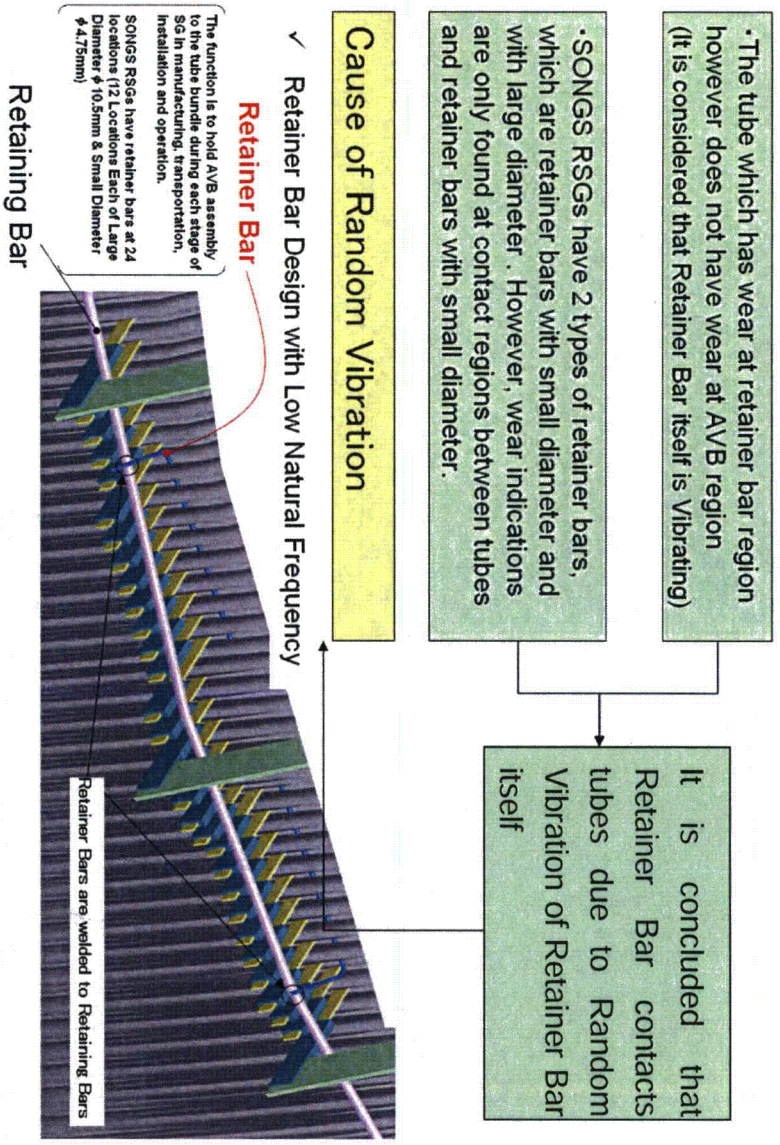

Fig.6.4-1 Type 4 Wear (RB wear) Mechanism

7. Conclusions

In the Unit-3 SGs, the following types of wear were identified:

(i) Type 1 (TTW)
(ii) Type 2 (AVB wear)
(iii) Type 3 (TSP wear)
(iv) Type 4 (RB wear)

The conclusions regarding mechanistic causes of tube wear are as follows:

- The concluded mechanistic cause of the Type 1 wear is tube FEI in the tube bundle U-bend region, which is caused by a combination of the SG secondary side thermal-hydraulic conditions (high fluid velocity and high void fraction) and inactive AVB support conditions in the in-plane direction.
- The concluded mechanistic cause of the Type 2 and 3 wear is random vibration of the tubes. The Type 2 wear is caused by the tube motion due to high void fractions and high flow velocities. The Type 3 wear is caused by high velocity flow across the straight leg sections of the tubes. △9
- The concluded mechanistic cause of the Type 4 wear type is vibration of the retainer bar, which is the same as in the Unit-2 SGs and is addressed in Reference 4.

The tube-to-AVB contact forces of Unit-3 were more likely to be insufficient to prevent the in-plane motion of tubes and the Unit-3 SGs were more susceptible to in-plane tube vibration than Unit-2 SGs because the average contact force in the Unit-3 SGs was found to be smaller than the average contact force in the Unit-2 SGs. The difference in the contact forces between the Unit-2 and Unit-3 SGs was caused by the manufacturing dimensional tolerance variations, mainly due to improvement of AVB dimensional control.

8. Countermeasures for Return to Service

The following short term actions should be taken in support of Unit 3 return to service for a limited period of time (if possible). In order to restore SONGS SGs' conformance to the CDS and make them capable of operating without time or reactor power level restrictions, more complex and involving actions (repairs) will be mandatory.

8.1 Tube Plugging

Tubes which exhibit a potential for losing their integrity during the next operating period due to progressive through-wall wear and/or susceptibility to FEI should be plugged. The number of tubes plugged for each type of tube wear is listed in Table 8.1-1.

8.1.1. Type 1 Wear

All tubes with ECT tube wear indications in the free span section should be plugged regardless of the wear depth. Furthermore, tubes with wear indications at the AVB and TSP locations, which are similar to those on the tubes with the wear indication in the free span section, should be preventatively plugged.

8.1.2. Type 2 Wear and Type 3 Wear

Tubes with wear equal to, or greater than, 35% should be plugged in accordance with Technical Specifications.

8.1.3. Type 4 Wear

Tubes with wear indications adjacent to the retainer bars should be plugged regardless of the wear depth. Furthermore, all tubes that have a possibility to come in contact with the retainer bars should be preventatively plugged.

NOTE:

As of this writing, tube plugging has already been performed in the Unit-2 and Unit-3 SGs, and the number of the tubes for each plugging type is listed in Table 8.1-1 below.

Table 8.1-1 Plugged Tubes

Wear Type/Plugging Type	Steam Generator				Total
	2E088	2E089	3E088	3E089	
Type 1 Wear (with wear indication)		2	161	165	328
Type 1 Wear (preventative plugging)	109	212	164	128	613
Type 2 Wear and Type 3 Wear	4		1		5
Type 4 Wear (with wear indication)	2	4	3	1	10
Type 4 Wear (preventative plugging)	92	90	91	93	366
Total	207	308	420	387	1322
% Tubes Plugged	2.2%	3.2%	4.4%	4.0%	

△9

△9

8.2 Operating at a Lower Thermal Power

As described in Section 6, the major contributor to the tube wear phenomenon in the SONGS SGs is the secondary side thermal-hydraulic conditions in the tube bundle U-bend region of interest at 100% reactor power. The major parameters making these conditions unfavorable from the tube wear perspective are high secondary fluid flow velocities and high void fractions (steam quality).

In general, decreasing the reactor power level will result in the fluid flow velocities and void fractions being lower, and hence tube margins to FEI being larger. Lowering the plant reactor power level to 70% is sufficient to decrease the fluid flow velocities and void fractions in the tube bundle region where tube wear, especially TTW, occurred during the previous operating period to the point at which the tubes remaining in service are not expected to become fluid elastic unstable, as shown in Fig. 8.2-1 (Details of the secondary side thermal-hydraulic conditions are described in Reference 5). △9

The effects of area plugging and power level reduction were investigated in the case study for their impact on tube stability (Reference 6). The results of this study indicate that the changes in the bundle thermal-hydraulic parameters reduce the stability ratios (increase margins to FEI) of the analyzed tubes slightly, but the ratios are still greater than 1.0 at 100% reactor power and the number of consecutive inactive AVB support points being 6 or more. Because no credit can be taken for a change in the tube support condition, as no modifications to the AVB support structure are possible in the short term, only reduction in power level can produce a beneficial reduction of the stability ratio (increase of margin to FEI) for the tubes remaining in service (not plugged).

Fig.8.2-1 Void Fraction or Steam Quality Distribution of Thermal Power Reduction

9. References

(1) Journal of Fluids and Structures, "Vibration analysis of shell-and-tube heat exchangers: an overview – Part 1:flow, damping , fluid elastic instability", M.J. Pettigrew, C.E. Taylor., March 2003

(2) ASME, "Fluidelastic Instability and Work-Rate Measurements of Steam-Generator U-Tubes in Air-Water Cross-Flow", V.P.Janzen, E.G.Hagberg, M.J.Pettigrew, C.E.Taylor. February 2005

(3) Flow-Induced Vibration,Meskell & Bennett (eds) ISBN 978-0-9548583-4-6, "Study on In-flow Fluid-elastic Instability of Circular Cylinder Arrays"], T.Nakamura, Y.Fujita, T.Oyakawa, Y.NI. July 2012

(4) MHI report, "Retainer Bar Tube Wear Report", L5-04GA561 the latest revision

(5) MHI report, "Case study of the input parameters and tube plugging impact on internal SG thermal hydraulic parameters", L5-04GA566 the latest revision

(6) MHI report, "Evaluation of Stability Ratio for Return to Service", L5-04GA567 the latest revision

(7) JSME, S016-2002, Guideline for Fluid-elastic Vibration Evaluation of U-bend Tube in SG, March 2002

(8) MHI report, "Screening Criteria for Susceptibility to In-Plane Tube Motion", L5-04GA571 the latest revision

(9) SCE project letter, "L5-04GA564, REV. 6, TUBE WEAR OF UNIT-3 RSG TECHNICAL EVALUATION REPORT", RSG-SCE/MHI-12-5757, August 2012

(10) MHI report, "Analytical Evaluations for Operating Assessment", L5-04GA585 the latest revision

(11) SCE project letter, "Updated ECT Data for Input to Return to Service and Repair Design Documents", RSG-SCE/MHI-12-5749, August 2012 △9

Appendix-1
ECT Data Evaluation of tubes with wear around Retainer Bar

1. Purpose

This appendix provides the ECT data evaluation of tubes with wear around the retainer bars in the two Unit-3 SGs.

2. Result

Table 2-1 shows tube wear identified at the intersections with AVB assembly retainer bars for Unit-3.

Table 2-1. Retainer Bar Tube Wear

SG	Row	Col	Location	Side	+Point depth	Circ extent	Axial extent
3B	117	137	B10 -0.42"	Out	44%	0.47"	0.35"
3B	125	49	B11 -0.50"	Out	28%	0.29"	0.27"
3B	128	126	B10 -0.44"	Out	41%	0.44"	0.32"
3A	124	130	B11 -0.47"	Out	46%	0.45"	0.27"

Note: The retainer bar is captured between two tube rows in each column. "Out" describes the tube with the larger bend radius.

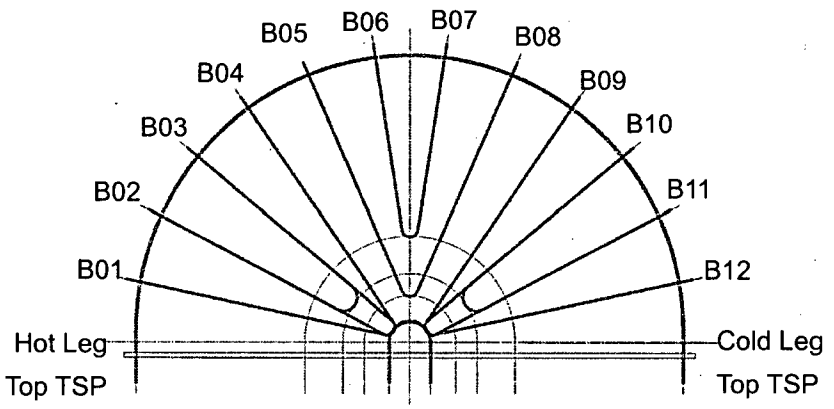

Fig.2-1 Retaining Bar and Retainer Bar Locations

Figures 2-2 and 2-3 provide an overview of the indication locations. Figure 2-4 shows a close-up view of the location with the deepest wear mark.

For these four tubes, it is confirmed by bobbin ECT data that no indication is detected at AVB and TSP contact points except the intersections with retainer bars, as shown in Table 2-2. This shows that the tube wear was not caused by the vibration of the tube but by the vibration of the retainer bar.

Table 2-2 Bobbin ECT results for tubes with retainer bar wear

SG	Row	Column	B01	B02	B03	B04	B05	B06	B07	B08	B09	B10	B11	B12
3B	117	137	-	-	-	-	-	-	-	-	-	W	-	-
	125	49	-	-	-	-	-	-	-	-	-	-	W	-
	128	126	-	-	-	-	-	-	-	-	-	W	-	-
3A	124	130	-	-	-	-	-	-	-	-	-	-	W	-

SG	Row	Column	TSH	01H	02H	03H	04H	05H	06H	07H	07C	06C	05C	04C	03C	02C	01C	TSC
3B	117	137	-	-	-	-	-	-	-	-	-	-	-	-	-	-	-	-
	125	49	-	-	-	-	-	-	-	-	-	-	-	-	-	-	-	-
	128	126	-	-	-	-	-	-	-	-	-	-	-	-	-	-	-	-
3A	124	130	-	-	-	-	-	-	-	-	-	-	-	-	-	-	-	-

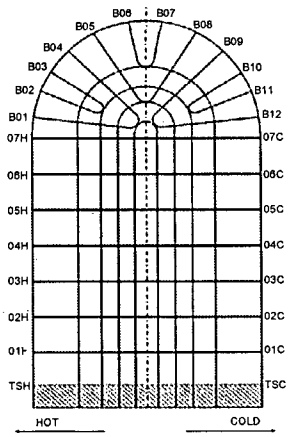

- : No wear

W : Wear at retainer bar location

3. Reference

1. ECT Data for Input to Return to Service and Repair Design Documents (RSG-SCE/MHI-12-5688), e-mail from SCEs Mr. Calhoun on March 23, 2012 (JST)

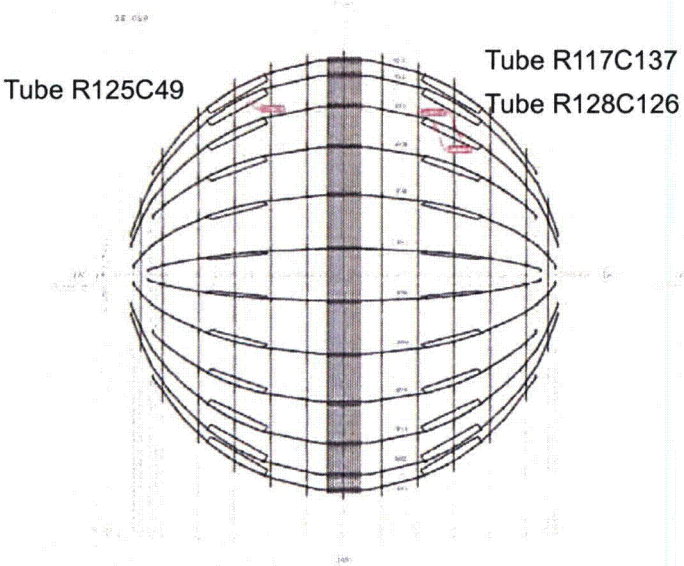

Fig.2-2 Indication locations for Unit-3B

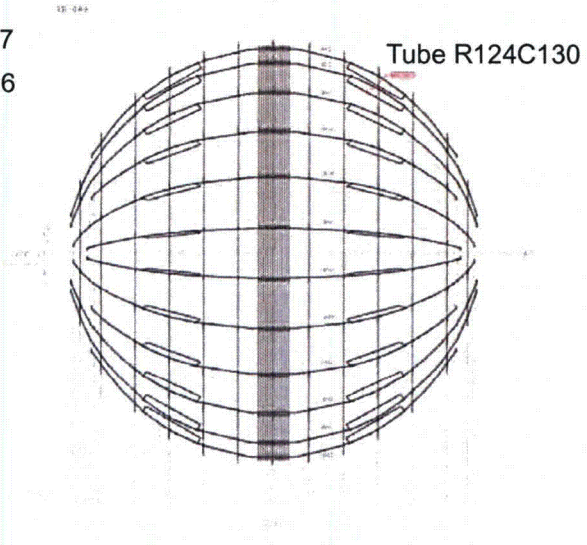

Fig.2-3 Indication location for Unit-3A

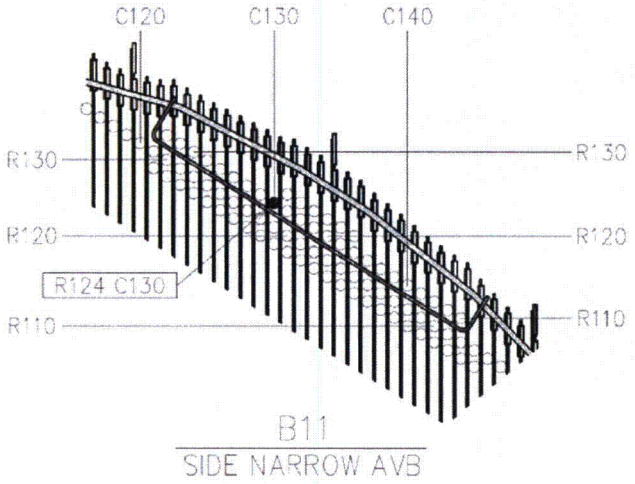

Fig.2-4 Location of 46% Wear (for Unit-3A, R124C130, AVB11 Retainer Bar)

Appendix-2
FEI Evaluation of Tube Straight Portion for Unit-2/3

1. Purpose

Tube-to-tube support plate (TSP) wears at tube straight portions are detected in SONGS-2/3 RSGs. It is possible that the cause of the wears is the fluid elastic instability (FEI) mechanism. The purpose of study provided in appendix-2 is to evaluate the possibility of FEI of the tube straight portion, through the thermal and hydraulic calculations by ATHOS/SGAP computer code and vibration calculations by FIVATS computer code (The evaluation of random excitation mechanism is provided in Appendix-2A).

2. Conclusion

In order to evaluate the possibility of FEI in the tube straight region the stability ratios defined in Section 6 for representative tubes are calculated with assuming TSPs effective supports because the gap between the tube and TSP is enough small. The analysis predicts that FEI of tube straight portions is not possible in case that all TSPs supports are effective. Thus, MHI concludes that the cause of tube-to-TSP wears in SONGS-2/3 RSGs is not due to FEI in the straight portion of tube due to the cross flow.

Table 2-1 Stability ratio calculations summary

Tube address	Stability ratio(*)			
	Conservative case (**)		Best estimated case (***)	
Row 1 Column 1	[ ]	Hot side	[ ]	Hot side
Row 1 Column 13	[ ]	Hot side	[ ]	Hot side
Row 1 Column 89	[ ]	Hot side	[ ]	Hot side
Row 53 Column 57	[ ]	Hot side	[ ]	Hot side
Row 80 Column 74	[ ]	Cold side	[ ]	Hot side
Row 101 Column 29	[ ]	Hot side	[ ]	Hot side
Row 137 Column 77	[ ]	Cold side	[ ]	Hot side

(*) Stability ratio over 1.0 implies a probability of FEI

(**) Critical factor (K=2.4) and damping ratio (h=1.5%) values are used.

(***) The critical factor depending on the volume flow rate quality (β) is used. The total damping which consist of the structural damping, two-phase damping, and squeeze film damping is used.

3. Assumption

9

(1) Nominal tube thickness and nominal tube length are used in the evaluation model because the effect of the tolerances of these dimensions on the natural frequency is negligible.

(2) Contact condition between tube and tube support plate is pin-supported. Fixed supported condition at No. 1 TSP is added.

(3) Contact condition between tube and active support points by the anti-vibration bar (AVB) is pin-supported. And all points are active.

(4) Modulus of elasticity of tube is interpolated based on the tube average temperature of $\frac{T_{av}+T_s}{2}$ from table of ASME Boiler and Pressure Vessel Code, Sec II, Materials, 1998 Edition, 2000 addenda (Ref.23).

Where,

T_{av} : Primary side average temperature (°F)

T_s : Secondary side temperature (°F)

(5) Tube has the virtual added mass supposing the fluid-structure interaction (FSI) effect as shown in the following formula (Ref.24).

$$m_v = \frac{\pi D_o^2 \rho_o}{4}\left\{\frac{(D_e/D_o)^2+1}{(D_e/D_o)^2-1}\right\} \text{(lbm/ft)} \quad \cdots\cdots (1)$$

$$D_e/D_o = \left(1+\frac{1}{2}P/D_o\right)P/D_o \quad \cdots\cdots (2)$$

Where,

m_v : Virtual added mass per unit length due to FSI effect;

ρ_o : Average density of water outside the tube;

D_o : Tube outside diameter

P : Tube pitch.

9

4. Acceptance criteria

Through the tube vibration analysis of the tube straight portion, the stability ratio to FEI is calculated. A stability ratio over 1.0 implies probability of FEI.

5. Design input

The nominal dimensions are obtained from the design drawings (Ref.3 to 20) and the manufacturing tolerances are not considered.

Flow characteristics are obtained from 3 dimensional thermal and hydraulic analysis (see Appendix 12) .Flow velocity, density, void fraction and hydrodynamic pressure are evaluated for representative 7 tubes (Table 5-1). The reason of selection of these tubes is provided in section 6.2.1.

The velocity, density distribution and volume flow rate quality for tube straight portion are provided in Fig.5-0 through 5-21.

The void fraction and velocity on the center vertical plane is provided in Fig.5-22.

The void fraction and velocity above each TSP are provided in Fig.5-24 through 5-31.

Table 5-1 Evaluated Tubes

Row	Column
1	1
1	13
1	89
53	57
80	74
101	29
137	77

(See Fig. 5-23)

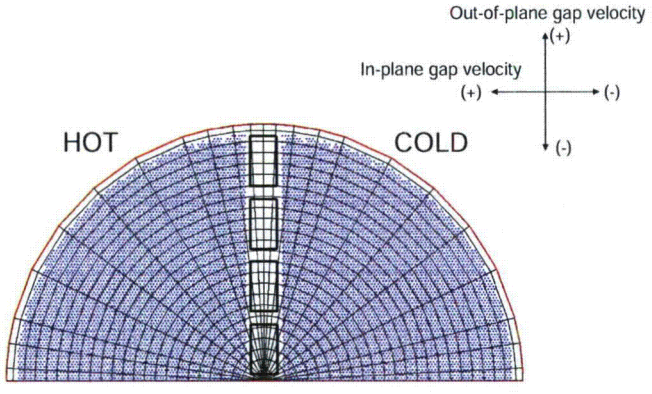

$V_{gap} = V_s \cdot P/(P-D)$

V_{gap} : gap velocity
V_s : superficial velocity
P : tube pitch
D : tube outside diameter

Fig.5-0 Definition of velocity direction

Fig.5-1 Cross flow velocity of tube straight portion (R1C1 tube)

Fig.5-2 Density of tube straight portion (R1C1 tube)

Fig.5-3 Volume flow rate quality (R1C1 tube)

Fig.5-4 Cross flow velocity of tube straight portion (R1C13 tube)

Fig.5-5 Density of tube straight portion (R1C13tube)

Fig.5-6 Volume flow rate quality (R1C13 tube)

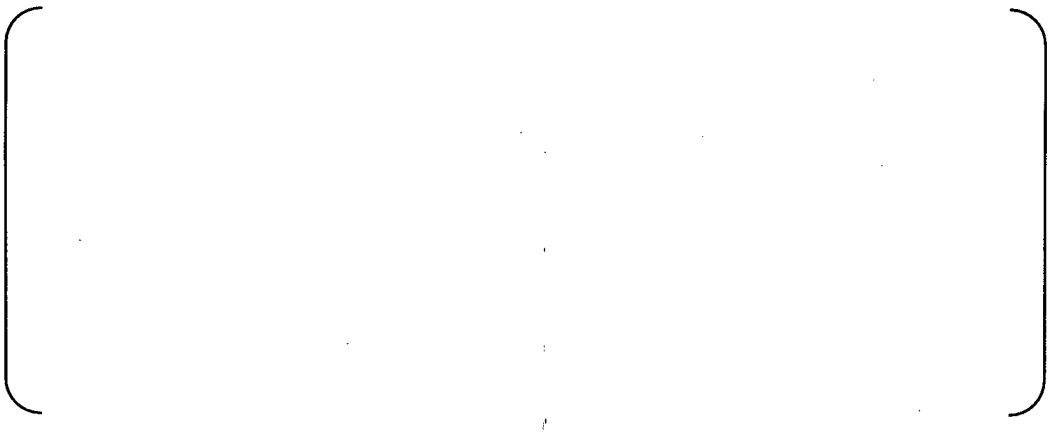

Fig.5-7 Cross flow velocity of tube straight portion (R1C89 tube)

Fig.5-8 Density of tube straight portion (R1C89 tube)

Fig.5-9 Volume flow rate quality (R1C89 tube)

Fig.5-10 Cross flow velocity of tube straight portion (R53C57 tube)

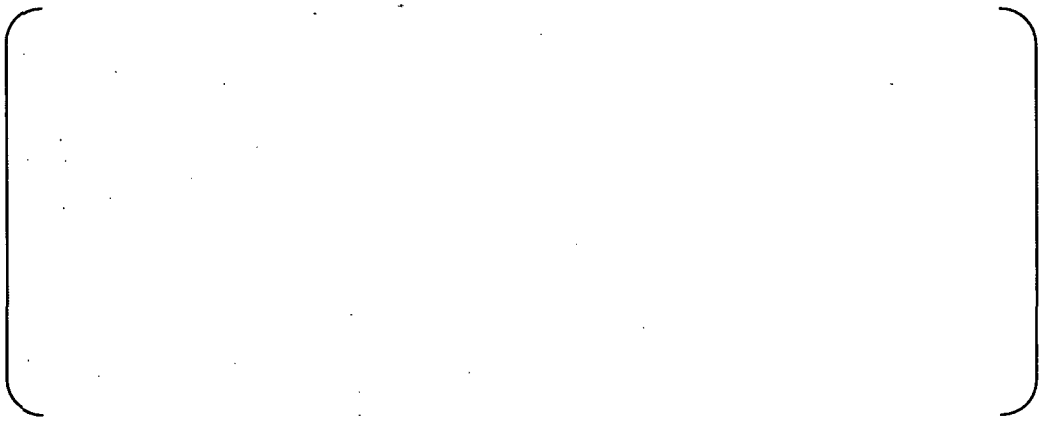

Fig.5-11 Density of tube straight portion (R53C57 tube)

Fig.5-12 Volume flow rate quality (R53C57 tube)

Fig.5-13 Cross flow velocity of tube straight portion (R80C74 tube)

Fig.5-14 Density of tube straight portion (R80C74 tube)

Fig.5-15 Volume flow rate quality (R80C74 tube)

Fig.5-16 Cross flow velocity of tube straight portion (R101C29 tube)

Fig.5-17 Density of tube straight portion (R101C29 tube)

Fig.5-18 Volume flow rate quality (R101C29tube)

Fig.5-19 Cross flow velocity of tube straight portion (R137C77 tube)

Fig.5-20 Density of tube straight portion (R137C77 tube)

Fig.5-21 Volume flow rate quality (R137C77 tube)

Fig.5-22 Distribution of void fraction and velocity

Fig.5-23 Evaluated tubes

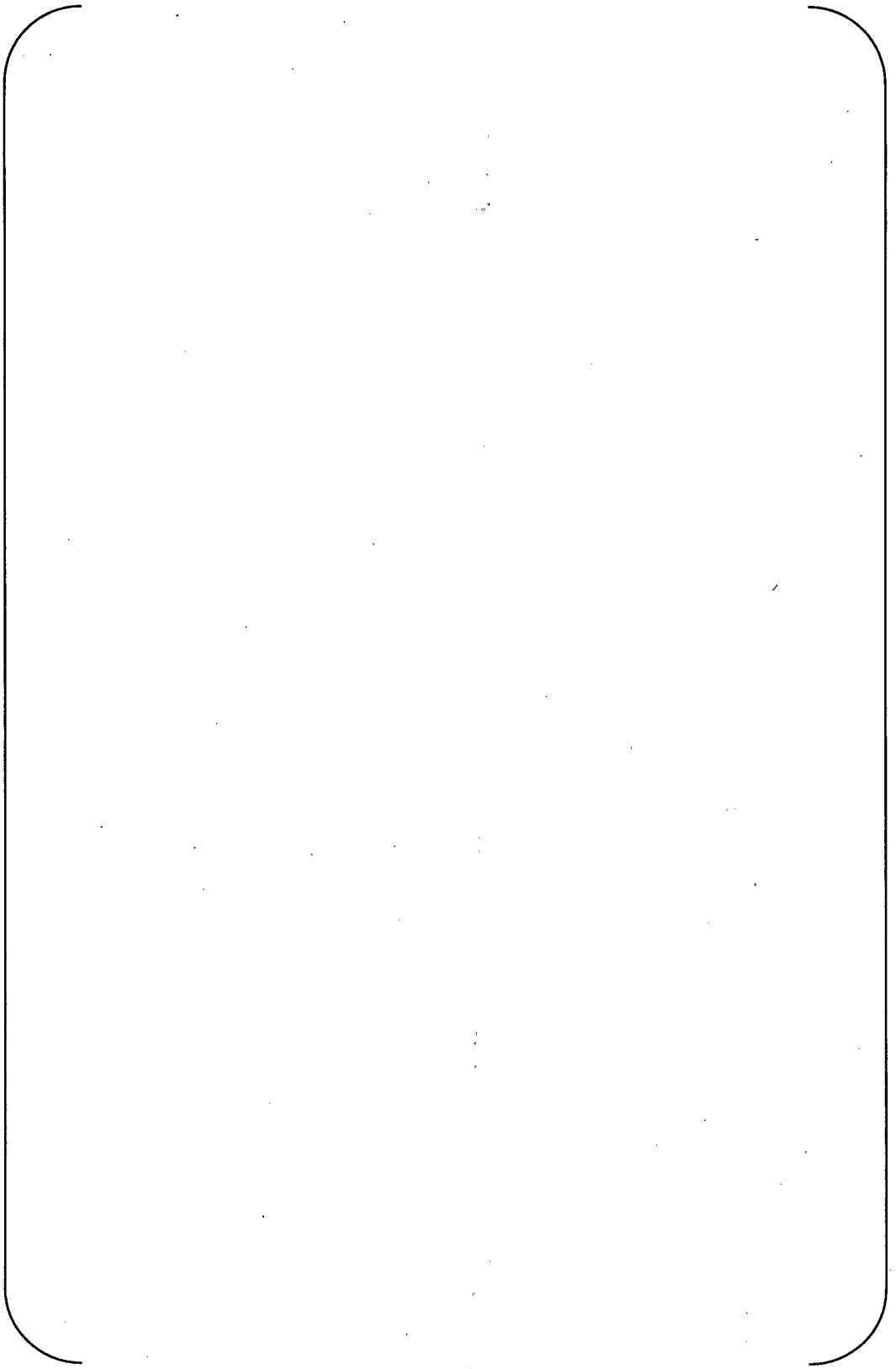

9

Fig.5-24 Distribution of void fraction and velocity above tube sheet

(Note 1)

Note that velocity of contour may mislead, because the velocity of outer circumference of the tube bundle is shown in lower velocity compared to that calculated by ATHOS/SGAP. The accurate values are provided in Appendix-2 Attachment-2.

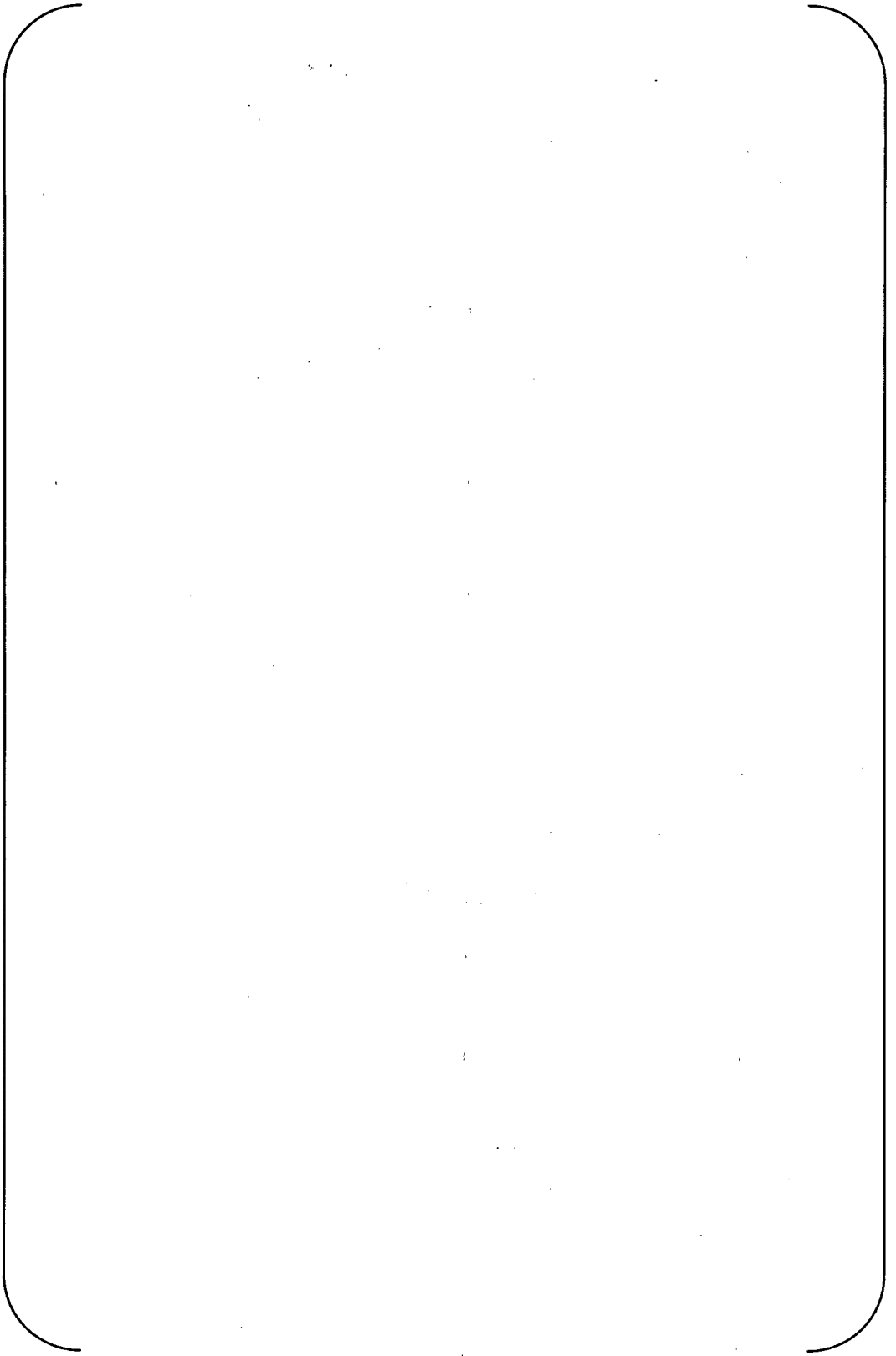

9

Fig.5-25 Distribution of void fraction and velocity at #1TSP

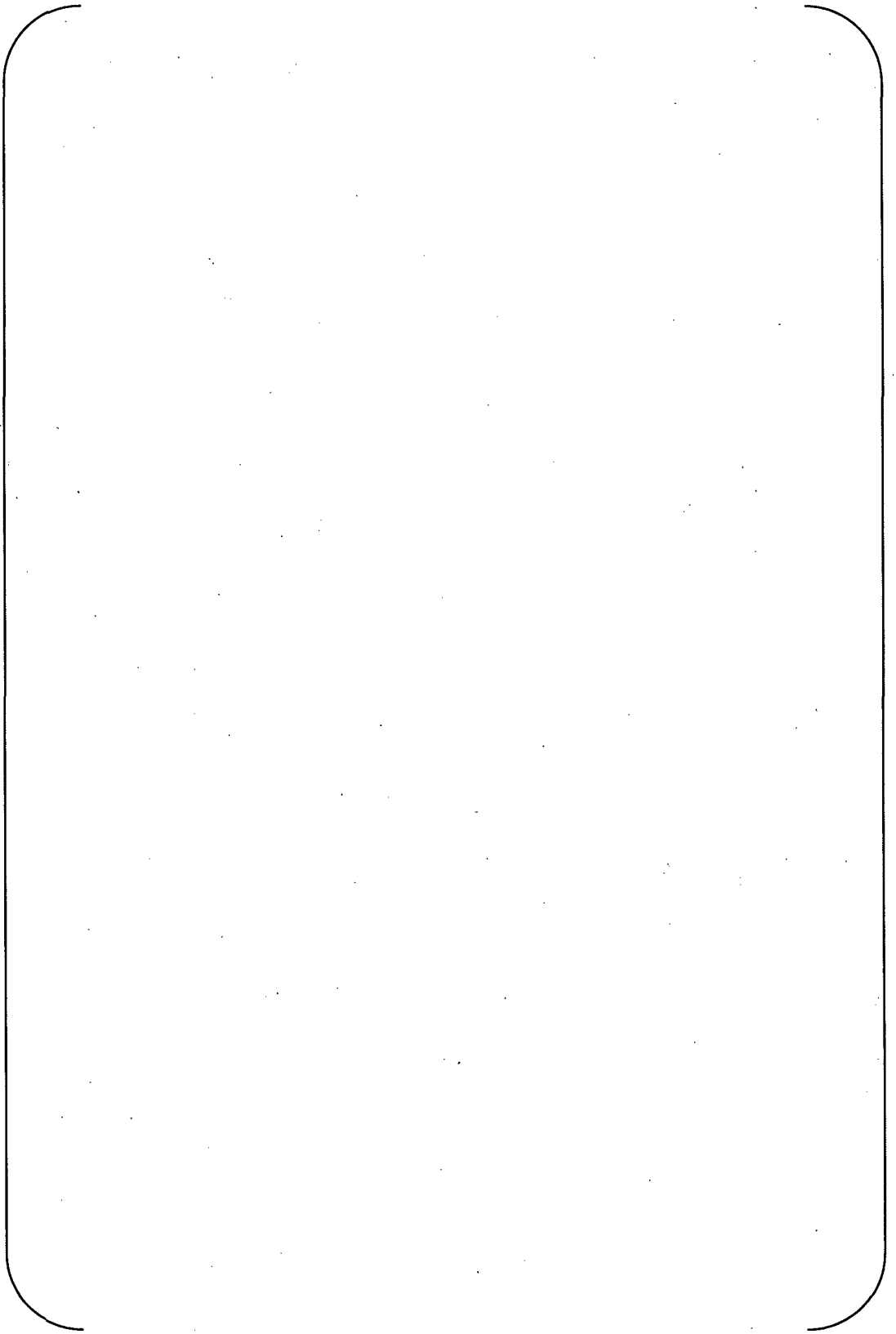

9

Fig.5-26 Distribution of void fraction and velocity at #2TSP

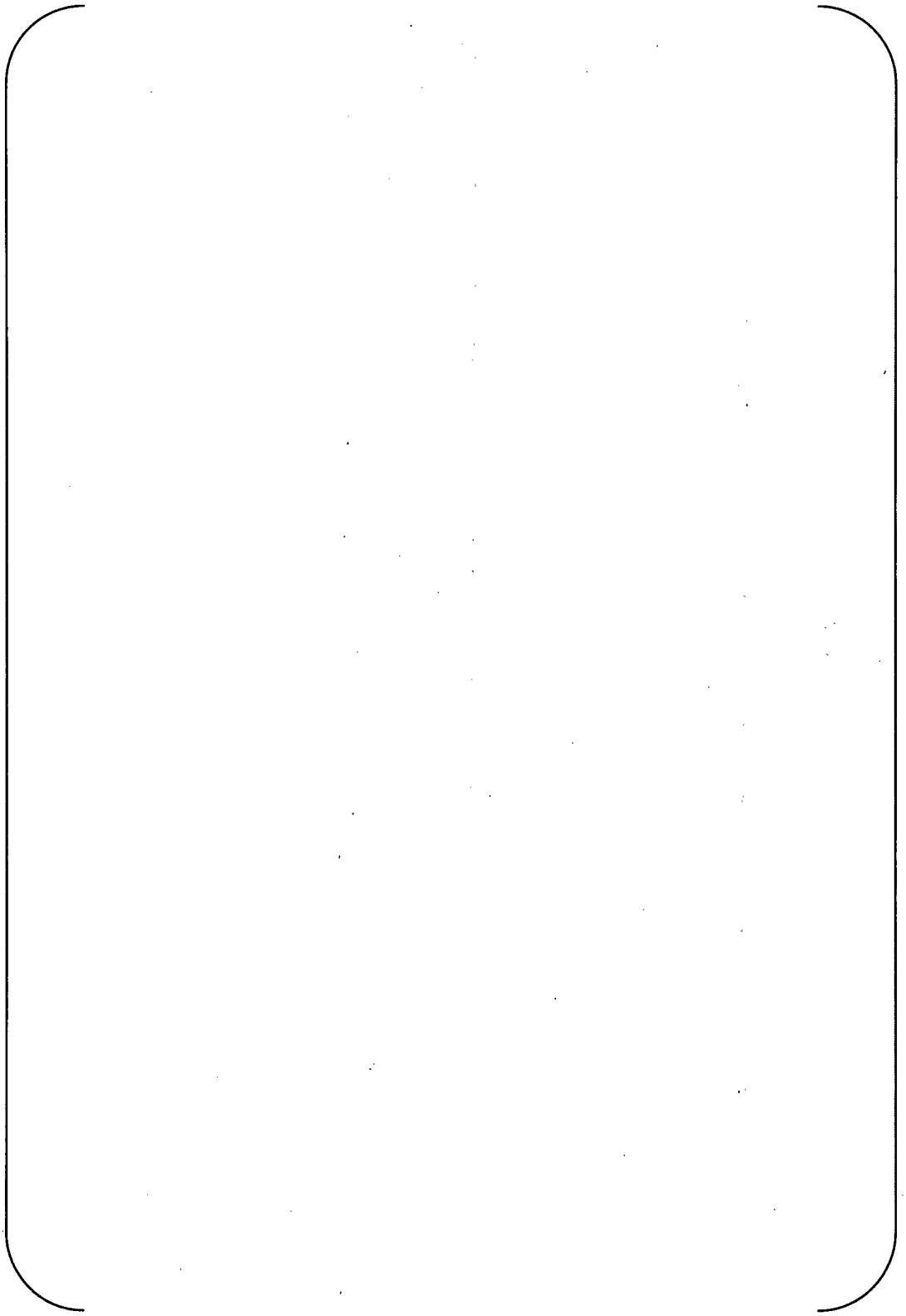

9

Fig.5-27 Distribution of void fraction and velocity at #3TSP

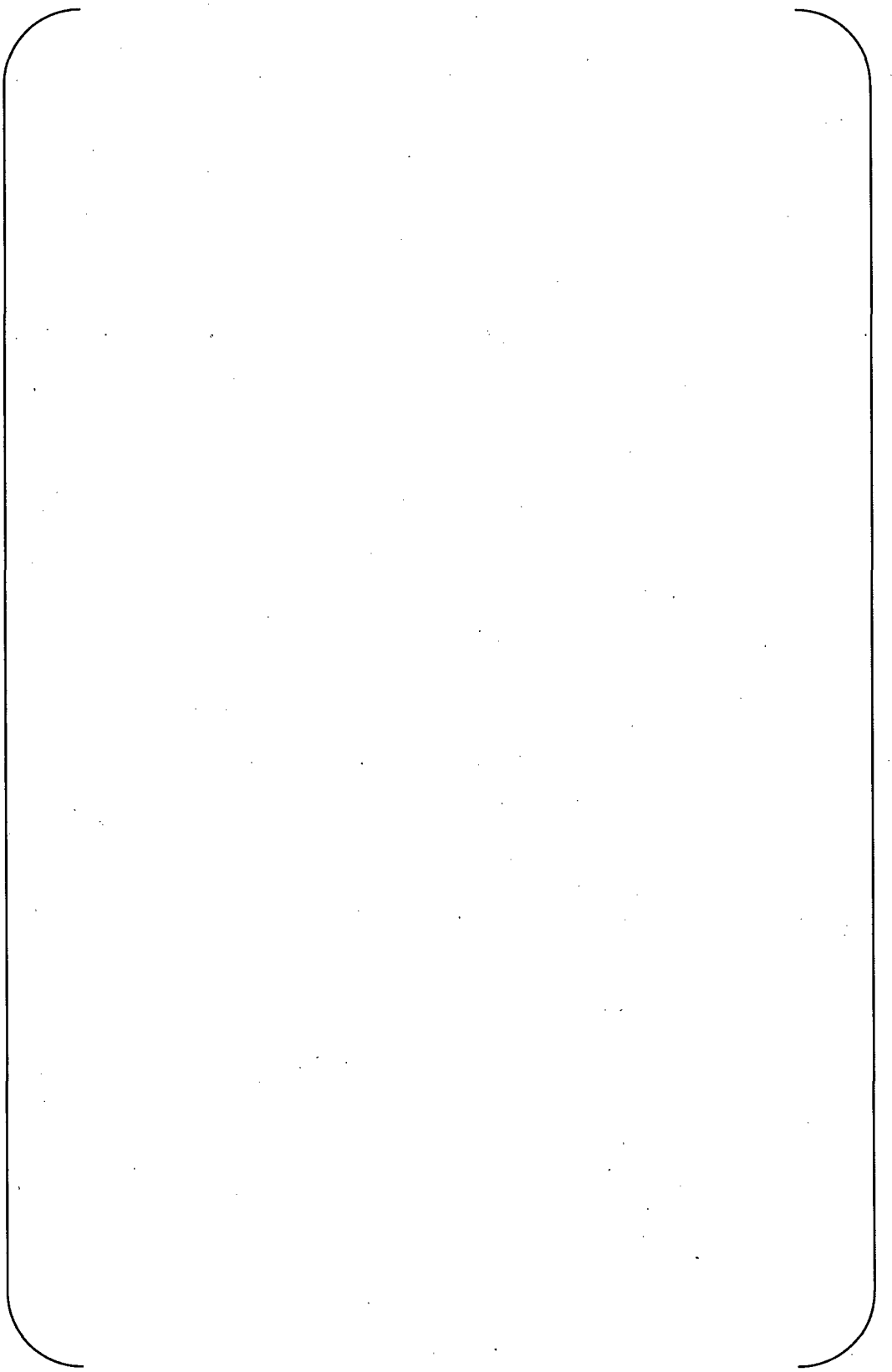

9

Fig.5-28 Distribution of void fraction and velocity at #4TSP

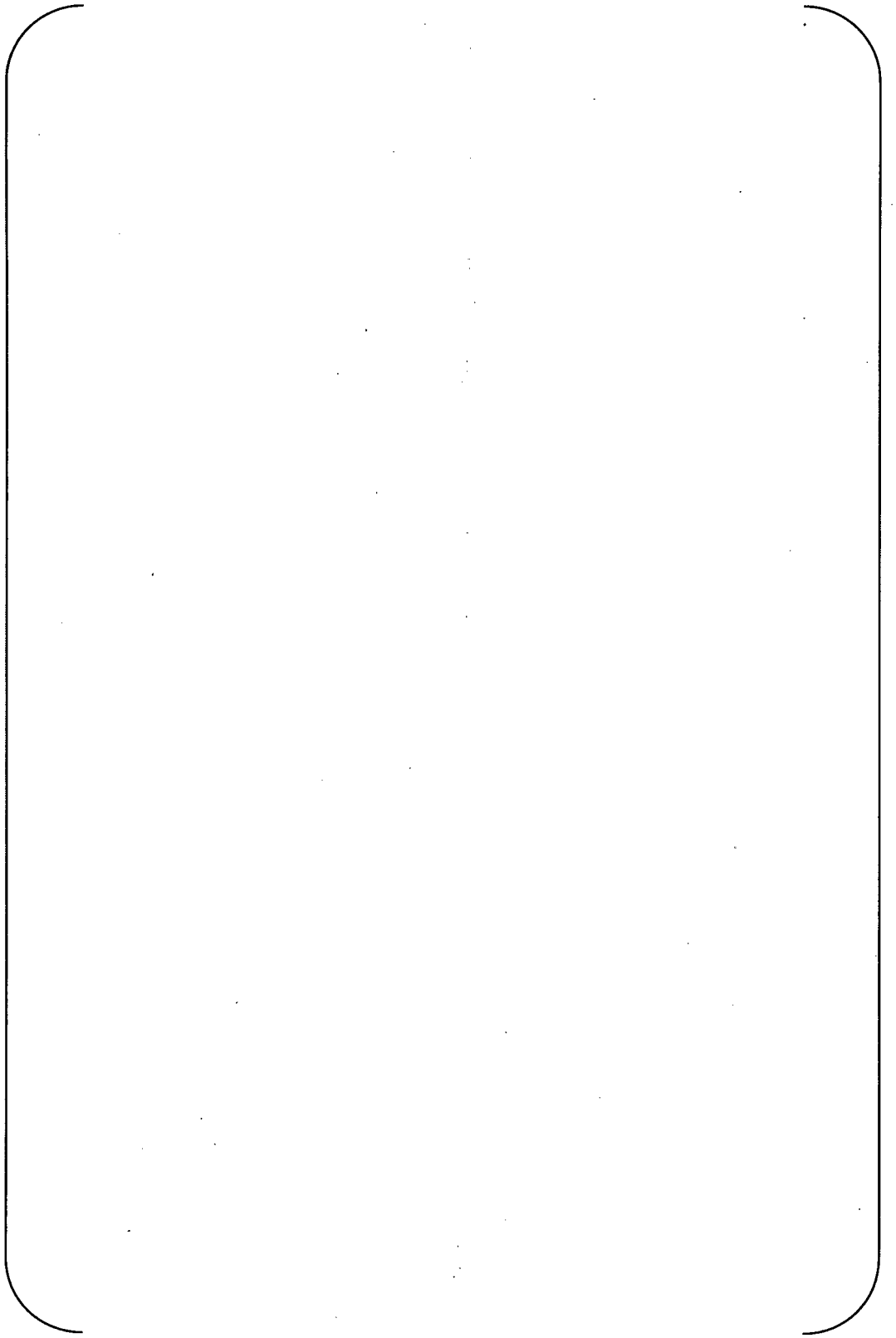

9

Fig.5-29 Distribution of void fraction and velocity at #5TSP

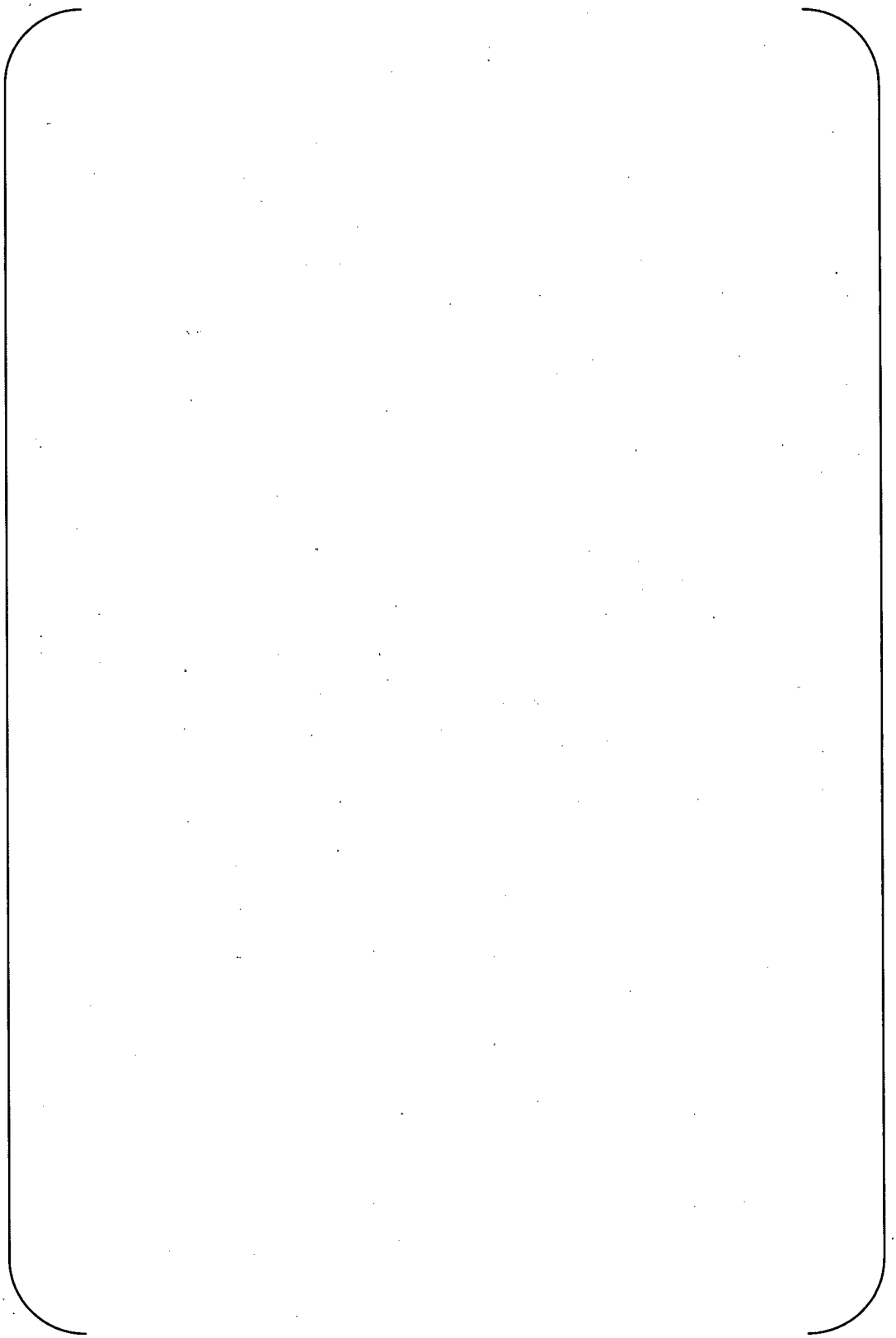

9

Fig.5-30 Distribution of void fraction and velocity at #6TSP

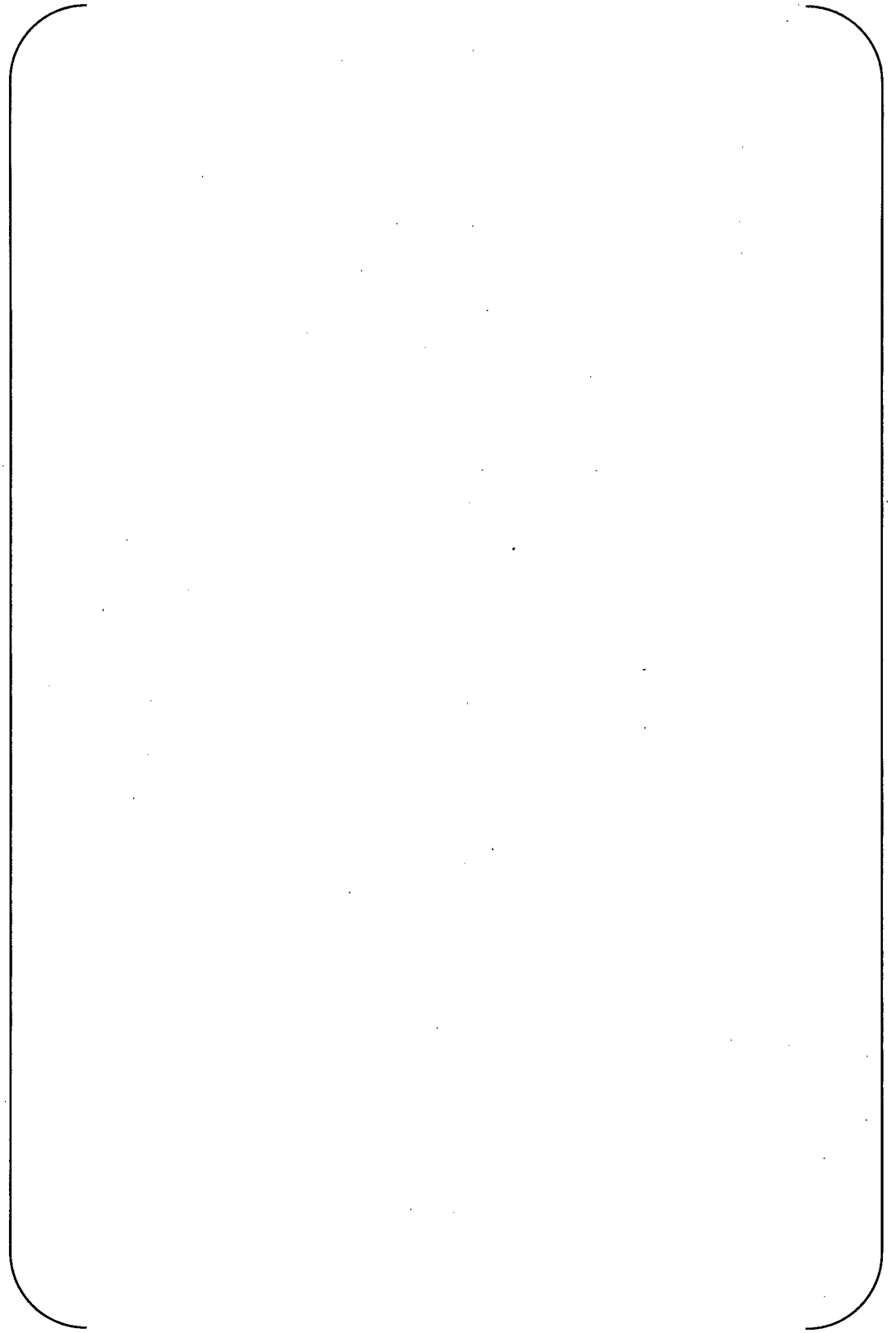

9

Fig.5-31 Distribution of void fraction and velocity at #7TSP

6. Methodology

6.1 Fluid elastic instability

6.1.1 Basic equation of tube vibration analysis

The term "fluid elastic instability" is generally used to refer to self-excited vibration of tube bundles due to cross flow. In 1969, Connors disclosed the presence of this phenomenon for the first time (Ref.24).

Causes of fluid elastic instability are considered to be the absorption of flow energy due to the interaction of fluid and structure. This phenomenon occurs on tube bundles, and is subjected to effects of tube bundle array. Thus, it is experimentally attempted to determine the criticality of occurrence in various tube bundle arrays.

The critical flow velocity U_c for generating fluid elastic instability is obtained in the following Connors' formula (Ref.24). This formula is employed in the TEMA (Standards of the Tubular Exchanger Manufactures Association), which is the industrial design standard in the United States.

$$\frac{U_c}{fD_o} = K\left[\frac{m_0\delta}{\rho_o D_o^{\,2}}\right]^{1/2} \quad \cdots\cdots (3)$$

Where,

U_c	: Critical flow velocity
f	: Tube natural frequency
D_o	: Tube outside diameter
K	: Critical factor
m_0	: Average tube mass per unit length
δ	: Tube logarithmic decrement(= $2\pi h$)
h	: Damping ratio
ρ_o	: Density of water outside the tube

The critical flow velocity U_c in eq. (3) is evaluated in case of tube vibration of single degree of freedom system with uniform cross flow along the tube axis. In actual tube, however, the vibration of the tube supported by the tube support plate is multi degrees of freedom system with beam type of vibration modes. Therefore, considering the vibration mode and fluid distribution, the effective flow velocity U_{en} is evaluated in the following formula.

$$U_{en} = \left[\frac{\int_0^L \frac{\rho(x)}{\rho_0}\cdot U(x)^2 \cdot \phi_n(x)^2\,dx}{\int_0^L \frac{m(x)}{m_0}\cdot \phi_n(x)^2\,dx}\right]^{1/2} \quad \cdots\cdots (4)$$

Where,

U_{en}	: Nth mode effective flow velocity
$\varphi_n(x)$	: Nth vibration mode
$\rho(x)$	:Fluid density distribution of water outside the tube in tube axis direction
$m(x)$	: Tube mass distribution per unit length in tube axis direction
$U(x)$	: Flow velocity distribution orthogonal to tube axis in tube axis direction
x	: Coordinate component along tube axis
ρ_o	: Average density of water outside the tube
m_o	: Average tube mass per unit length
L	: Tube length

The stability ratio is determined as follows in each vibration mode by calculating the ratio of eq. (3) and eq. (4).

$$SR_n = \frac{U_{en}}{U_{cn}} \quad \cdots\cdots (5)$$

where,

$$\frac{U_{cn}}{f_n \cdot D_o} = K\left[\frac{m_0 \delta}{\rho_o D_o^{\,2}}\right]^{1/2} \quad \cdots\cdots (6)$$

This value is called the n-th mode stability ratio SR_n, and if $SR_n > 1$, fluid elastic instability occurs. Generally, the maximum stability ratio in each mode is called the stability ratio of the tube, which is simply expressed as SR.

6.2. Critical factor and damping ratio

It is considered that the ASME code provides the conservative critical factor and damping ratio for the low void fraction region such as the tube straight region (Conservative case). In order to calculate the more realistic stability ratio, we can use the best estimated critical factor and the damping factor.

6.2.1 Conservative case

K=2.4 of the critical factor and h=1.5 % of damping ratio are used as recommended in ASME Sec.III Appendix N-1330 as a code calculation.

6.2.2 Best estimated case

Best estimated values based on recent experiential data are used in this case as follow.

6.2.2.1 Damping ratio

The damping ratio is calculated as the sum of the structural damping (1.0%), two phase damping, and squeeze film damping.

$$h = h_{ST} + h_{TP} + h_{SF} \quad \cdots\cdots (7)$$

where

h : Total damping ratio

h_{ST} : Structural damping ratio

h_{TP} : Two phase damping ratio

h_{SF} : Squeeze film damping ratio

(1) Structural damping

Since MHI test result (Figure 6.2-1, Ref.26) show the average structural damping value is 1.0% (0.2% in minimum), 1.0% is used for the evaluation.

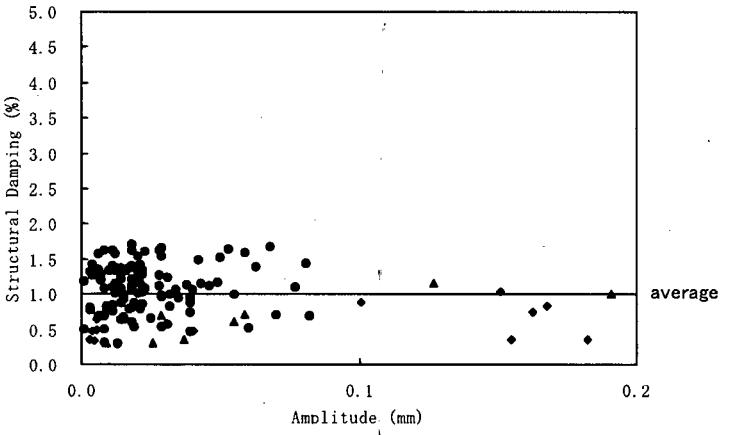

Fig.6.2-1 Structural Damping

(2) Two-phase damping

Pettigrew's test result of the two phase damping (Figure 6.2-2, Ref.27), which is the function of superficial void fraction, is used to calculate the effective two-phase damping along the tube length by considering vibration mode using the following equation.

$$\frac{\int h_{TP}(\beta(x))\phi^2 dx}{\int \phi^2 dx} \quad \cdots\cdots (8)$$

Where,

h_{TP}	: Two-phase damping
β	: Superficial void fraction
Φ	: Vibration mode
x	: Tube axis

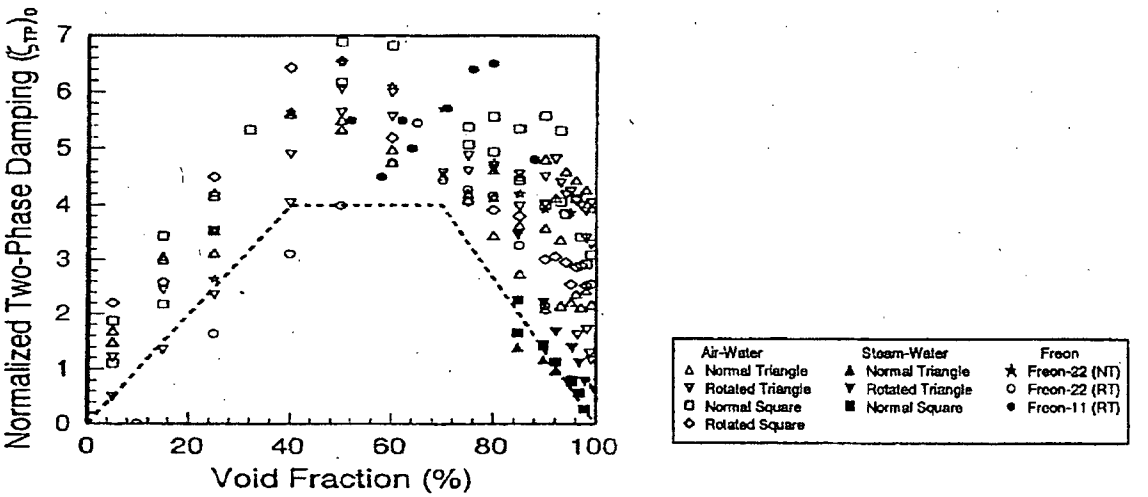

$$(\bar{\zeta}_{TP})_D = \zeta_{TP}(\rho_\ell D^2/m)^{-1}\{[1+(D/D_c)^3]/[1-(D/D_c)^2]^2\}^{-1}$$

Fig 6.2-2 Effect of void fraction on two-phase damping

(3) Viscous damping

Since the viscous damping is negligible in high void fraction (Ref.28), it is neglected in this analysis.

(4) Squeeze film damping

Squeeze film damping takes place at the supports and the following equation is based on the available experimental data. (Ref.27)

$$h_{SF} = \left(\frac{N-1}{N}\right)\left[\frac{(1460)}{f}\left(\frac{\rho D^2}{m}\right)\left(\frac{L}{\ell_m}\right)^{\frac{1}{2}}\right] \quad \cdots\cdots (9)$$

Where,

h_{SF}	: Squeeze film damping
ρ	: Homogeneous density
D	: Tube outside diameter
N	: Number of the support
f	: Natural frequency
L	: Support thickness
l_m	: Characteristic tube length

6.2.2.2 Critical Factor

(1) Effect of the void fraction

Based on MHI experimental data (Ref.30), the critical factor K is evaluated using the equation shown in Figure 6.2-3 which indicates the relation between the superficial void fraction and the critical factor. This experiment was performed under two-phase flow condition using the straight tube bundle of the triangular pitch as shown in Table 6.2-1 and Fig.6.2-4.

The effective superficial void fraction along the tube length is calculated by considering vibration mode and using the following equation in the same manner as the two-phase damping. The obtained critical factor obtained is K, when the value of P/D is 1.33.

$$\overline{\beta} = \frac{\int \beta(x)\phi^2 dx}{\int \phi^2 dx} \quad \cdots\cdots (10)$$

$$K = f(\overline{\beta}) \quad \cdots\cdots (11)$$

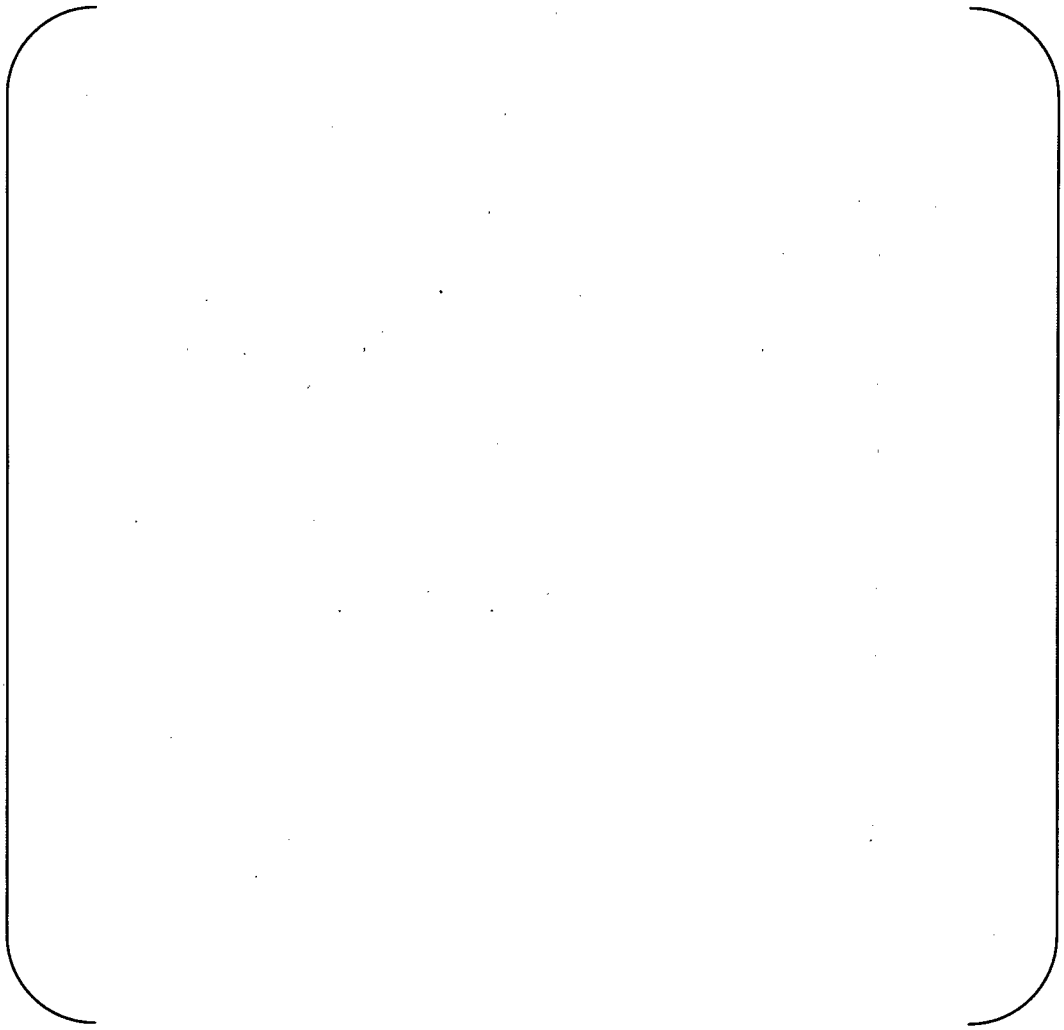

Fig.6.2-3 MHI Experimental Test Result (Relation between Critical Factor and Superficial Void Fraction)

Table 6.2-1 MHI Test Condition

Tube diameter	[
Tube pitch	
Number of tubes	
Flow condition	
Pressure	
Temperature	
Superficial void fraction	]

[

]

Fig.6.2-4 MHI Test Equipment

6.3. Flow of the evaluation

Evaluation of occurrence of fluid elastic instability in U-tubes is carried out in the following steps :

① Using a 1-dimensional Thermal and Hydraulic parameter code (SSPC), determine the tube bundle circulation ratio and other secondary side operating conditions for the normal operating condition (Ref.21).

② Using the flow analysis code (ATHOS/SGAP), determine the distributions of flow velocity U(x) and density of the fluid ρ(x) along the tube axis.

③ For the damping ratio h and critical factor K, the suggested values based on ASME Sec III Appendix N-1330 are used in conservative case, or eqs. (7), (11) are used in the best estimated case. And from eqs. (3) ~ (5) stability ratio is evaluated (Ref.25)

Figure 6.3-1 describes this process.

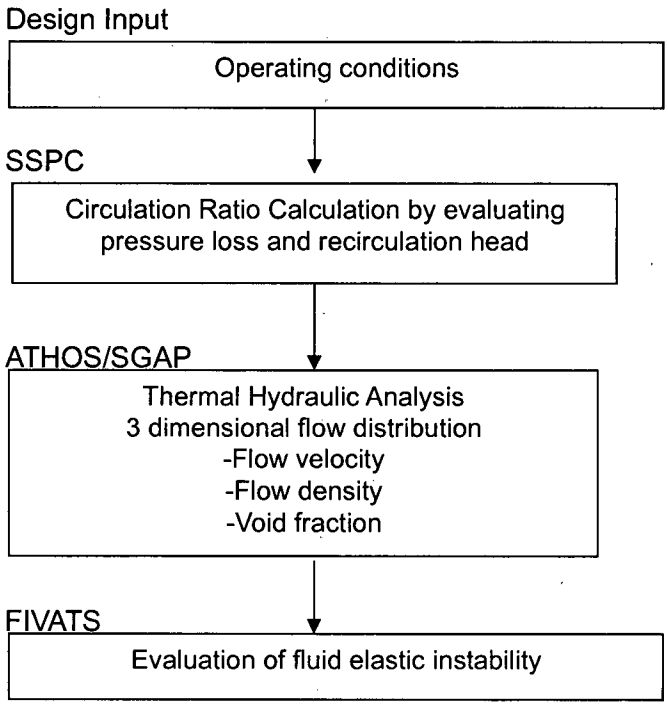

Fig.6.3-1 Flow of the evaluation

6.4 Evaluation Parameters

In general, larger thermal power is more severe for vibration, because the steam flow rate increases. At constant thermal power, lower steam pressure is more severe for vibration than higher pressure, because ρU^2 increases - (the lower ρ causes the higher U).

Basic parameters required for calculations are shown in Table 6.4-1.

Table 6.4-1 Basic parameters for calculation

	Condition of Cycle 16
Plugging	[
T_{cold} (°F)	
T_{hot} (Tsg-in) (°F)	
$T_{sg\text{-}out}$ (°F)	
$T_{feedwater}$ (°F)	
Saturation Steam Pressure (psia)	
Steam Mass Flow (lb/hr)	
Circulation ratio	
Thermal power (MWt/SG)	]

6.5 Evaluation of fluid elastic instability

6.5.1 Selection of tubes to be evaluated

The locations of Tube-to-TSP wear at tube straight portions detected in SONGS-2/3 RSGs are shown in Fig. 6.5-1 thorough 6.5-4. In all SGs, tube-to-TSP wear is present in many Row 1 tubes that border on the tube-free-lane. In addition many of the tubes on the bundle periphery with large bend radii (i.e. Rows 131-142) of 2B-SG exhibit tube-to-TSP wear.

Table 6.5-1 through Table 6.5-3 provides the maximum 10 tube wear depth in each SG. The tube-to-TSP wear distributions at each TSP elevation in each RSGs are provided in Appendix-2 Attachment-1.

Among Row1 tubes, the tube on the bundle periphery (Row 1 Column 1), the tube in column center region (R1C89), and the tube outside of the column region (R1C13) are selected for evaluation. Note that R1C1 tube has the second deepest wear indication at the TSP.

Among bundle periphery tubes, the tube which has the largest wear depth in peripheral tubes (R137C77) and the tube in the middle (R101C29) are selected for evaluation.

In the tube bundles, the tube which has the largest wear depth in all tubes (R80C74) and the tube in the middle of column (R53C57) are selected for evaluation.

As shown in Fig. 5-23, it is considered that the selected tubes cover wide range of tube bundle.

In general, the tube is supported by AVBs so that the tube vibration in U-bend region does not have much effect on the tube vibration of the tube straight part. Thus, the tube vibration model simulating only tube straight part is used for the evaluation.

Table 6.5-1 Max.10 Tube-to-TSP wear depth in 2A-SG

Table 6.5-2 Max.10 Tube-to-TSP wear depth in 2B-SG

Table 6.5-3 Max.10 Tube-to-TSP wear depth in 3A-SG

Table 6.5-4 Max.10 Tube-to-TSP wear depth in 3B-SG

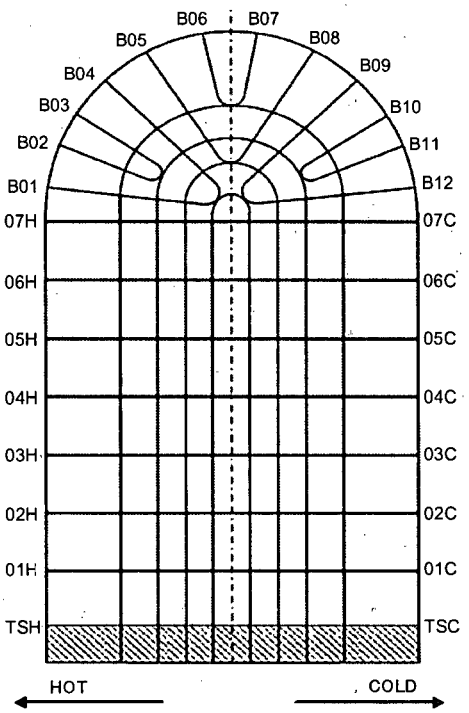
B06
B07
B05
B08
B04
B09
B03
B10
B02
B11
B01
B12
07H
07C
06H
06C
05H
05C
04H
04C
03H
03C
02H
02C
01H
01C
TSH
TSC
HOT
COLD

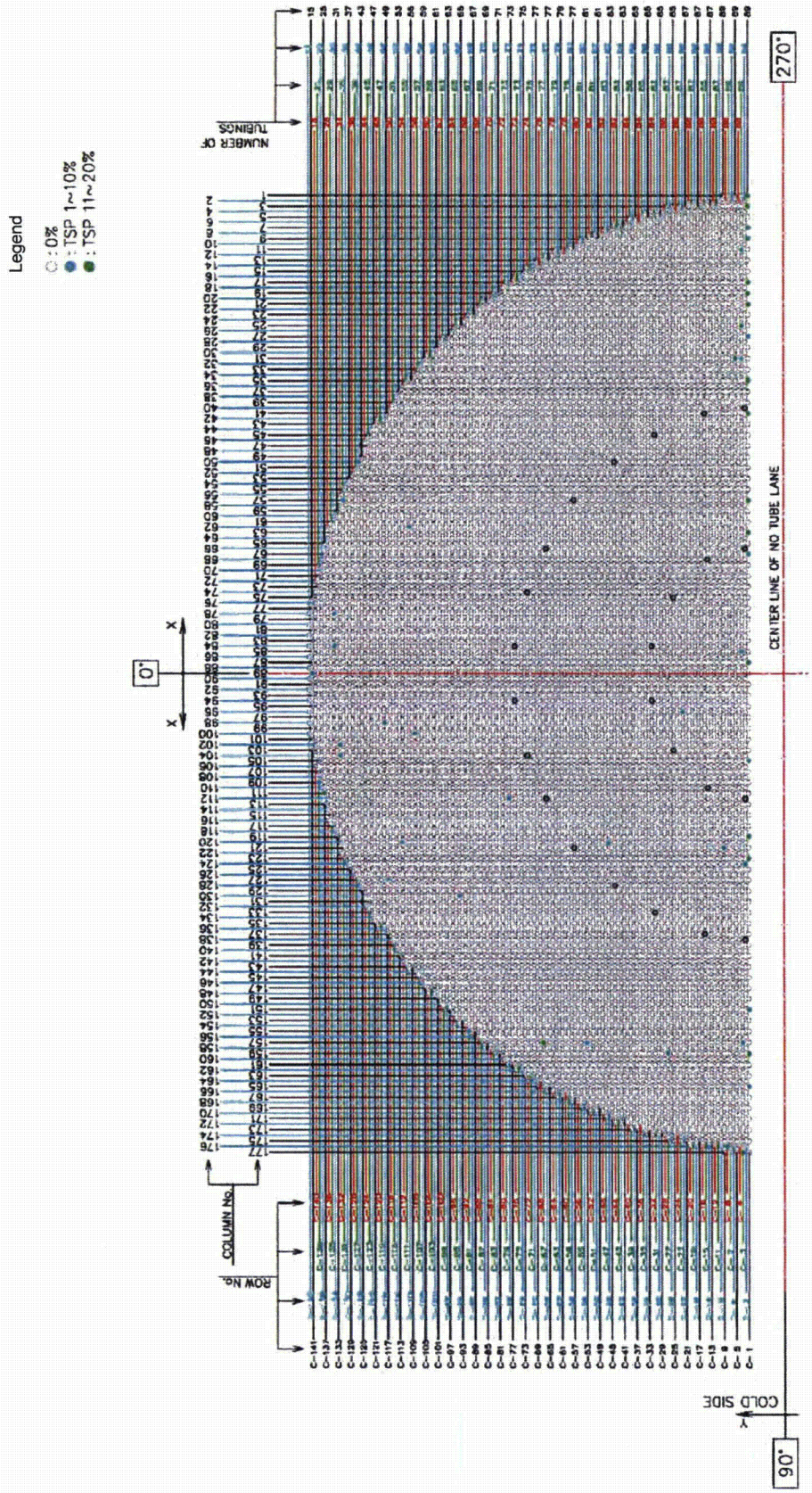

Fig. 6.5-1 Tube-to-TSP wear in 2A-SG

9

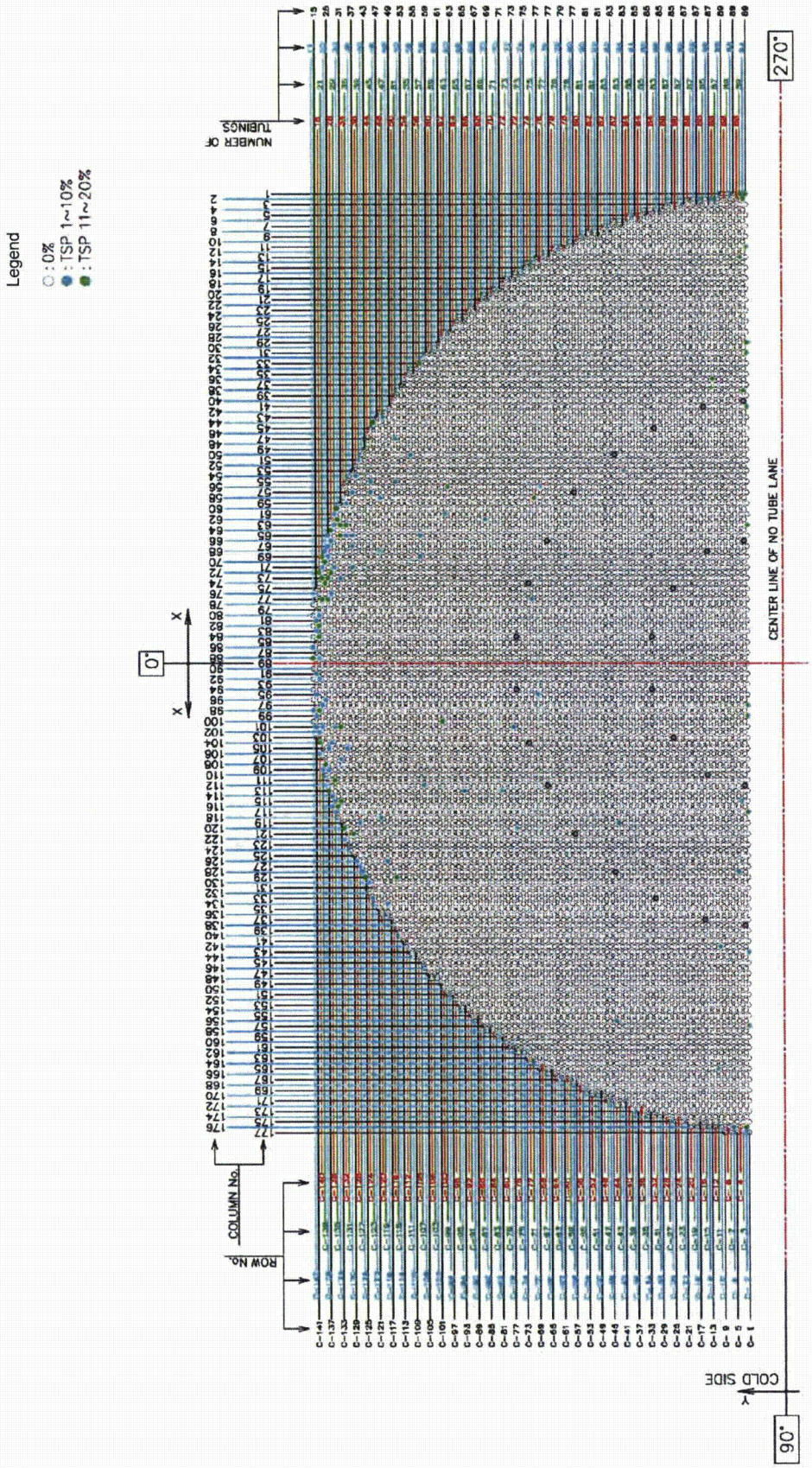

Fig. 6.5-2 Tube-to-TSP wear in 2B-SG

9

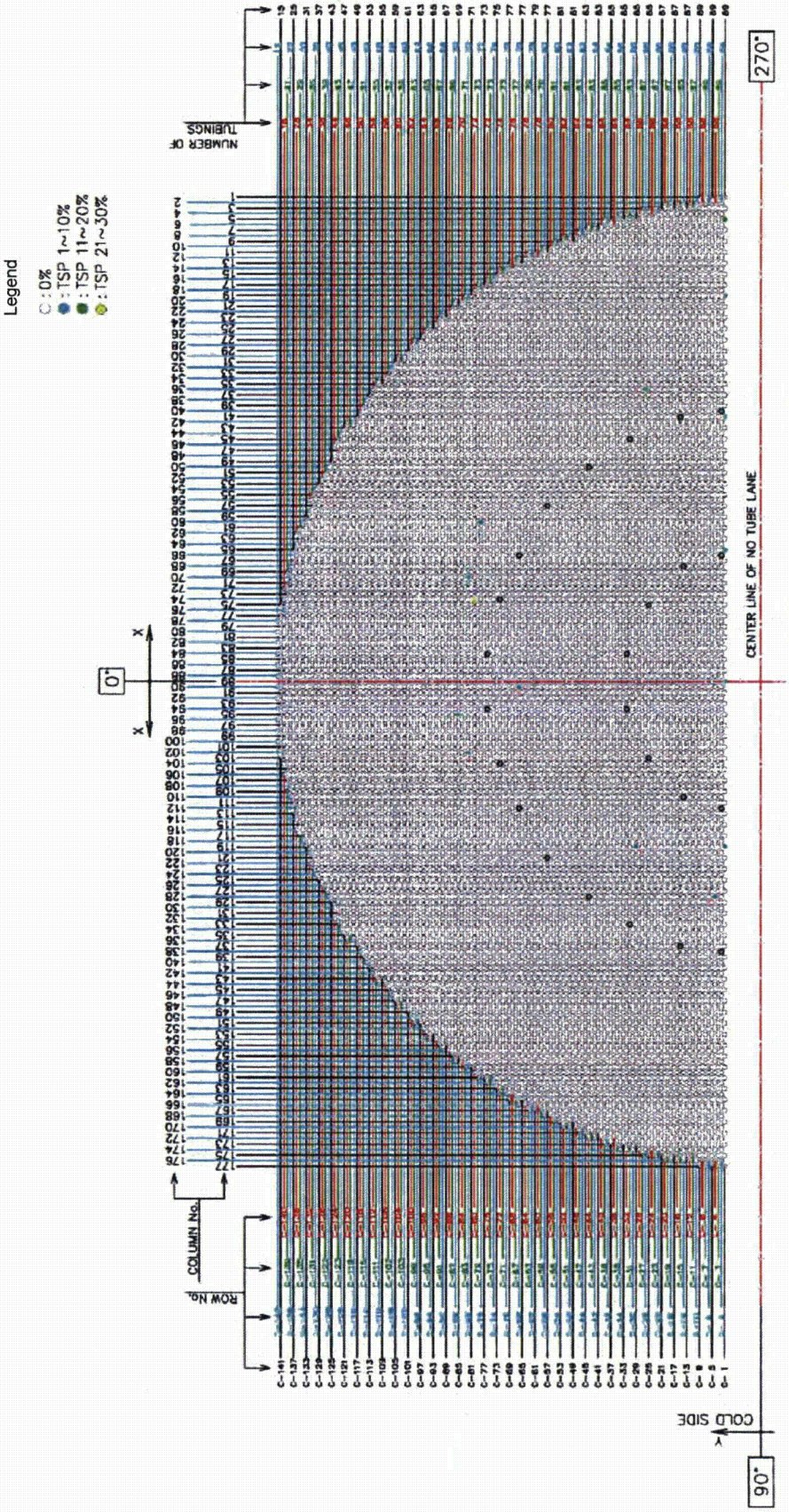

Fig. 6.5-3 Tube-to-TSP wear in 3A-SG

9

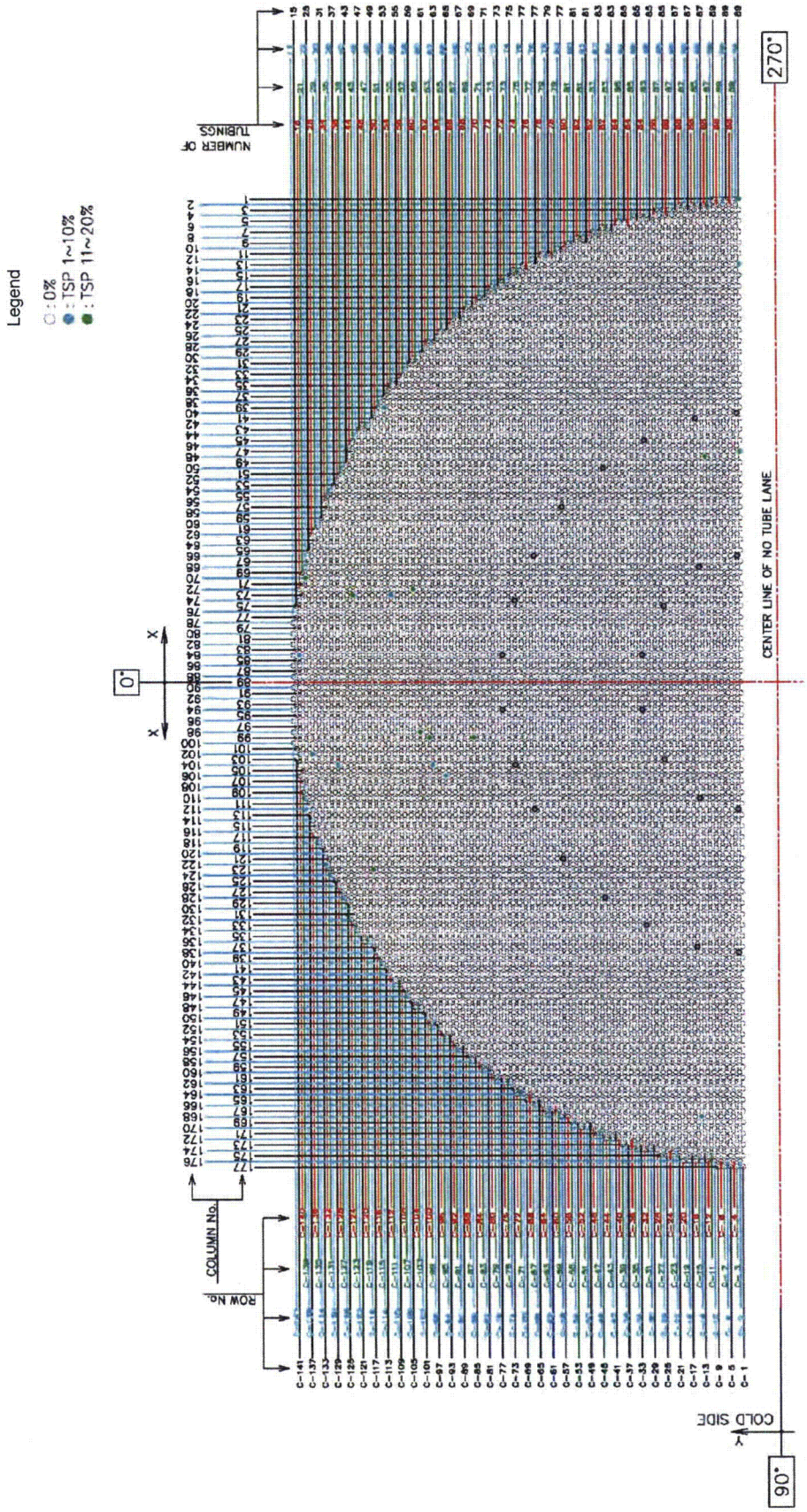

Fig. 6.5-4 Tube-to-TSP wear in 3B-SG

9

7. Results

(1) Conservative case

The vibration analysis results in case of conservative case (K=2.4, h=1.5%) are shown in Table 7-1 and Fig. 7-1 through 7-3. The maximum stability ratio is 0.67 for R1C1 tube in hot leg. Since the stability ratios are less than 1.0, the analyses imply no FEI occurrence of tube straight portion.

Table 7-1 Stability ratio (conservative case)

Tube		Leg	Mode	Frequency (Hz)	Critical velocity (ft/s)	Effective velocity (ft/s)	Stability ratio
Row	Column						
1	1	COLD					
		HOT					
1	13	COLD					
		HOT					
1	89	COLD					
		HOT					
53	57	COLD					
		HOT					
80	74	COLD					
		HOT					
101	29	COLD					
		HOT					
137	77	COLD					
		HOT					

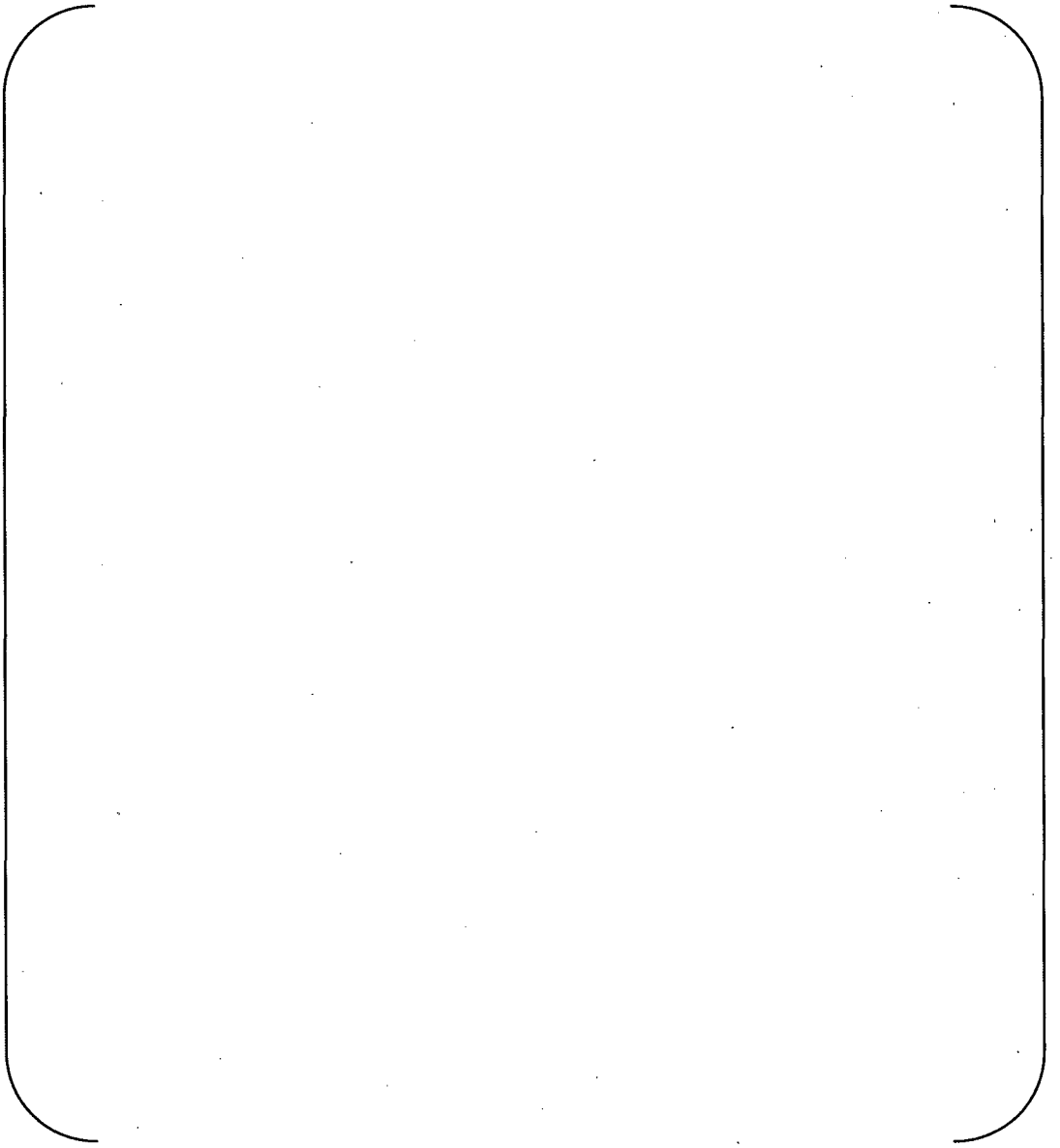

(a) Hot side (b) Cold side

Fig.7-1 Vibration mode diagram for R1C1 tube

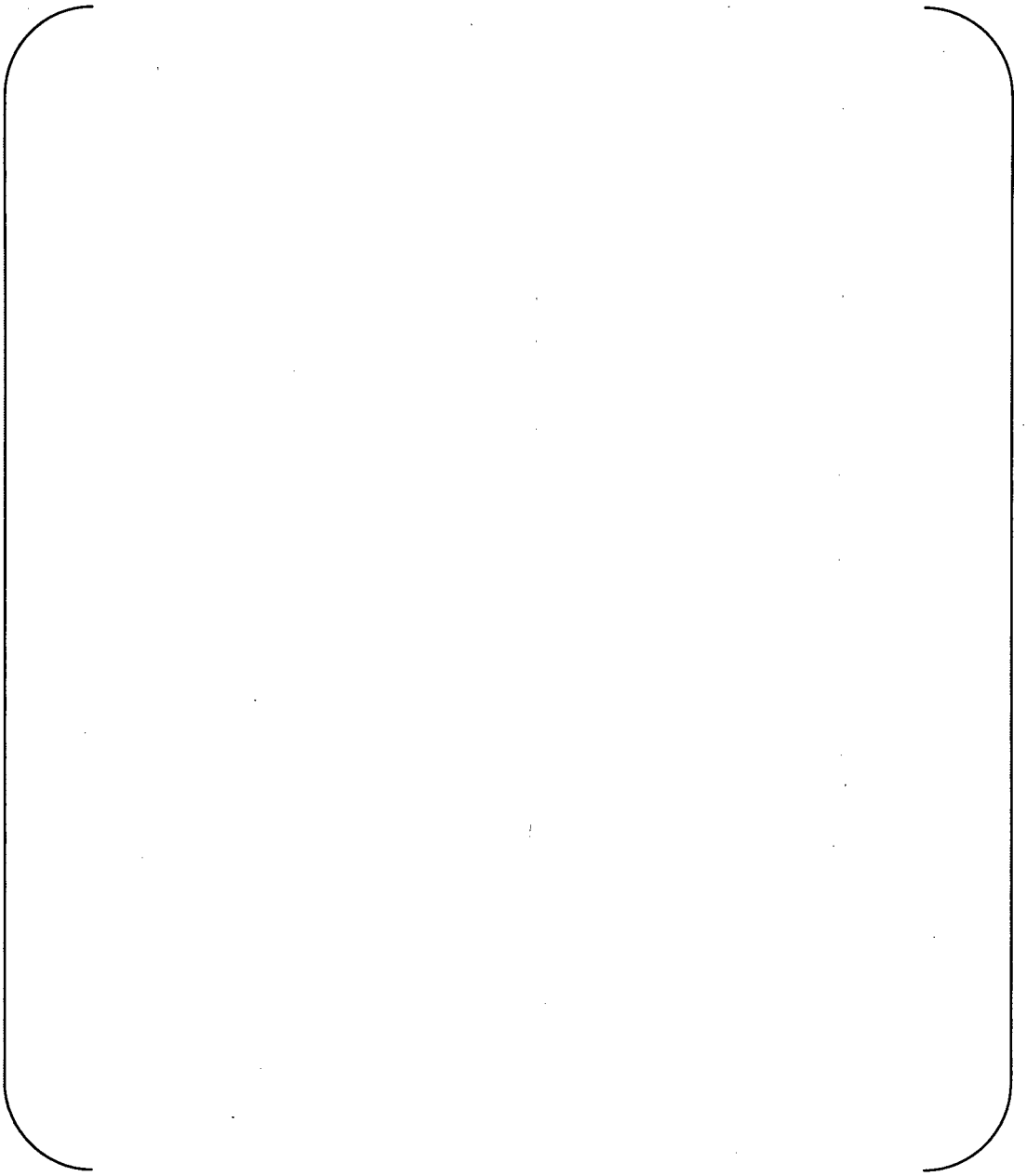

(a) Hot side (b) Cold side

Fig.7-2 Vibration mode diagram for R80C74 tube

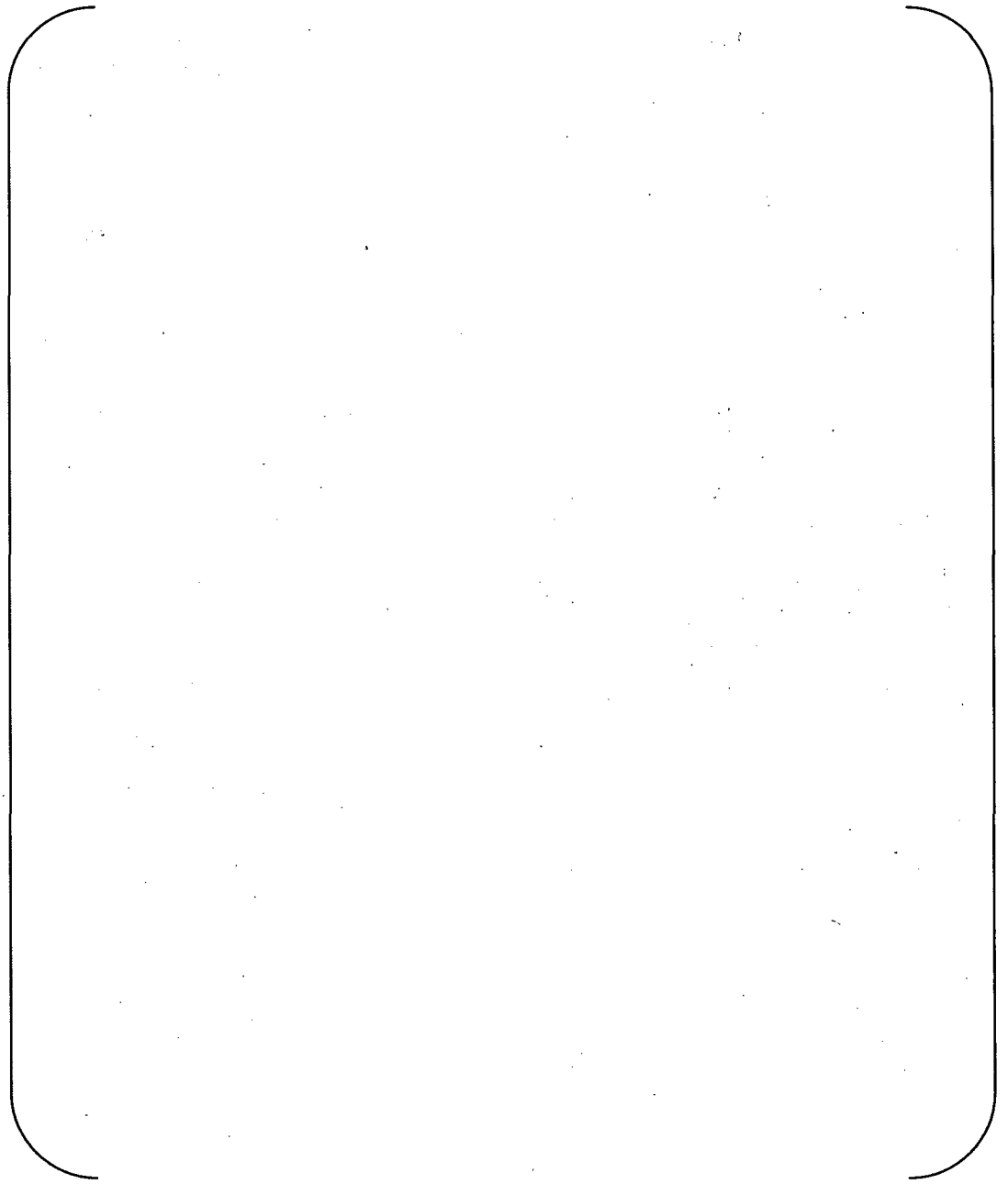

(a) Hot side (b) Cold side

Fig.7-3 Vibration mode diagram for R137C77 tube

(2) Best estimated case

In this case, the best estimated critical factors and damping ratios are calculated based on the recent experimental data. The critical factor and damping ratio are provided in Table 7-2.

Table 7-2 Critical factor and damping ratio(refined case)

Tube		Leg	Mode	Frequency (Hz)	Critical factor	Two phase damping (%)	Squeeze film damping (%)	Total damping (%)(*1)
Row	Column							
1	1	COLD						
		HOT						
1	13	COLD						
		HOT						
1	89	COLD						
		HOT						
53	57	COLD						
		HOT						
80	74	COLD						
		HOT						
101	29	COLD						
		HOT						
137	77	COLD						
		HOT						

(*1) Total damping = (Structural damping [1.0%]) + (two phase damping) + (squeeze film damping).

The vibration analysis results in case of refined case (K and h are calculated in detail) are shown in Table 7-3 and Fig. 7-4 through 7-6. The maximum stability ratio is [ ] for R1C89 tube in hot leg. Since the stability ratios are less than 1.0, the analyses imply no FEI occurrence of tube straight region.

The tube inspection identified the largest tube-to-TSP wear at R80C74 at hot #3-TSP. On the other hand, the calculated stability ratio for R80C74 is [ ], which is not so large compared to the other tubes. In addition, the tube inspection identified the relatively large tube wear in Row1 tubes in cold leg. However, the stability ratios of Row1 tubes in cold side are smaller than those in hot side. It is evaluated that the stability ratio evaluation does not match the tube wear inspection results. Thus, MHI concludes that the cause of tube-to-TSP wears in SONGS-2/3 RSGs is not due to FEI in the straight portion of tube due to the cross flow.

Table 7-3 Stability ratio (refined case)

Tube		Leg	Mode	Frequency (Hz)	Critical velocity (ft/s)	Effective velocity (ft/s)	Stability ratio
Row	Column						
1	1	COLD					
		HOT					
1	13	COLD					
		HOT					
1	89	COLD					
		HOT					
53	57	COLD					
		HOT					
80	74	COLD					
		HOT					
101	29	COLD					
		HOT					
137	77	COLD					
		HOT					

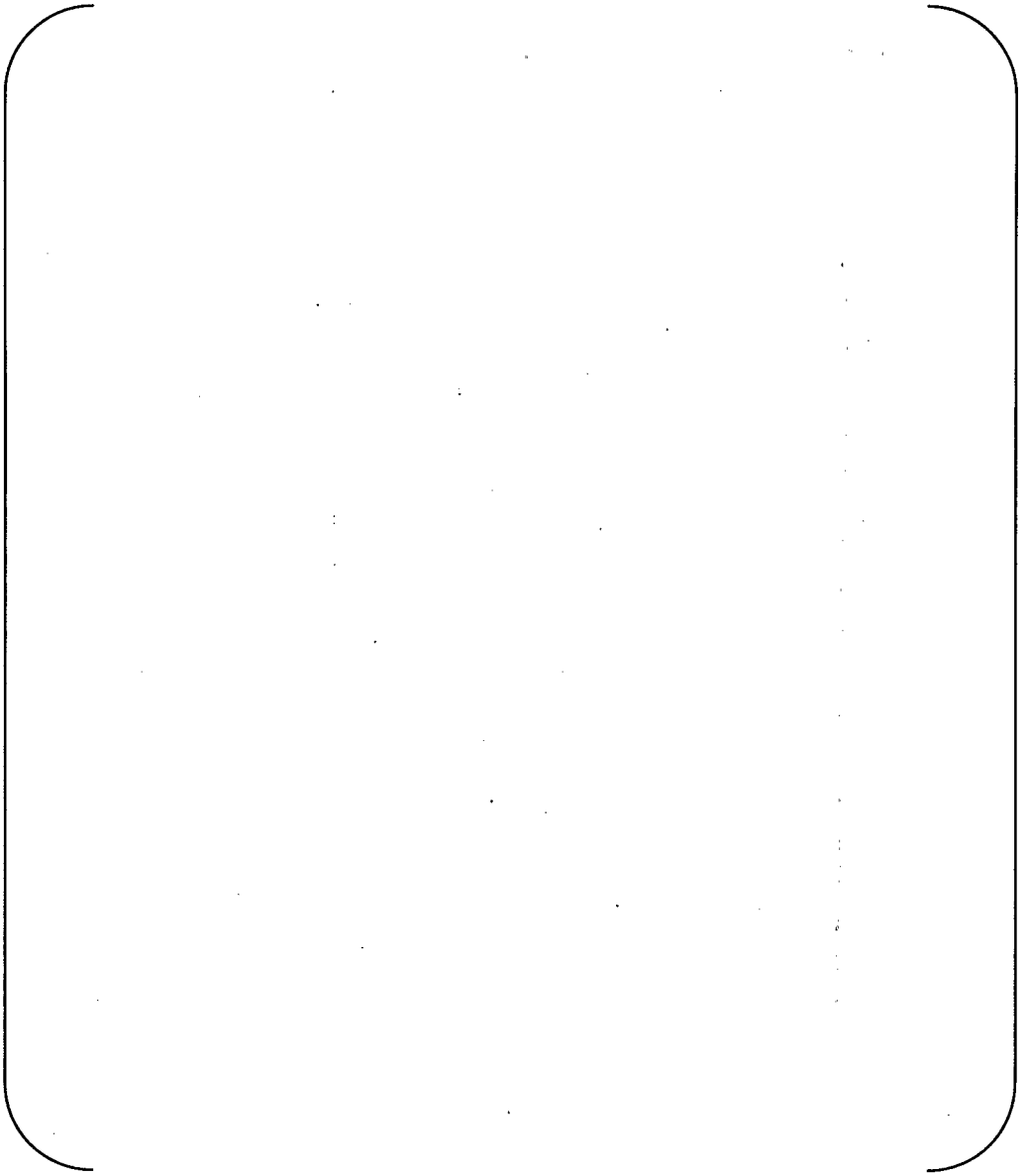

(a) Hot side (b) Cold side

Fig.7-4 Vibration mode diagram for R1C1 tube

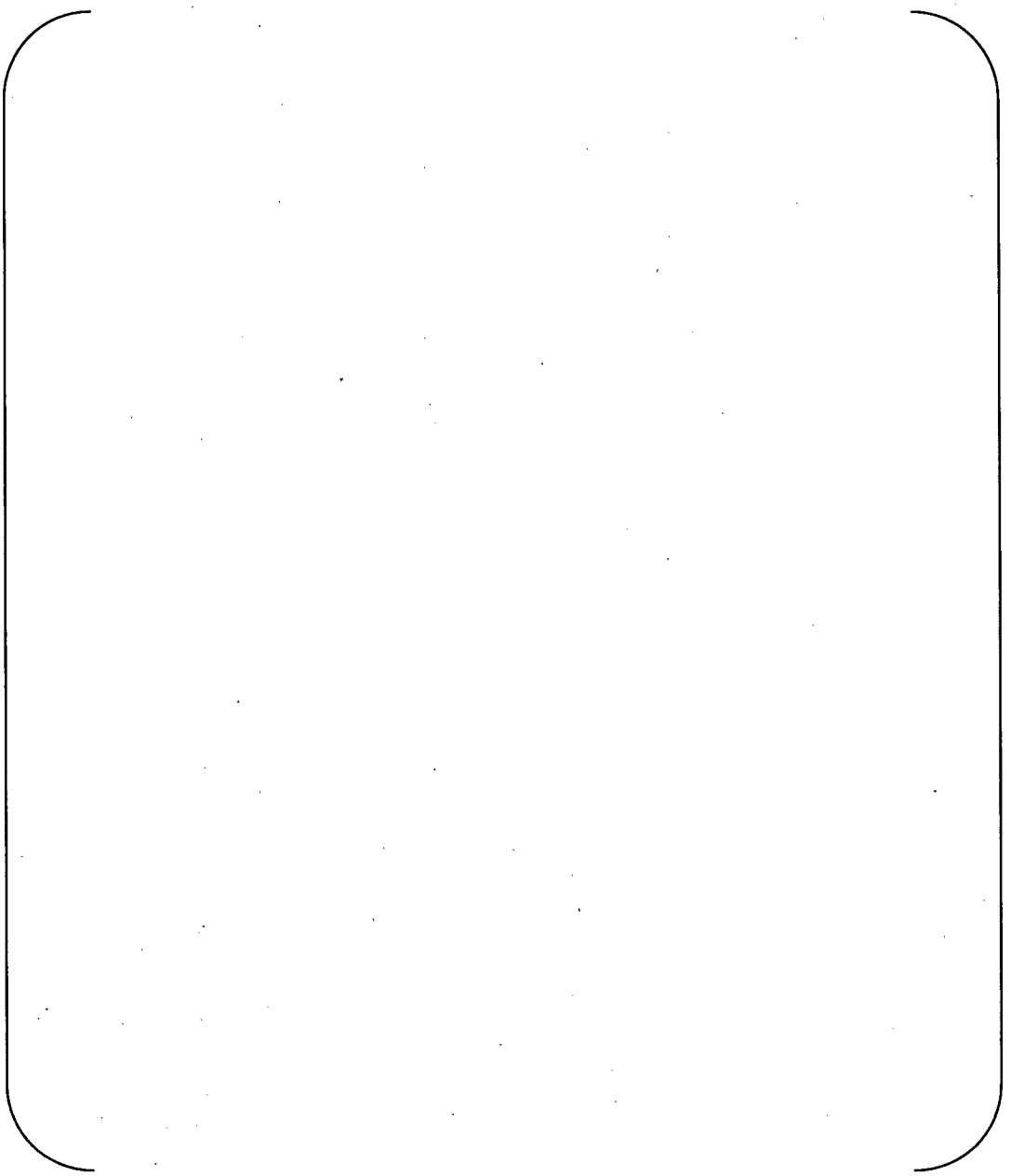

(a) Hot side (b) Cold side

Fig.7-5 Vibration mode diagram for R80C74 tube

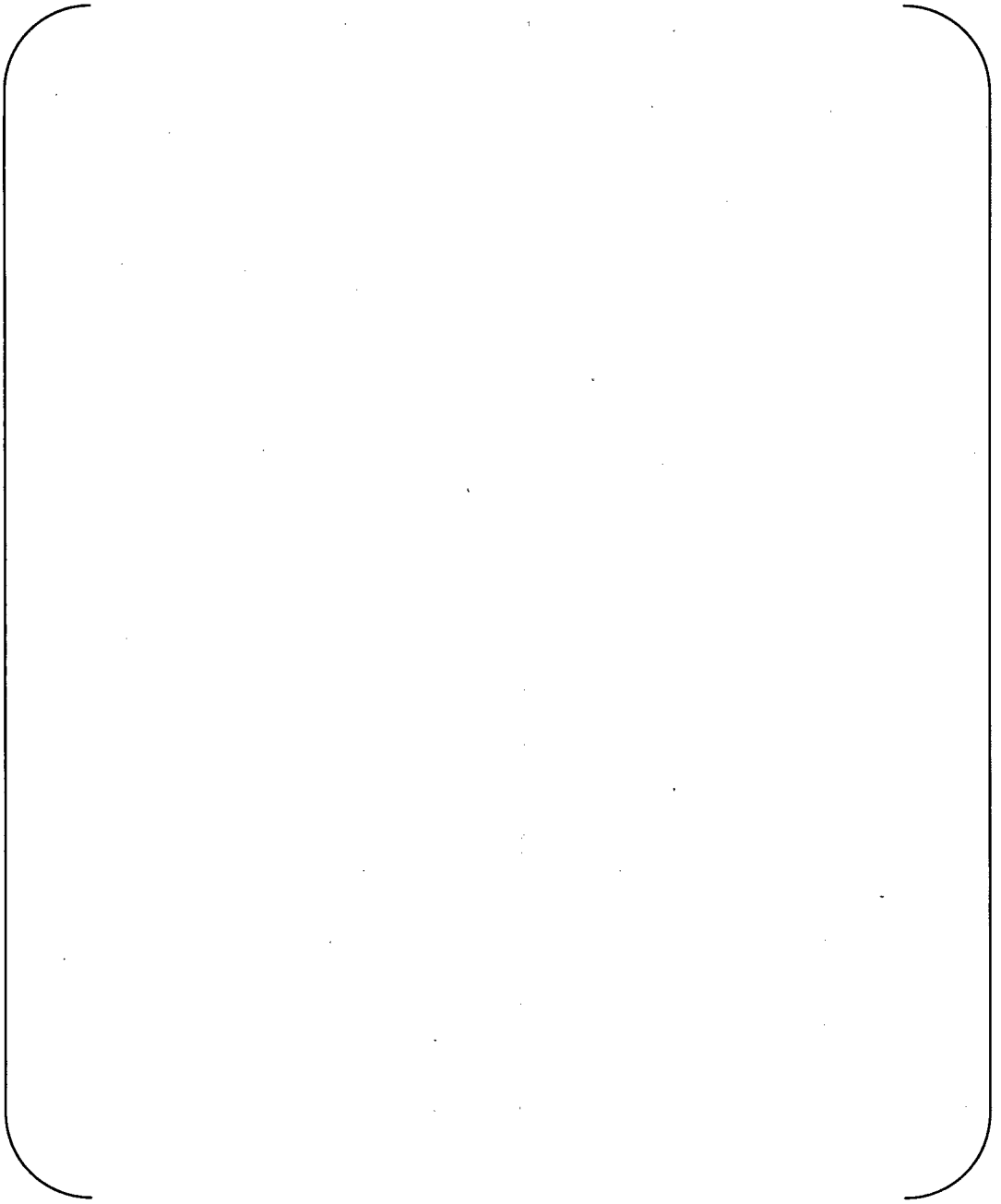

(a) Hot side (b) Cold side

Fig.7-6 Vibration mode diagram for R137C77 tube

8. References

1) Deleted
2) Deleted
3) L5-04FU001 the latest revision, Component and Outline Drawing 1/3
4) L5-04FU002 the latest revision, Component and Outline Drawing 2/3
5) L5-04FU003 the latest revision, Component and Outline Drawing 3/3
6) L5-04FU021 the latest revision, Tube Sheet and Extension Ring 1/3
7) L5-04FU022 the latest revision, Tube Sheet and Extension Ring 2/3
8) L5-04FU023 the latest revision, Tube Sheet and Extension Ring 3/3
9) L5-04FU051 the latest revision, Tube Bundle 1/3
10) L5-04FU052 the latest revision, Tube Bundle 2/3
11) L5-04FU053 the latest revision, Tube Bundle 3/3
12) L5-04FU111 the latest revision, AVB assembly 1/9
13) L5-04FU112 the latest revision, AVB assembly 2/9
14) L5-04FU113 the latest revision, AVB assembly 3/9
15) L5-04FU114 the latest revision, AVB assembly 4/9
16) L5-04FU115 the latest revision, AVB assembly 5/9
17) L5-04FU116 the latest revision, AVB assembly 6/9
18) L5-04FU117 the latest revision, AVB assembly 7/9
19) L5-04FU118 the latest revision, AVB assembly 8/9
20) L5-04FU119 the latest revision, AVB assembly 9/9
21) L5-04GA510 the latest revision, Thermal and Hydraulic Parametric Calculations
22) Vibration analysis of shell-and-tube heat exchanger : an overview – Part 1 : flow, damping, fluidelastic instability, M.J. Pettigrew, C.E. Taylor, Journal of fluids and structural 18 (2003) 469-483
23) ASME Boiler and Pressure Vessel Code, Sec II, Materials, 1998 Edition through 2000 addenda.
24) Connors, H.J., Fluid Elastic Vibration of Tube Arrays Excited by Cross Flow, ASME Annual Meeting, 1970.
25) Blevins, R. D., "Flow-induced Vibration", Krieger Publishing Company.
26) T. Nakamura, et al., "An advanced method to estimate fluid elastic instability of steam generator U-bend tube bundle.", ASME PVP 2001
27) M.J. Pettigrew.,et.al.,2003,"Vibration analysis of shell-and-tube heat exchangers" Journal of Fluids and Structures 18 (2003) 469-483
28) S. M. Fluit and M. J. Pettigrew, "Simplified method for predicting vibration and fretting-wear in nuclear steam generator U-bend tube bundle", ASME PVP 2001
29) M.J. Pettigrew.,et.al.,2000, "The effects of tube bundle geometry on vibration in two-phase cross-flow"
30) WJS16263, MHI Test Report of Fluid Elastic Vibration